

**Biochemical and functional studies on DafA, a
member of the DnaK chaperone system from
*Thermus thermophilus***

Dissertation

zur Erlangung des Grades
Doktor der Naturwissenschaften
des Fachbereichs Chemie der Universität Dortmund

vorgelegt von

Dipl. Biochem.

Georgeta Liliana Dumitru

Max-Planck-Institut für molekulare Physiologie

Dortmund 2004

Die vorliegende Arbeit wurde in der Zeit vom Januar 2000 bis zum Mai 2004 in der Abteilung Physikalische Biochemie am Max-Planck-Institut für molekulare Physiologie in Dortmund unter der Anleitung von Herrn PD. Dr. Jochen Reinstein und Herrn Prof. Dr. Roger S. Goody angefertigt.

1. Gutachter: Prof. Dr. Roger Goody
2. Gutachter: Prof. Dr. Roland Winter

Hiermit versichere ich, dass ich diese Arbeit selbständig verfaßt und keine anderen als die angegebenen Hilfsmittel benutzt habe.

Dortmund, Mai 2004

INDEX

1	INTRODUCTION	1
1.1	Protein folding	1
1.2	Molecular chaperones	2
1.2.1	Hsp100/Clp family	4
1.2.2	Hsp60 or chaperonins	5
1.2.3	Hsp70/DnaK family	7
1.3	Aims	13
2	MATERIALS AND METHODS	15
2.1	Materials	15
2.1.1	Chemicals	15
2.1.2	Enzymes	15
2.1.3	Reagent kits	16
2.1.4	Chromatography material	16
2.1.5	Microorganisms	16
2.1.6	Vectors and PCR-primers	16
2.1.7	Media	18
2.2	Methods	19
2.2.1	Methods related to nucleic acids	19
2.2.2	Methods related to proteins	22
2.2.3	Spectroscopic methods	30
2.2.4	Calorimetry	34
3	RESULTS	35
3.1	Biochemical and biophysical characterization of DafA(L2V)_{Tth} and DnaK_{Tth}-DnaJ_{Tth}-DafA(L2V)_{Tth} complex	35
3.1.1	Optimization of DafA(L2V) _{Tth} purification	35
3.1.2	Optimization of DafA(L2V) _{Tth} solubility	36
3.1.3	Effect of chaotropic agents on DafA(L2V) _{Tth} structure analyzed by fluorescence spectroscopy	41
3.1.4	Stability of DnaK _{Tth} -DnaJ _{Tth} -DafA(L2V) _{Tth} complex in urea	43
3.1.5	Thermal stability of DafA(L2V) _{Tth} analyzed by DSC	44
3.1.6	Inhibitory effect of DafA(L2V) _{Tth} on luciferase refolding assisted by DnaK _{Tth} chaperone system	47
3.1.7	Cysteine mutants engineering	49
3.1.8	Dynamics of DnaK _{Tth} -DnaJ _{Tth} -DafA(L2V) _{Tth} complex formation at equilibrium	50
3.1.9	Structural analysis of DafA(L2V) _{Tth} using HSQC-NMR spectroscopy	53
3.1.10	Analysis of various DafA(L2V) _{Tth} mutants	55

3.2	Functional analysis of DafA_{Tth}	59
3.2.1	Identification of new potential interaction partners of DafA(L2V) _{Tth}	59
3.2.2	Analysis of 70 S ribosome-DafA(L2V) _{Tth} complex in correlation with DnaK _{Tth} -DnaJ _{Tth} -DafA(L2V) _{Tth}	68
3.2.3	DafA(L2V) _{Tth} binding to 70 S ribosomes from <i>T. thermophilus</i> and <i>E. coli</i> : fluorescence anisotropy studies	71
3.3	<i>In vitro</i> refolding studies using <i>E. coli</i> cell lysate containing co-expressed DnaK, DnaJ, GrpE and ClpB chaperones from <i>T. thermophilus</i>	78
3.3.1	Co-expression of DnaK _{Tth} and ClpB _{Tth} chaperone systems in <i>E. coli</i>	78
3.3.2	Refolding of model substrates using <i>E. coli</i> cells lysate co-expressing DnaK _{Tth} , DnaJ _{Tth} , GrpE _{Tth} and ClpB _{Tth}	80
4	DISCUSSION	87
4.1	Properties of free DafA(L2V)_{Tth}	87
4.1.1	DafA(L2V) _{Tth} is a thermostable protein	87
4.1.2	Denaturing agents have different effects on DafA(L2V) _{Tth} stability	87
4.1.3	Structural considerations	88
4.2	DafA(L2V)_{Tth} and its relationship with DnaK_{Tth} and DnaJ_{Tth}	90
4.2.1	DnaK _{Tth} -DnaJ _{Tth} -DafA(L2V) _{Tth} complex is unable to assist protein refolding	90
4.2.2	DnaK-DnaJ-DafA(L2V) complex possesses high affinity and low rates of association and dissociation	91
4.2.3	Point mutations in DafA(L2V) _{Tth} and the stability of the ternary complex	92
4.3	Functional studies reveal new potential functions for DafA_{Tth}	92
4.3.1	DafA _{Tth} is not implicated in transcriptional regulation of <i>dnaK_{Tth}</i> operon	93
4.3.2	The 70 S ribosome, the new interaction partner of DafA(L2V) _{Tth}	94
4.3.3	Ribosome-DafA(L2V) _{Tth} complex and its relationship with DnaK-DnaJ-DafA(L2V) _{Tth} complex	94
4.4	Outlook	96
5	SUMMARY	99
6	REFERENCES	101
7	APPENDIX	115
7.1	Derivations	115
7.1.1	Determination of the k_{on} and k_{off} via k_{obs}	115
7.2	Abbreviations	116
ACKNOWLEDGEMENTS		119

CURRICULUM VITAE**121****Publications****121**

1 INTRODUCTION

1.1 Protein folding

Proteins accomplish numerous and various structural and catalytic functions in the cell. Protein biosynthesis represents a complex and efficient cellular process. An *E. coli* cell utilizes up to 20000 ribosomes to produce an estimated total of 30000 polypeptides per minute (Bukau et al., 2000). After synthesis on the ribosome, polypeptides need to gain their unique three-dimensional structure in order to become fully functional. Anfinsen discovered in 1961 that, *in vitro*, small denatured proteins could spontaneously regain their native structure upon removal of the denaturant. It was thus demonstrated that the information for the tertiary structure of a protein is determined by its amino acid sequence (Anfinsen et al., 1961; Anfinsen, 1973). Consequently, the native state is the thermodynamically most stable conformation of a polypeptide. However, later studies have shown that spontaneous folding *in vitro* is efficient for small, single-domain proteins that bury exposed hydrophobic amino acid residues rapidly (Dobson and Karplus, 1999). A significant number of proteins, especially larger proteins composed of multiple domains, usually refold inefficiently *in vitro* leading to the formation of partially folded intermediates, including misfolded states that lead to aggregates formation (Jaenicke, 1987; Goldberg et al., 1991).

In contrast to the *in vitro* systems, protein folding in the cell represents a far more complex process (Ellis and Hartl, 1999). There are two major differences between the refolding of a denatured protein chain in a test tube and the folding of a newly synthesized chain inside the cell (Hartl, 1996). First, protein chains are produced inside the cells in a vectorial fashion by the ribosome (Frydman et al., 1994). In many cases, the rate of this process is slower than the rate of protein folding (Radford, 2000). Thus, there is the possibility that the elongating chain will misfold before its completion, be degraded because it is not fully folded and hence is susceptible to proteases or can aggregate with similar close by chains. A way of bypassing these negative effects is the co-translational folding of the emerging polypeptide chain before termination of synthesis (Frydman and Hartl, 1996). However, since the formation of stable tertiary structure is a cooperative process at the level of protein domains (50-300 amino acid residues), an average domain can be fully folded only when its entire sequence has emerged from the ribosome (Jaenicke, 1991).

A second major problem uncounted by newly synthesized polypeptides is the cellular milieu, a very crowded and dynamic environment. The effective protein concentration inside a typical cell has been estimated to be as high as 300 mg/ml (Minton, 2000; Ellis, 2001). Crowding is predicted to greatly increase the risk that newly synthesized chains will

not fold correctly into monomers, but will aggregate with one another to form nonfunctional structures (Ellis and Hartl, 1999).

Besides folding problems encountered by the newly synthesized polypeptide chains, environmental factors as high temperature, high concentration of oxidizing substances or metals, changes in pH values or in cell osmolarity can damage the folded state of proteins resulting in loss of function. Damaged proteins have to be either rescued or permanently eliminated through degradation (Wickner et al., 1999). Therefore, to maintain the normal protein homeostasis, cells have developed specialized systems that enable proteins to gain their tertiary structure and to repair damaged proteins (molecular chaperones) or to remove proteins that cannot be longer recovered (proteasome).

There are circumstances in which these reparatory mechanisms are disturbed. As a consequence, misfolded proteins and aggregates that accumulate may lead to serious diseases. For example, defects in protein folding represent the cause of several affections as cystic fibrosis or familial hypercholesterolemia (Thomas et al., 1995; Choudhury et al., 1997). The so called “amyloidoses” or prion diseases, which involve aberrant deposition of proteins in the form of amyloid fibrils or plaques, are encounter in both, humans (variant Creutzfeldt-Jakob disease, Alzheimer disease) and animals (bovine or sheep spongiform encephalopathies) (Dobson, 1999; Selkoe, 2002).

1.2 Molecular chaperones

The terminology “molecular chaperones” describes a class of ubiquitary and highly conserved proteins that facilitate protein folding. Molecular chaperones interact with nascent and translocating polypeptides to stabilize them and prevent them from undergoing nonproductive reaction such as aggregation (Figure 1-1). Chaperones participate in folding of other proteins without being a component of the final structure (Ellis and van der Vies, 1991). Although present in all organisms and organelles, the number and the type of chaperones are variable and connected to the complexity of the organism (Pahl et al., 1997).

The level of molecular chaperone expression in the cell is highly stimulated during stress conditions, e.g. heat shock. Therefore the term “heat shock proteins” (Hsp) is also currently used to describe those molecules (Pelham, 1986). However, this description is inappropriate because molecular chaperones are also produced under normal growth conditions (Georgopoulos and Welch, 1993). These constitutively expressed chaperones are known as “Heat shock cognates” (Hsc). Molecular chaperones have been classified function of their molecular weight in small Hsps, Hsp60, Hsp70, Hsp90 and Hsp100.

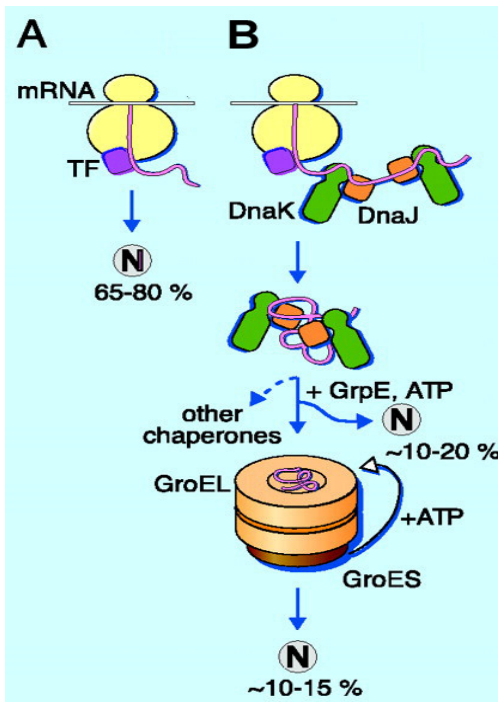


Figure 1-1: Model for the folding of newly synthesized polypeptides in the eubacterial cytosol (Hartl and Hayer-Hartl, 2002). (A) *Unassisted folding.* Nascent chains emerging from the ribosome probably interact generally with trigger factor (TF), a ribosome-associated chaperone found at the polypeptide exit tunnel. Most small uni-domain proteins fold rapidly upon synthesis without additional assistance. (B) *Folding assisted by chaperones.* Another fraction of newly synthesized chains, representing usually larger or multi-domain proteins, require the assistance of DnaK/DnaJ chaperones for their folding. These chaperones are able to bind the polypeptide chain while still bound on ribosome, but also after its release. About 10-15 % of partially folded chains are subsequently interacting with GroEL/GroES system.

The classical molecular chaperones increase the yield of the refolding reaction without affecting the refolding rate, except for protein disulfideisomerases and peptidyl prolyl cis/trans isomerases, two classes of chaperones that stimulate the rate limiting steps of refolding (Freedman et al., 1995; Schmid, 2001). Although different in shape and dimension, chaperones seem to bind their substrates following the same principle: they recognize and bind non-covalently hydrophobic residues and/or unstructured backbone regions in their substrates. These are features typically exposed by nonnative proteins but normally buried within a correctly folded structure. Thus, the association of several segments of different polypeptides, which would otherwise lead to aggregation, is prevented (Ellis, 1994a; Hayer-Hartl et al., 1995). This buffering activity of chaperones is called “holder” function and can be exerted independent of ATP. Refolding into the active three-dimensional structure requires the “folder” function, which is an ATP-dependent process (Mogk et al., 2002).

Numerous evidences have shown that several mechanistically distinct chaperones are cooperating in protein folding (Frydman et al., 1994; Deuerling et al., 1999; Teter et al., 1999). In this manner molecular chaperones are mediating not only the folding of newly synthesized polypeptides or damaged proteins but they are also involved in protein

transport through membranes (Ryan et al., 1997; Ryan and Pfanner, 2001) or in regulation of signal transduction (Buchner, 1999; Pearl and Prodromou, 2001).

Chaperone systems are also cooperating with the protein degradation machinery. When substrate proteins cannot be recovered by the chaperone systems they are recognized and degraded by specialized proteases (Gottesman et al., 1997; Maurizi, 2002).

1.2.1 Hsp100/Clp family

The Hsp100 or Clp (caseinolytic protease) chaperone family is found in all prokaryotes and some eukaryotic organisms. This family comprises several homologous ATPases involved in various processes in the cell including thermotolerance (Sanchez and Lindquist, 1990), proteolysis (Wickner et al., 1994) and regulation of transcription (Schirmer et al., 1996). They are able to disassemble large protein structures and dissolve protein aggregates (Glover and Lindquist, 1998; Zolkiewski, 1999) and they cooperate with other chaperone systems in protein folding (Diamant et al., 2000; Ben Zvi and Goloubinoff, 2001). The best characterized Hsp100 family members are the *E. coli* homologues Clp-ATPases ClpA (Gottesman et al., 1990), ClpB (Squires et al., 1991), ClpX (Gottesman et al., 1993) and ClpY (HslU) (Chuang et al., 1993; Rohrwild et al., 1997). The Hsp100/Clp chaperones are classified according to the number of nucleotide binding domains (NBD). Class one proteins contain two nucleotide binding sites (ClpA and ClpB from *E. coli*, Hsp104 from *S. cerevisiae*), whereas class two members contain only one nucleotide binding site (ClpY from *E. coli*). In ClpB and Hsp104, ATP hydrolysis at both NBDs was shown to be necessary for the chaperone activity of the Clp proteins (Parsell et al., 1994; Schlee et al., 2001). Gel filtration experiments, electron microscopy and later on the crystal structure have shown that Hsp100/Clp proteins build ring-shaped hexameric structures in the presence of ATP (Parsell et al., 1994; Kim et al., 2000).

ClpB and Hsp104 chaperones cooperate functionally with the Hsp70/DnaK system in protein disaggregation (Glover and Lindquist, 1998; Mogk et al., 1999; Zolkiewski, 1999). This collaboration is very important especially at elevated temperature, e.g. heat shock, when the amount of denatured proteins can lead to the formation of large aggregates and further to death. The reactivation of protein aggregates cannot be accomplished by ClpB/Hsp104 alone, but in collaboration with Hsp70/DnaK system. In the first phase of the disaggregation, both chaperone systems cooperate and modify the aggregates in a manner that enable them to be reactivated only by the DnaK system in the second phase of the process (Goloubinoff et al., 1999; Ben Zvi and Goloubinoff, 2001). The mechanism of ClpB and DnaK cooperation is not yet understood. Recently, a physical interaction between ClpB and DnaK was observed for the *T. thermophilus* homologues under conditions that stabilize a high-order oligomeric state of ClpB (Schlee et al., 2004).

1.2.2 Hsp60 or chaperonins

Hsp60 chaperones, known also as chaperonins, are classified in two groups: the GroEL family found in prokaryotes and organelles, and the TriC family which is found in the cytosol of archaeobacteria and eukaryotes (Frydman et al., 1992; Cowan and Lewis, 2001).

The most intensively studied chaperonin is the GroEL homologue from *E. coli*. GroEL forms together with the Hsp10-homologue GroES a large complex of ca 1000 kDa (Goloubinoff et al., 1989; Xu et al., 1997). Structurally, a GroEL molecule is constructed from two rings (*cis* ring and *trans* ring) comprising seven identical monomers that assemble into a cylindrical structure (Figure 1-2). Each monomer consists of two discrete domains (apical and equatorial) joined by a hinge-like intermediate domain (Braig et al., 1994). The equatorial domains contain the ATP-binding pocket, whereas the apical domains contain a patch of hydrophobic amino acids exposed at the interior of the cavity. These hydrophobic residues bind the unfolded substrate polypeptide through hydrophobic contacts (Chen et al., 1994; Xu et al., 1997; Chen and Sigler, 1999).

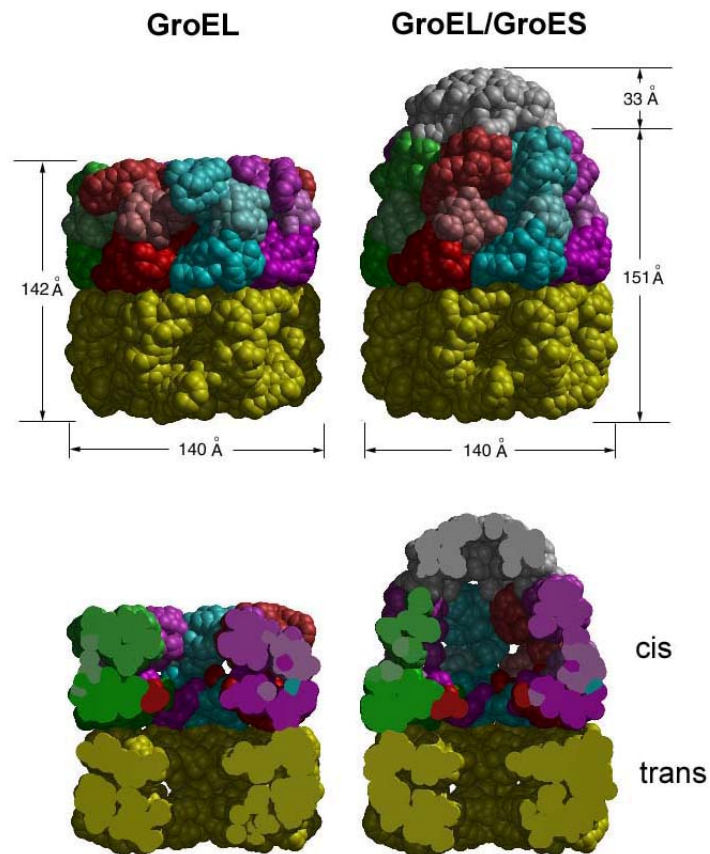


Figure 1-2: Overall architecture and dimensions of GroEL and GroEL/GroES-(ADP), represented by van-der-Waals space-filling models (Sigler et al., 1998). Upper panels show the outside views, while the lower ones show the insides of the assemblies. Various colors are used to distinguish the subunits of GroEL in the *cis* ring. The domains are indicated by shading (equatorial is dark blue, apical is medium hue and intermediate domain is light hue). The *trans* GroEL ring is colored in yellow. GroES is uniformly gray.

A ring of seven molecules of GroES can bind on both sides of the GroEL₁₄ cylinder (Hunt et al., 1996; Roseman et al., 1996; Saibil et al., 2001). The binding of ATP to a GroEL *cis* ring (the ring associated with GroES and the folding polypeptide) is cooperative and has a negative cooperative effect on the ATP binding on the *trans* ring (Yifrach and Horovitz, 1994; Horovitz et al., 2001). The binding of the GroES₇ to the *cis* ring stimulates the cooperativity of ATP hydrolysis at this level (Gray and Fersht, 1991; Todd et al., 1994) and impairs the binding of a second GroES₇ to the opposite *trans* ring. Thus, the two rings do not occur in the same nucleotide-bound state. The GroES₇·ADP₇·GroEL₇/GroEL₇ complex is considered to be the “acceptor form” of GroE that is able to bind polypeptides (Weissman et al., 1995).

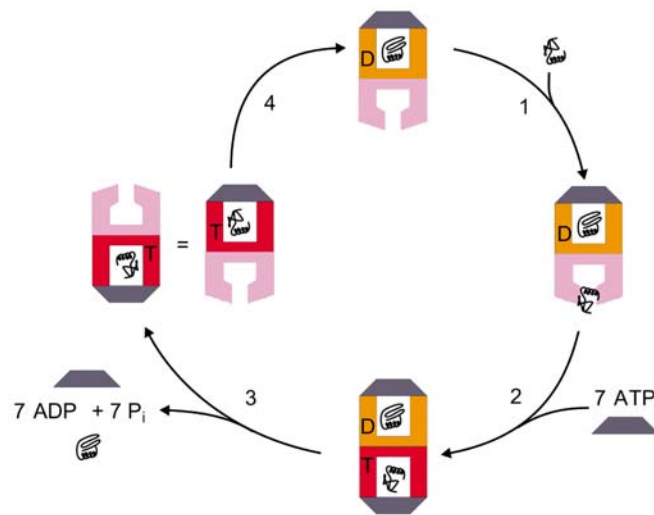


Figure 1-3: GroEL/GroES chaperone cycle (Walter and Buchner, 2002). Here, both rings are active at the same time, but they are in different phases of the cycle. In a first step of the cycle (1) a hydrophobic polypeptide is prevented from aggregation by binding to the nucleotide-free *trans* ring (lilac) of GroEL. Binding of GroES (gray) and ATP₇ (T) to this ring (step 2) induces structural changes in GroEL (red ring) leading to the polypeptide release and folding into the closed cavity of GroEL. The binding of ATP to this ring (red) induces the release of GroES, ADP (D) and polypeptide (step 3) from the opposite ring (orange). Subsequent hydrolysis of ATP (step 4) induces a second conformational change in GroEL (top ring, orange), which allows the *trans* ring (bottom ring, lilac) to bind polypeptide and start a new cycle. Note: the orientation of the GroEL molecule is reversed after step 3 (i.e. the polypeptide does not “move” to the top ring as shown).

In a chaperone cycle (Figure 1-3), in the presence of ATP, GroES binds to this GroEL ring and induces a conformational change in the apical domains that displaces the substrate from its binding sites. The substrate is thus released and locked into the central cavity (Mayhew et al., 1996), which is now covered with hydrophilic side chains (Roseman et al., 1996). It was proposed that the enclosed cavity functions like an “Anfinsen-cage” where the substrate is allowed to refold in a protective environment according to its thermodynamic potential (Ellis, 1994b). The binding of GroES and ATP to the *cis* ring leads to a decrease in the affinity of the *trans* ring for ADP and GroES resulting in their dissociation from GroEL (Todd et al., 1993; Hayer-Hartl et al., 1995). A

refolding cycle takes ca. 10 s, timed by the ATP hydrolysis in the *cis* ring (Rye et al., 1997). Upon completion of hydrolysis, binding of seven ATP molecules to the *trans* ring triggers the opening of the *cis* ring cage. After the refolding cycle, the released substrate might be fully folded or it might be found in an intermediate folding state. To gain its native state, it might fold further free in the solution, it might rebind to the GroEL for another refolding cycle or might be recruited by other chaperone machineries.

Although GroEL/GroES chaperone system is essential for the viability of *E. coli* (Fayet et al., 1989), protein refolding in the GroEL chamber is limited to proteins smaller than 60 kDa (Sakikawa et al., 1999). About 10-15% of newly synthesized polypeptides are dependent on the GroEL assisted folding in *E. coli* (Ewalt et al., 1997; Houry et al., 1999).

1.2.3 Hsp70/DnaK family

Hsp70s form a highly conserved family of proteins, distributed ubiquitously in all prokaryotes and in cellular compartments of eukaryotic organisms. Some cell compartments contain multiple Hsp70 homologs with distinct cellular functions. Hsp70s are involved in various processes including the co-translational stabilization of the newly synthesized polypeptide (Deuerling et al., 1999), protein translocation through the organelles (Pfanner et al., 1997) disassembly of protein oligomers (Zylicz et al., 1989), cell cycle and apoptosis (Hohfeld and Jentsch, 1997; Zeiner et al., 1997) and dissociation of protein aggregates (Sherman and Goldberg, 1996).

The structural and mechanistic aspects of the Hsp70 system are best understood for the eubacterial Hsp70, termed DnaK (Mayer et al., 2001). Hsp70 chaperones consist of two functionally coupled domains, which have been crystallized separately (Figure 1-4). The highly conserved 44 kDa N-terminal domain mediates ATP binding (Flaherty et al., 1990), whereas the 27 kDa C-terminal domain binds the substrates (Zhu et al., 1996; Bukau and Horwich, 1998). A structure of the entire Hsp70 molecule which could offer structural insights into the coupling between nucleotide-DnaK interaction and substrate binding and release is not available until present.

In contrast to the GroEL/GroES system, DnaK does not bind the entire substrate but is able to recognize and bind peptides of about seven residues that are typically hydrophobic in their central region, with leucine and isoleucine residues being preferred by DnaK (Hartl, 1996; Rudiger et al., 1997). Because of its hydrophobic nature, this binding motif would typically be located in the interior of a correctly folded protein. The peptides are bound to DnaK in an extended state through hydrophobic side-chain interactions and hydrogen bonds with the peptide backbone (Zhu et al., 1996) (Figure 1-4B). These binding sites occur statistically every ca. 40 residues in proteins and are recognized with affinities of 5 nM to 5 μ M (Bukau and Horwich, 1998). Similarly to the GroEL/GroES chaperone machinery, DnaK-assisted protein folding requires repeated cycles of binding and release

(Szabo et al., 1994; Buchberger et al., 1996), frequently at a stoichiometry of a single DnaK monomer per substrate molecule (Bukau and Horwich, 1998).

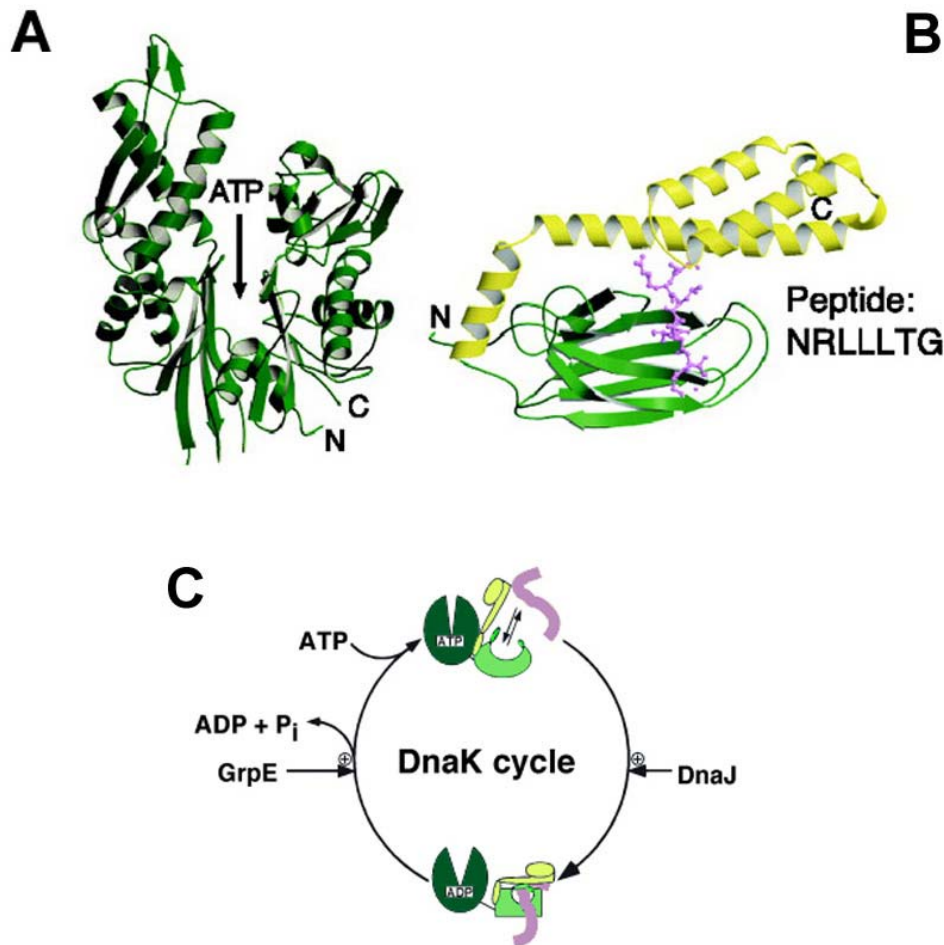


Figure 1-4: The structure of DnaK and model for the DnaK cycle. (A) Structure of the ATPase domain of DnaK from *E. coli*. ATP indicates the position of the nucleotide binding site. (B) Structure of the peptide-binding domain of DnaK from *E. coli*. The α -helical latch of the peptide binding domain is shown in yellow. The extended peptide substrate is shown in lilac. (C) The model for the DnaK cycle in *E. coli*. In the ATP-bound state the DnaK_{Eco} binds and releases substrates very fast. In the ADP-bound form of DnaK_{Eco} the substrate is locked in the peptide-binding domain. The transition between the low affinity ATP-state and high affinity ADP-state is determined by the ATP-hydrolysis, which occurs through the interaction between the substrate and the co-chaperone DnaJ_{Eco}. The return of DnaK_{Eco} to the ATP-state is regulated by the GrpE_{Eco} co-chaperone. (A) and (B): reproduced after (Hartl and Hayer-Hartl, 2002) and (C) after (Mogk et al., 2002).

The nucleotide state of DnaK determines its substrate binding properties (Buchberger et al., 1995; McCarty et al., 1995). Whereas a rapid but weak peptide binding occurs in the ATP-bound state of DnaK, a slow but tight binding takes place in the ADP-bound form. This change in substrate binding kinetic can be explained by the nucleotide-induced modifications occurring at the level of the substrate binding site. The substrate binding domain of DnaK is formed by two subdomains: a β -sheet comprising region representing the principal substrate binding site and an α -helical region that functions as a latch above the β -sheet subdomain. In the ATP-bound state the α -helical latch over the peptide-binding

cleft is in an open conformation (Figure 1-4C). Stable holding of peptide involves its closing. This conformational change is achieved by hydrolysis of bound ATP to ADP (“locking in” concept (Greene et al., 1995)). Thus, the hydrolysis of ATP is essential for a stable interaction between substrate and DnaK (Buchberger et al., 1995).

The cycling of DnaK between the two different nucleotide states is regulated by its two cochaperones: DnaJ, a member of the Hsp40 family, and GrpE, a nucleotide exchange factor (Liberek et al., 1991; McCarty et al., 1995). DnaJ binds to DnaK and accelerates its ATPase activity (Mayer et al., 2000b; Pellicchia et al., 2000) whereas GrpE induces the release of ADP from DnaK (Harrison et al., 1997).

The Hsp40 homologues are present in almost every cellular compartment populated by Hsp70. DnaJ proteins consist of four domains that are conserved to various degrees among the homologues. The N-terminal 76-amino acid J-domain defines proteins as members of the DnaJ/Hsp40 family and is, thus, present in all members of this family (Hennessy et al., 2000). It contains the conserved tripeptide His-Pro-Asp, which is essential for the DnaJ-DnaK interactions and for the stimulation of the ATPase activity of DnaK (Wall et al., 1994; Greene et al., 1998; Genevaux et al., 2002). Adjacent to the J-domain resides the glycine and phenylalanine-rich G/F domain which, together with the J-domain, is essential for maximal stimulation of the ATPase activity of DnaK (Karzai and McMacken, 1996). The central domain of DnaJ is the zinc-binding cysteine-rich domain, which is followed by a poorly conserved C-terminal (Lu and Cyr, 1998). Since not all DnaJ/Hsp40 homologues contain all four domains, the members of this family are classified according to the number of domains contained. Class I DnaJ homologues contain all domains, class II lack the central cysteine-rich zinc binding domain and class III representatives have only the J-domain in common (Linke et al., 2003).

DnaJ from *E. coli*, a type I homologue, is able to stimulate the ATP-hydrolysis of DnaK at least of 500-fold (Pellicchia et al., 1996; Laufen et al., 1999; Russell et al., 1999). Also, similar to other type I DnaJ homologues, DnaJ_{Eco} has the ability to bind by itself substrates with a rate and substrate specificity similar to the one of DnaK·ATP (Gamer et al., 1992; Rudiger et al., 2001). Besides its DnaK-ATPase stimulating activity, DnaJ_{Eco} can also recruit substrate protein for DnaK_{Eco} (Liberek et al., 1991; Wickner et al., 1991; Langer et al., 1992). Identification of a DnaK-DnaJ complex in *E. coli* was possible only in the presence of ATP (Wawrzynow and Zylicz, 1995).

The GrpE co-chaperone, a homodimer of 20 kDa/monomer, binds to DnaK in a 2:1 ratio and functions as a nucleotide exchange factor (Liberek et al., 1991; Dekker and Pfanner, 1997; Harrison et al., 1997). Structurally, GrpE consists of two domains: a long α -helical structure and a globular β -sheet domain at the C-terminus. The crystal structure of GrpE bound to the ATPase domain of DnaK_{Eco} shows that the most important contact region for the interaction involves the β -sheet domain of GrpE that binds both subdomains forming the nucleotide binding site of DnaK-ATPase domain (Harrison et al., 1997).

The binding of GrpE_{Eco} to DnaK_{Eco}·ADP leads to a 5000-fold stimulation of the nucleotide exchange and reduces the affinity of DnaK_{Eco} for nucleotides with a factor of 200 (Packschies et al., 1997). Since the ATP concentration inside the cell is exceeding the one of ADP, nucleotide-free DnaK_{Eco} is able to rebind ATP. This leads to the dissociation of the DnaK_{Eco}-peptide complex, completing the DnaK chaperone cycle (Figure 1-4C). DnaK_{Eco} can now rebind substrates and a new chaperone cycle might take place.

The cycles of substrate binding and release are fairly short and most likely have to be repeated many times until a protein is refolded and no longer recognized as a substrate. However, the mechanism of DnaK-assisted refolding is not yet clarified. According to one hypothesis DnaK unfolds the substrate locally in contrast to the global unfolding by GroEL (Mayer et al., 2000a).

In contrast to the GroEL/GroES system, substrate binding by the DnaK system is not constrained by the substrate molecular weight. *In vivo* experiments in *E. coli* have shown that proteins larger than 60 kDa, which do not fit into the central cavity of the GroEL, constitute an appreciable fraction of DnaK substrates suggesting that folding of large multidomain proteins is more dependent on DnaK chaperone action (Mogk et al., 1999; Deuerling et al., 1999).

The DnaK chaperone system from *Thermus thermophilus*

The DnaK chaperone system was also identified in the eubacterium *Thermus thermophilus*, an organism that normally grows at temperatures ranging between 40 to 85°C (Motohashi et al., 1994; Osipiuk and Joachimiak, 1997). The organization of the *dnaK*_{Th} operon is substantially different from the one of *E. coli*. Whereas in *E. coli* the *dnaK* operon comprises only *dnaK* and *dnaJ* genes, in *T. thermophilus* the genes encoding for DnaK, DnaJ and GrpE are controlled by the same promoter. In addition, the thermophilic *dnaK* operon comprises the gene encoding for the ClpB chaperone and for a small protein of unknown function named DafA (Motohashi et al., 1996). The arrangement of the genes in this operon is following the sequence: *dnaK-grpE-dnaJ-dafA-clpB*. The promoter of the *dnaK*_{Th} operon shows similarities with the σ^{32} -depending heat shock promoter of *E. coli* and it is believed therefore that expression of the genes comprised in *dnaK*_{Th} operon is controlled by a similar mechanism (Osipiuk and Joachimiak, 1997).

DnaK_{Th}, DnaJ_{Th} and GrpE_{Th} share with their counterparts from *E. coli* a sequence identity of 56 %, 43 % and 27 % respectively. Also, ClpB_{Th} shows high homology with ClpB_{Eco} (56 %). The product of *dafA* gene is the only member of the DnaK_{Th} system for which no homologues were yet identified (Motohashi et al., 1996; Klostermeier, 1998).

When compared to the *E. coli* system, the DnaK chaperone system from *T. thermophilus* shows similar features but also important differences (Schlee and Reinstein, 2002). Despite the high degree of homology, the thermophilic chaperones possess increase thermostability when compared to their mesophilic counterparts

(Klostermeier et al., 1998; Groemping and Reinstein, 2001). This supports the idea that thermostability can be achieved by only subtle structural changes (Jaenicke, 1996).

A characteristic feature of DnaK_{Tth} is its co-existence with its co-chaperone DnaJ_{Tth} as a highly stable complex that can be isolated from *Thermus* cells (Motohashi et al., 1994). It was only later discovered that for a stable association of the DnaK_{Tth} and DnaJ_{Tth} DafA_{Tth} protein is indispensable (**D**naJ-**D**naJ **A**ssembly **F**actor **A**) (Motohashi et al., 1996). This ternary complex comprises three copies of each protein species and could be visualized with the help of electron microscopy (Motohashi et al., 1994). The complex is shaped as a trigonal particle of ca. 11 nm in length with a ca 3 nm wide cavity. The formation of this heterotrimeric complex seems to occur in a highly synergic manner since binary complexes of DnaK_{Tth} and DnaJ_{Tth} or DafA_{Tth} are not detectable (Klostermeier et al., 1999).

Similar to DnaK_{Eco}, DnaK_{Tth} is also able to recognize and bind hydrophobic patches of polypeptides and its substrate binding properties are regulated as well by the nucleotide state (Klostermeier et al., 1999). The binding and releasing of nucleotide is very slow at 25°C compared to *E. coli* and a temperature shift of 50°C stimulates the nucleotide on/off rates only with a factor of three (Klostermeier et al., 1999). ATP-hydrolysis by DnaK_{Tth} is, in the unstimulated DnaK_{Tth} cycle, in the same range as for DnaK_{Eco} (Theysen et al., 1996). Therefore, whereas for *E. coli* DnaK the rate limiting step is the ATP hydrolysis, in *T. thermophilus* the nucleotide binding and release represent the rate-limiting steps in the absence of cofactors.

DnaK_{Tth} accomplishes its chaperone activity accompanied by the two co-chaperones DnaJ_{Tth} and GrpE_{Tth} similar to the system from *E. coli*. However, significant differences regarding the regulation of the DnaK chaperone cycle by these co-factors have been reported (Klostermeier et al., 1999; Groemping et al., 2001).

DnaJ_{Tth}, a member of class II Hsp40/DnaJ family, does not possess the zinc-finger domain considered to be important for the substrate binding (Banecki et al., 1996). In contrast to DnaJ_{Eco}, DnaJ_{Tth} does not stimulate the ATPase activity of DnaK_{Tth} either in the absence or in the presence of peptide substrates. It is also unable to bind peptides by itself (Klostermeier et al., 1999). However, substoichiometric concentrations of DnaJ_{Tth} are necessary for DnaK_{Tth} chaperone activity (Groemping et al., 2001).

In contrast to DnaJ_{Tth}, GrpE_{Tth} stimulates the ADP release from DnaK_{Tth}·ADP complex by a factor of 80000 (Groemping et al., 2001) and is therefore much more effective than the GrpE_{Eco} (5000-fold stimulation). Thus, the DnaK_{Tth} cycle nucleotide regulation seems to be exclusively under the control of GrpE_{Tth} since DnaJ_{Tth} does not appear to exert any regulatory role at this level (Groemping et al., 2001).

Similar to *E. coli*, substrate binding to DnaK_{Tth} is coupled to the nucleotide state of DnaK_{Tth}. At 25°C in the ATP-form DnaK_{Tth} binds and releases substrates very fast, whereas in the ADP-form the substrates are bound or released slowly. In the presence of

GrpE_{Th} and ATP the rates are increased with a factor of 30 for the binding and of 50 for the release (Klostermeier et al., 1998). The binding and releasing of peptide substrates to DnaK_{Th} is strongly influenced by temperature. A shift of temperature from 25°C to 75°C leads to a 200-300-fold stimulation of the on/off rates (Klostermeier et al., 1998). Under these conditions, ATP has no additional influence.

As mentioned before, DafA_{Th} represents a mandatory element required for stabilization of the DnaK_{Th}-DnaJ_{Th} complex (Motohashi et al., 1996). This 8.7 kDa protein is the only member of DnaK_{Th} chaperone system with no correspondent homologue in other organisms. It was speculated that a protein with a similar function in mediating DnaK-DnaJ interaction may exist in other organisms as well. Evidences that could confirm this suggestion are, at least until present, not available. The amino acid sequence of DAF_{Th} shares no significant homology with any other protein found in the current databases. Moreover, the high degree of sequence homology between DnaK, DnaJ and GrpE from *T. thermophilus* and their counterparts from the moderately thermophilic *Meiothermus ruber* (81,96 % for DnaK, 58 % for DnaJ and 49,72 % for GrpE) does not imply the existence of a corresponding DafA homologue. DnaK and DnaJ from *M. ruber* associate into a stable complex in an ATPdependent manner without the help of an accessory protein (Pleckaityte et al., 2003). In comparison, the assembly of DnaK-DnaJ-DafA complex in *T. thermophilus* is a nucleotide-independent process (Klostermeier et al., 1999).

Except for its mediating role in the formation of DnaK_{Th}-DnaJ_{Th}-DafA_{Th} complex, little is known about the specific function of DafA_{Th}. Studies with fluorescent peptides indicated that, in the presence of DnaJ_{Th}, DafA_{Th} is interfering with substrate binding to DnaK_{Th} (Klostermeier et al., 1999). Also, substrate already bound to DnaK_{Th} is replaced by DafA_{Th} in the presence of DnaJ_{Th}. From these studies, Klostermeier et al. drew the conclusion that DafA_{Th} and DnaJ_{Th} compete with the substrate for the binding site on DnaK_{Th} and that the DnaK_{Th}-DnaJ_{Th}-DafA_{Th} isolated cannot represent the active species in DnaK_{Th} chaperone cycle. Consequently, a model describing the DnaK_{Th} chaperone cycle and its regulation by co-chaperones was proposed (Klostermeier et al., 1999). According to this model (Figure 1-5) DnaK₃-DnaJ₃-DafA₃ complex represents the inactive chaperone species cycling slowly between the ATP- and ADP-bound forms of DnaK_{Th} and being activated only at high concentrations of substrates produced under stress condition (e.g. heat shock) which displace DafA_{Th}. After ATP-hydrolysis the substrates can only dissociate slowly from the complex formed with DnaK_{Th} and DnaJ_{Th}. Only after the GrpE_{Th} stimulated ADP-dissociation DnaK_{Th} rebind ATP and the substrate is released. The cycle may be repeated through rebinding of substrates or may switch off by rebinding DafA_{Th}.

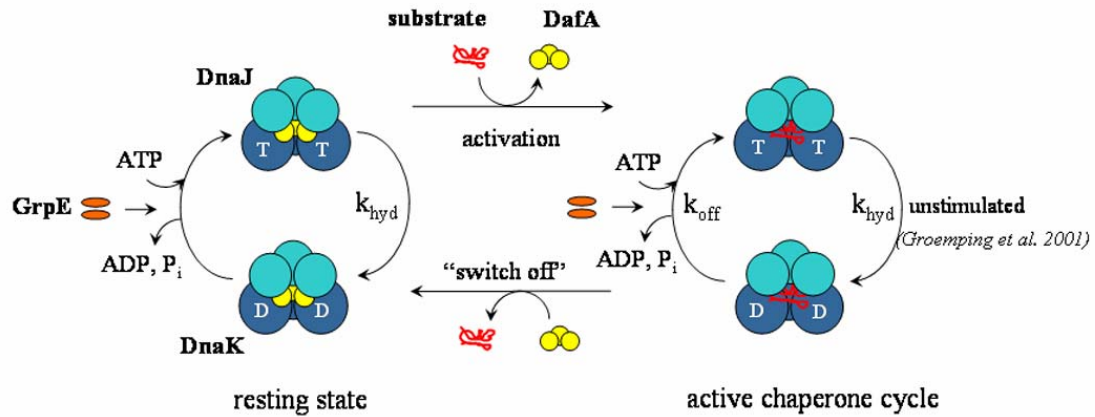


Figure 1-5: The model for the regulated cycle of DnaK_{Tth} (adapted from Klostermeier et al., 1999). DnaK₃-DnaJ₃-DafA₃ complex represents the resting state of the chaperone system. At high concentration of substrate, DafA_{Tth} is replaced by denatured protein and the system is activated. In the active chaperone cycle, DnaK·ATP scans rapidly substrate through fast binding and release, whereas DnaK·ADP binds substrate tightly and with low exchange rates. As Groemping et al. (2001) showed the ATPase activity of DnaK_{Tth} is not stimulated by DnaJ_{Tth} in contrast to other DnaK systems. ATP rebinding to DnaK_{Tth} is mediated by GrpE_{Tth} and leads to substrate release. The cycle may continue with another round of substrate binding or is switched off by rebinding DafA_{Tth}.

1.3 Aims

The main aim of this work is to characterize DafA_{Tth} from the biochemical and functional point of view. This study should be applied to free DafA_{Tth} as well as to DafA_{Tth} found in association with its two partners, DnaK_{Tth} and DnaJ_{Tth}.

In a first step, efforts should be made in order to enhance the stability of DafA_{Tth} produced in *E. coli* as DafA(L2V)_{Tth}, since this protein is prone to aggregation. At the same time, conditions that assure higher protein purity, a necessary condition for a reliable DafA_{Tth} characterization, have to be found. In parallel with the biochemical analysis the structural properties of DafA_{Tth} represent an important issue of this work. With its 8.7 kDa molecular weight as a monomer, DafA_{Tth} is a good candidate for structure determination using NMR-spectroscopy.

The enhanced stability of the DnaK_{Tth}-DnaJ_{Tth}-DafA_{Tth} complex observed in various experiments resides in a high affinity existent between the three protein species. Thermodynamic experiments following the formation of the complex have given an apparent dissociation constant of 10-40 nM (Klostermeier et al., 1999). Since these values do not represent the true K_D for the complex association, measurements that allow a more accurate determination have to be performed. In this respect, insertion of a cysteine residue in otherwise cysteine deficient DafA_{Tth} by replacing a defined amino acid would be the first step. The subsequent labeling of the cysteine mutant (-s) with fluorescent dyes would permit the analysis of the ternary complex formation via fluorescence spectroscopy. In this

manner, the rates constant characterizing the complex association and dissociation might be also determined.

An interesting aspect of the DnaK_{Th} chaperone cycle is the inhibition of peptide binding to DnaK_{Th} induced by DafA(L2V)_{Th} (Klostermeier et al., 1999). This finding has led to the hypothesis that DafA_{Th} and the substrate are competing for the same binding sites on DnaK_{Th} and therefore DnaK_{Th}-DnaJ_{Th}-DafA_{Th} complex cannot represent the active chaperone specie (see Figure 1-5). Here it should be tested whether this assumption is also valid when substrate proteins are used instead of model peptides.

Considering the model proposed by Klostermeier et al. for the DnaK_{Th} chaperon cycle, DafA has to be replaced by the denatured substrate from DnaK_{Th}-DnaJ_{Th}-DafA_{Th} complex. On the other side, once the refolding activity of DnaK_{Th}-DnaJ_{Th} is not needed anymore, DafA_{Th} has to rebind to inactivate the cycle. Naturally, the question “What is happening to DafA_{Th} between these two events?” is arising. To answer this question, functional analyses should be carried out. In this context, new potential interaction partners of DafA_{Th} have to be identified. Since DafA_{Th} might be the key element in DnaK_{Th} cycle regulation under stress conditions, this search will involve a repertoire of potential candidates representing important regulatory sites in the cell.

Another line of experiments will be concentrated on the ability of thermophilic DnaK and ClpB chaperone systems to collaborate in reactivation of protein aggregates in the absence of DafA(L2V)_{Th}. It was shown previously (Groemping Y., 2000) that the presence of ClpB_{Th} in refolding assays together with DnaK_{Th} system leads to the stimulation of both rate and the yield of reactivation. Thermophilic systems present an advantage relative to their mesophilic counterparts that resides in their enhanced thermostability. From the biotechnological point of view this advantage can be seen as a huge potential for the reactivation of various proteins obtained in an inactive form in *E. coli* expression systems. Of a particular interest is the *in vivo* reactivation of such problematic proteins. This would imply however the co-expression of the two chaperone systems. Therefore, conditions that will allow for aggregate reactivation using co-expressed DnaK_{Th} and ClpB_{Th} systems should be first established *in vitro*. In a further step, the *in vitro* conditions should be adapted for *in vivo* procedures.

2 MATERIALS AND METHODS

2.1 Materials

2.1.1 Chemicals

The chemicals used and the corresponding suppliers are presented in Table 2-1.

Table 2-1: Chemicals and their suppliers

Supplier	Chemical
Amersham	ECF-Western blotting Reagent, Protein G Sepharose 4 Fast Flow, Low Molecular Weight Calibration Kit for SDS Electrophoresis
AppliChem (Darmstadt)	30% Acrylamid 4K-solution, (NH ₄) ₂ SO ₄
Calbiochem (Darmstadt)	NDSB-256
J.T.Baker (Deventer, NL)	Ethanol, Acetic acid, HCl, HClO ₄ , Isopropanol, K ₂ HPO ₄ , KH ₂ PO ₄ , MgCl ₂ , NaCl, NaOH, Na ₂ SO ₄ , Urea
BioGenes (Berlin)	Anti-DafA(L2V) antibodies
BioRad (München)	Agarose, Polypeptide SDS-PAGE Molecular Weight Standards, PVDF membrane
Fluka (Neu-Ulm)	TCA, DMSO, Brij58
Gerbu (Gailberg)	Boric acid, DTE, EDTA, GdmCl, Glycerol, HEPES, IPTG, Kanamycin, MOPS
GibcoBRL (Karlsruhe)	Agar, Yeast extract, Peptone
Hampton Research (CA, USA)	NDSB-195, -201
Molecular Probes (via MoBiTec in Göttingen)	Fluorophores (IANBD-ester, IAEDANS I-14, Alexa488-Maleinimide), Luciferin
New England Biolabs (Schwalbach)	1 kb DNA-Ladder
Promega (Mannheim)	RNasin Ribonuclease Inhibitor
Roche Diagnostics (Mannheim)	Protease Inhibitor, Western Blotting Blocking Reagent,
Roth (Karlsruhe)	Glycin, Tris, Rotiphorese Gel 40 (19:1)
Serva (Heidelberg)	APS, Bromphenolblue, Coomassie blue-R250/G250, SDS, TEMED, Xylencyanol
Sigma-Aldrich (Taufkirchen)	AlO ₃ beads, ATP, Betaine, BSA, CHAPS, DEPC, Ethidiumbromide, 2-Mercaptoethanol, PMSF, para-Nitrophenylglucoside, Sucrose, Tricine, tRNA yeast

2.1.2 Enzymes

Alcaline Phosphatase	Roche (Mannheim)
Firefly luciferase	Promega (Madison, USA)
DNase I, RNase I	Roche (Mannheim)
Dpn I	Stratagene (Amsterdam, Holland)

Pfu-Turbo-DNA-Polymerase	New England Biolabs (Schwalbach)
Polynucleotide Kinase A	New England Biolabs (Schwalbach)

2.1.3 Reagent kits

QIAprep Spin Miniprep Kit	Quiagen (Hilden)
QuikChange Site Directed Mutagenesis Kit	Stratagene (Amsterdam, Holland) (Braman et al., 1996)
BigDye Terminator Cycle Sequencing Kit	Applied Biosystems (Langen)
DyeEx Spin Kit	Quiagen (Hilden)

2.1.4 Chromatography material

EMD-DEAE Sepharose	Merck (Darmstadt)
Superdex S-200	Amersham-Pharmacia (Freiburg)
ProbeQuant G50 Micro-columns	Amersham-Pharmacia (Freiburg)
MonoQ	Amersham-Pharmacia (Freiburg)
NAP-5, PD-10	Amersham-Pharmacia (Freiburg)
TLC plate Polygram Cel 300 PEI/UV254	Macherey-Nagel (Düren)

2.1.5 Microorganisms

<i>E. coli</i> TG-1	K12, supE, hsd Δ 5, thi, Δ (lac-proAB), F'[traD36, proAB ⁺ , lacI ^q , lacZ Δ M15] (Gibson, 1984)
<i>E. coli</i> XL-1 Blue	recA1, endA1, gyrA96, thi-1, hsdR17, supE44, relA1, lac [F'proAB lacI ^q Z Δ M15 Tn10]
<i>E. coli</i> BL21 (DE3)	B, F ⁻ , hsdS _B (r _B ⁻ , m _B ⁻), gal, dcm, ompT, λ (DE3) (Studier und Moffatt, 1986)
<i>Thermus thermophilus</i> HB 8	Wild type <i>T.thermophilus</i> strain non-transformable (ex Oshima and Imahori, 1974) (Manaia et al., 1995)
<i>Thermus thermophilus</i> HB 27	Wild type <i>T.thermophilus</i> strain transformable (ex Oshima and Imahori, 1974) (Manaia et al., 1995)

2.1.6 Vectors and PCR-primers

pET-27 derivates (Novagen, Schwalbach)	pRS-DafA(L2V) _{Tth} , pRS-DnaK _{Tth} •DnaJ _{Tth} •DafA(L2V) _{Tth} complex
ptac	Δ DafA-genomic DnaK _{Tth} -ClpB _{Tth} system

pET-41a (Novagen, Schwalbach) pET-GST-DafA(L2V)_{Tth}
 pETM-60 (EMBL, Heidelberg) pETM-60-NusA-DafA_{Tth}(L2V)

The pRS and ptac constructs were kindly provided by Dr. Ralf Seidel. The pET-GST-DafA(L2V)_{Tth} and pETM-60-NusA-DafA_{Tth}(L2V) constructs were produced and kindly provided by Sabine Zimmermann (MPI for Medical Research, Heidelberg).

The overexpression of the *T. thermophilus* chaperones in *E. coli* BL21 (DE3) strain is under the control of a T7-Polymerase-dependent promoter that precedes the lac-operator sequence. The defective prophage DE3 contains the gene for T7-Polymerase whose transcription is controlled by the IPTG-inducible *lacUV5*-promoter. Addition of IPTG to the cell culture derepresses the T7-Polymerase transcription and induces the expression of the *T. thermophilus* proteins.

The various point mutants of DafA(L2V)_{Tth} were constructed using the QuikChange Site Directed Mutagenesis Kit. The primers were obtained from firma MWG-Biotech (Ebersberg) and are shown in Table 2-2. Wild type DafA_{Tth} was engineered by inserting a second Methionine at the N-terminus and replacing the following Valine with a Leucine residue.

Table 2-2: Primer sequences

Mutant	Primer	Sequence
DafA(L2V)-W7C	DafA(L2V)W7C for	5' -GTC GCG CGT AGC GGT TGC CTT TCC CTC GAG GCC-3'
	DafA(L2V)W7C rev	5' -GGC CTC GAG GGA AAG GCA ACC GCT ACG CGC GAC-3'
DafA(L2V)-S14C	DafA(L2V)S14C for	5' -C CTC GAG GCC CTC TGC GAG TAC GGC CTT TCC-3'
	DafA(L2V)S14C rev	5' -GGA AAG GCC GTA CTC GCA GAG GGC CTC GAG G-3'
DafA(L2V)-V27C	DafA(L2V)V27C for	5' -GCC GTG CGG GCC TAC TGC GAG ATC GGC TTC GTG G-3'
	DafA(L2V)V27C rev	5' -C CAC GAA GCC GAT CTC GCA GTA GGC CCG CAC GGC-3'
DafA(L2V)-F31C	DafA(L2V)F31C for	5' -GCC TAC GTG GAG ATC GGC TGC GTG GAG CCT TTG G-3'
	DafA(L2V)F31C rev	5' -C CAA AGG CTC CAC GCA GCC GAT CTC CAC GTA GGC-3'
DafA(L2V)-W41C	DafA(L2V)W41C for	5' -G GAG GTG GGC GGG GCC TGC TAC TTC CGG GAG GAG G-3'
	DafA(L2V)W41C rev	5' -C CTC CTC CCG GAA GTA GCA GGC CCC GCC CAC CTC C-3'
DafA(L2V)-M51C	DafA(L2V)M51C for	5' -G GAG GAC CTC CTG AGG TGC GCC AAG GCC GAA CGC-3'
	DafA(L2V)M51C rev	5' -GCG TTC GGC CTT GGC GCA CCT CAG GAG GTC CTC C-3'
DafA(L2V)-A69C	DafA(L2V)A69C for	5' -CC AAC CTC ATC GGG GCG TGC CTC GTC GTC GAG ATC C-3'
	DafA(L2V)A69C rev	5' -G GAT CTC CAC CAC CAG GCA CGC CCC GAT GAG GTT GG-3'
DafA(wt)	DafA(wt) for	5' -GA AGG AGA TAT ACC ATG ATG CTG GCG CGT AGC GGT TGG-3'
	DafA(wt) rev	5' -CCA ACC GCT ACG CGC CAG CAT CAT GGT ATA TCT CCT TC-3'
All mutants	T7-Promoter	5' -TTA ATA CGA CTC ACT ATA GGG GAA-3'
All mutants	T7-Terminator	5' -CTA GTT ATT GCT CAG CGG TGG C-3'

Bold letters = codon encoding for the inserted or muted amino acid

2.1.7 Media

2-TY Medium

16 g/l Peptone-140, 10 g/l yeast extract, 5 g/l NaCl, pH 7.2

Luria Bertani (LB) Medium

10 g/l Bactotryptone, 5 g/l yeast extract, 10 g/l NaCl, pH 7.0

TSS Medium

50 mM MgCl₂, 5 % DMSO, 10 % PEG 8000 in LB Medium, pH 6.5 (not adjusted)

Minimal Medium for *E.coli*

Na ₂ HPO ₄	7.5 g	<i>10 x SL4:</i>	
K ₂ HPO ₄	3 g	EDTA	0.5 g
NaCl	0.5 g	FeSO ₄ •7H ₂ O	0.2 g
MgSO ₄ •7H ₂ O	0.25 g		
CaCl ₂ •2H ₂ O	0.014 g	<i>SL6:</i>	
Glucose	10 g	MnCl ₂	0.03 g
NH ₄ Cl (or N ¹⁵ H ₄ Cl)	1 g	ZnSO ₄	0.1 g
Trace elements (see below)	10 ml	H ₃ BO ₃	0.3 g
Distilled water	to 1.0 l	CuCl ₂	0.010 g
		Na ₂ MoO ₄	0.025 g
		CoCl ₂ •6H ₂ O	0.2 g
<i>Trace elements:</i>		NiCl ₂	0.020 g
10 x SL4	9 ml	Na ₂ MoO ₄	0.030 g
SL6	10 ml	Distilled water	to 1.0 l
Distilled water	to 100 ml		

T.thermophilus HB8 Medium

8 g/l Peptone-140, 4 g/l yeast extract, 2 g/l NaCl, pH 7.5

T.thermophilus HB27 Medium

4 g/l Peptone-140, 2 g/l yeast extract, 1 g/l NaCl, 1x Castenholz salts, pH 7.5

10x Castenholz Salts:

Nitrilotriacetic acid	1g
Nitsch's Trace Elements (see below)	10 ml
FeCl ₃ solution (0.4%)	10 ml
CaSO ₄ •2H ₂ O	0.6 g
MgSO ₄ •7H ₂ O	1 g
NaCl	0.008 g
KNO ₃	1.03 g
NaNO ₃	6.89 g
Na ₂ HPO ₄	1.11 g
Distilled water	to 1.0 l

Nitsch's Trace Elements:

H ₂ SO ₄	0.5 ml
MnSO ₄	3.16 g
ZnSO ₄	0.5 g
H ₃ BO ₃	0.5 g
CuSO ₄	0.016 g
Na ₂ MoO ₄	0.025 g
CoCl ₂ •6H ₂ O	0.046 g
Distilled water	to 1.0 l

The media were sterilized at 121°C for 20 minutes. For the overexpression of the chaperone proteins in *E. coli* the 2-YT medium was supplemented with 50 µg/ml kanamycine.

2.2 Methods

2.2.1 Methods related to nucleic acids

2.2.1.1 Isolation of plasmid DNA

The isolation of plasmids from *E. coli* cells was performed using the Qiagen Mini- and Midi-Prep Kit following the instructions of the supplier. This isolation technique is based on the alkaline lysis of the cells and precipitation of the proteins with SDS. The plasmid-DNA is then purified from the supernatant *via* anion-exchange chromatography.

2.2.1.2 Agarose gel electrophoresis

DNA fragments were analyzed using horizontal agarose gel electrophoresis. Gels of 0.7-1 % agarose in 1 x TBE-buffer containing ethidium bromide (500 µg/l) were used. Prior to electrophoresis the samples were mixed with 1 x DNA-Sample Buffer. The gels were run at room temperature at a voltage of 10 V/cm. As molecular weight marker 500 ng of 1 kb DNA-Ladder was used. Stained DNA bands were visualized using UV light at 302 nm and documented using a Polaroid camera.

- TBE-Buffer: 90 mM Tris, 90 mM boric acid, 2 mM EDTA (pH ~8.3, not adjusted)
- 5 x DNA-Sample Buffer: 0.05 % (w/v) bromphenolblue, 0.05 % (w/v) xylencyanol, 50 % (w/v) glycerol

2.2.1.3 Analytical polyacrylamide-urea gel electrophoresis

DNA or RNA molecules are separated at a high resolution in analytical polyacrylamide-urea gel electrophoresis. The gels used were prepared using the following components: 20 % Rotiphorese Gel 40 (19:1) (RNase free-acrylamide:N,N'-methylene-bis-acrylamide solution in a 19:1 ratio), 1 x TBE buffer and 7 M urea RNase free. The polymerization of the gels was started by addition of 5 µl 10 % APS and 2.5 µl TEMED per ml solution. Prior to electrophoresis, the samples were mixed with an equal volume of Formamide Buffer and denatured for 3 minutes at 95°C. The gel electrophoresis was carried out at room temperature in 1 x TBE buffer at 200 V in a Protean Minigel System II chamber (BioRad, München). After electrophoresis the nucleic acid bands were stained with ethidium bromide and visualized by UV light.

- Formamide Buffer: 80 % formamide, 1 mg/ml bromphenolblue, 1 mg/ml xylencyanol, 1 x TBE

2.2.1.4 Polymerase chain reaction (PCR)

With the help of the PCR technique DNA fragments are selectively amplified *in vitro* (Mullis and Faloona, 1987). For the engineering of DafA(L2V)_{Tth} mutants or of wild type DafA_{Tth} the QuikChange Site Directed Mutagenesis was used. This technique is based on the PCR amplification of the whole plasmid-DNA isolated from *E. coli* using two primers

that contain the desired point mutation. In comparison to the parental DNA, the PCR product is not methylated and can be separated from the PCR template via Dpn I digestion. Dpn I endonuclease is specific for methylated and hemimethylated DNA and is used to digest the parental DNA template and to select for mutation-containing synthesized DNA.

For the mutagenesis every PCR reaction was carried out by mixing the following components in a total volume of 50 μ l: 0.1-0.2 μ g template (plasmid-DNA), 1.25 μ l 100 μ M 5'-primer, 1.25 μ l 100 μ M 3'-primer, 10 μ l dNTP mixture (each 1 mM), 10 μ l 10 x Reaction-Buffer and 1 μ l (2.5 U/ μ l) PfuTurbo DNA Polymerase. The thermocycler was programmed as shown in the Table 2-3. Subsequent cycling the PCR products were treated with 1 μ l Dpn I, incubated for 1 hour at 37°C and then stored at -20°C.

Table 2-3: Cycling parameters for QuikChange Site Directed Mutagenesis PCR

Step	Cycles	Temperature	Time	Reaction
1	1	95°C	30 seconds	dsDNA denaturation
2	16	95°C	30 seconds	dsDNA denaturation
		55°C	1 minute	Primer annealing
		68°C	11 minutes	Elongation
3	1	68°C	4 minutes	Extension time
4		4°C	no limit	Reaction stop

dsDNA = double stranded DNA

For the sequencing PCR the reaction mixture was the following: 0.5-1 μ g DNA template, 10 pMol T7-Promoter primer, 10 pMol T7- Terminator primer, 2 μ l DMSO, 4 μ l BigDye Terminator Cycle Sequencing Kit (containing AmpliTaq-Polymerase and fluorescent dideoxynucleotides) in 20 μ l final volume. The PCR parameters are shown in Table 2-4.

Table 2-4: Cycling parameters for Sequencing PCR

Step	Cycles	Temperature	Time	Reaction
1	1	96°C	10 seconds	dsDNA denaturation
2	25	96°C	10 seconds	dsDNA denaturation
		50°C	5 seconds	Primer annealing
		60°C	4 minutes	Elongation
3	1	60°C	4 minutes	Extension time
4		4°C	no limit	Reaction stop

Prior to sequencing procedure the PCR products were purified with the DyeEx Spin Kit and analyzed by capillary-electrophoresis in an ABI PRISM 3700 DNA Analyzer (Applied Biosystems, Langen).

2.2.1.5 Preparation of competent cells

Electrocompetent cells

The *E. coli* XL-1 and BL21(DE3) strains were grown in LB-medium at 37°C to an OD₆₀₀ of 0.6 and then cooled down on ice and pelleted (5000 g, 10 minutes, 4°C). The cell pellet was re-suspended in 80 ml of 5 % sterile glycerol and supplemented with another 320 ml glycerol after re-suspension. Cells were again centrifuged (5000 g, 10 minutes, 4°C), re-suspended in 20 ml of 5 % glycerol and brought to a final volume of 400 ml with 5 % glycerol. After another centrifugation of 10 minutes (5000 g, 4°C) the cells were re-suspended in 15 ml of 5 % glycerol and supplemented with 30 ml of 5 % glycerol. In the end, the cells were again centrifuged (5000 g, 10 minutes, 4°C), re-suspended in ca. 5 ml of 5 % glycerol, aliquoted (80 µl/aliquot), shock-frozen in liquid N₂ and stored at -80°C. For the preparation of the electrocompetent cells all the solutions and material used were chilled prior usages.

DMSO-competent cells

The *E. coli* XL-1 Blue and TG-1 strains were grown over night in 30 ml LB-medium at 37°C. This culture was used to inoculate a larger volume of LB-medium (dilution factor 1:100). The cells were grown to an OD₆₀₀ of 0.3-0.4 and then cooled down on ice and pelleted (1500 g, 15 minutes, 4°C). The cells were resuspended in 1/10 of previous volume in ice-cold TSS-medium, aliquoted (500 µl/aliquot), shock-frozen in liquid N₂ and stored at -80°C.

2.2.1.6 Transformation of the *E. coli* cells with circular DNA

Transformation of electrocompetent cells

80 µl of electrocompetent *E. coli* XL-1 Blue and BL21(DE3) cells were slowly mixed with 5-50 ng DNA and incubated on ice for 2 minutes. The transformation was made by electroporation with a BioRad Gene Pulser apparatus (2 mm distance between electrodes, 1.5 kV voltage gradient, 800 Ohm resistance, 25 µF capacity). After transformation the cells were resuspended in 1 ml antibiotic-free 2-TY medium, incubated for 30-60 minutes at 37°C and then plated out on selective medium (agar plates containing 30 µg/ml Kanamycin).

Transformation of DMSO-competent cells

500 µl of DMSO-competent *E. coli* XL-1 Blue and TG-1 cells were slowly mixed with 5-50 ng DNA and incubated on ice for 30 minutes. The cells were transformed by heat shock at 42°C for 2 minutes and then resuspended in 1 ml antibiotic-free 2-TY medium, incubated for 30-60 minutes at 37°C and plated out on selective medium (agar plates containing 30 µg/ml Kanamycin).

2.2.1.7 Radiolabeling of DNA and RNA

The ^{32}P -labeled pkRNA was kindly provided by Dr. Laurent Chaloin.

The labeling of DNA molecules with $[\gamma\text{-}^{32}\text{P}]\text{ATP}$ was carried out via T4 Polynucleotide Kinase (T4 PNK) that catalyze the transfer of the gamma-phosphate from ATP to the 5'-hydroxyl of single- or double-stranded DNA, RNA, and nucleoside 3'-monophosphates. The labeling reaction was performed as described previously (Sambrook et al., 1989). The radio-labeled nucleic acids were extracted from the reaction mixture with a phenol:chloroform:isoamyl alcohol (25:24:1, pH 8) solution and purified on ProbeQuant G 50 Micro-columns. To estimate the labeling efficiency 1 μl (diluted 1:5) of labeled nucleic acid was applied on a PEI-cellulose plate and subjected to thin layer chromatography (TLC) using the TLC-Buffer. After the leading edge of the solvent front had reached the end of the plate, the plate was dried, and then exposed to a photosensitive plate for 5 minutes. This plate was scanned using a BioRad GS-525 Phosphoimager and the radioactive spots were quantified with Molecular Analyst software (BioRad). By comparing the counts per minute (cpm) of the labeled oligonucleotides of nucleic acids before and after purification from free $[\gamma\text{-}^{32}\text{P}]\text{ATP}$ it is possible to determine their concentration.

The radiolabeled DNA was used in further experiments as single stranded DNA (ssDNA) or it was hybridized with the unlabeled complementary strand and used as double stranded DNA (dsDNA). For the hybridization reaction the complementary strands were mixed in a 1:1.5 ratio labeled:unlabeled DNA in 20 mM Tris/HCl pH 7.5, 25 mM NaCl. The mixture was heated at 95°C for 2 minutes and then slowly cooled down on the bench.

- TLC-Buffer: 0.6 M KH_2PO_4 pH 3.5.

2.2.1.8 Extraction and digestion of nucleic acids from DafA(L2V)_{Tth} sample

The extraction of the nucleic acids present within DafA(L2V)_{Tth} sample was carried out via phenol/chloroform extraction followed by ethanol precipitation (Sambrook et al., 1989). After ethanol precipitation the pellet of nucleic acids was resuspended in DEPC-water (double distilled water previously treated with DEPC; see section 7.2) and store at -20°C until usage. Digestions were carried out for 1 hour at 37°C by using 50 $\mu\text{g}/\text{ml}$ RNaseA in 10 mM Tris/HCl pH 7.5. To estimate roughly the molecular mass of the nucleic acids a 33-mer RNA was used as marker.

2.2.2 Methods related to proteins

2.2.2.1 Protein overexpression

The overexpression of all DafA_{Tth} variants was carried out in *E. coli* BL21(DE3) strain following the conditions presented in Table 2-5. For the individual *T. thermophilus* chaperones or the DnaK_{Tth}-DnaJ_{Tth}-DafA(L2V)_{Tth} complex the overexpression parameters

were described previously (Klostermeier et al., 1998; Klostermeier et al., 1999; Groemping et al., 2001).

After induction times indicated in Table 2-1 the cells were cooled down and pelleted by centrifugation (5000 g, 20 minutes, 4°C). The cell pellet was washed with 50 mM Tris/HCl pH 7.5, 50 mM KCl and re-centrifuged (5000 g, 20 minutes, 4°C). The final pellet was shock-frozen in liquid N₂ and stored at -80°C until usage.

Table 2-5: Overexpression conditions for *T. thermophilus* chaperones

Protein	Medium	Antibiotic	Induction at OD ₆₀₀	[IPTG] (mM)	T (°C)	Induction time (hours)
DafA(L2V)	2 x TY	50 µg/ml Kan	0.6	0.5	28	18
N ¹⁵ -DafA(L2V)	Minimal medium with N ¹⁵ H ₄ Cl	50 µg/ml Kan	0.5	1	28	24
DafA(L2V)W7C	2 x TY	50 µg/ml Kan	0.6-0.8	1	37	4
DafA(L2V)S14C	2 x TY	50 µg/ml Kan	0.6-0.8	1	37	4
DafA(L2V)V27C	2 x TY	50 µg/ml Kan	0.6-0.8	1	37	4
DafA(L2V)F31C	2 x TY	50 µg/ml Kan	0.6-0.8	1	37	18
DafA(L2V)W41C	2 x TY	50 µg/ml Kan	0.6-0.8	1	37	4
DafA(L2V)M51C	2 x TY	50 µg/ml Kan	0.6-0.8	1	37	4
DafA(L2V)A69C	2 x TY	50 µg/ml Kan	0.6-0.8	1	37	4
GST-DafA(L2V)	2 x TY	50 µg/ml Kan	0.6	1	37	4
NusA-DafA(L2V)	2 x TY	50 µg/ml Kan	0.6	1	37	3.5
DafA(wt)	2 x TY	50 µg/ml Kan	0.7	various	various	various
DnaK, DnaJ, GrpE, ClpB co-expression	2 x TY	50 µg/ml Kan	0.6-0.8	2	37	4

OD₆₀₀= absorption at 600 nm; wt = wild type; Kan = kanamycin

2.2.2.2 Protein purification

The purification of the various thermophilic proteins was performed using a Waters FPLC 650E system connected to a 490E Programmable Multiwavelength Detector and an Analog Plotter (Linseins).

Purification of DafA(L2V)_{Tth} and its mutants

The purification protocol of DafA(L2V)_{Tth} and its mutants is based on the protocol established by Klostermeier et al. (1999) to which additional improvements were made.

The *E. coli* cell pellet was re-suspended in Lysis Buffer in the presence of protease inhibitors and disrupted using a microfluidizer (Microfluidics, Newton, Mass, USA) at a pressure of 600 kPa. The cell lysate was centrifuged for 30 minutes at 35000 rpm and 4°C in a Beckman Ti-45 rotor. The cell pellet containing DafA(L2V)_{Tth} expressed as inclusion bodies was re-suspended in Washing Buffer and homogenized by slowly stirring for 30 minutes at 4°C. The suspension was centrifuged (30 minutes, 35000 rpm, 4°C) and the resulting pellet was re-suspended in Extraction Buffer containing 4 M urea. DafA(L2V)_{Tth}

was brought into the soluble fraction by slowly stirring for 60 minutes at 4°C. After solubilization of DafA(L2V)_{Tth} the solution was centrifuged (30 minutes, 40000 rpm, 4°C, Beckman Ti-60 rotor) and the supernatant fraction was kept for the subsequent purification step. The protein solution was applied on a Superdex S-75 preparative gel filtration column equilibrated over night in the GF-Buffer and eluted at a flow of 2 ml/min (3 injections of ca. 3 ml each). The gel filtration pool of DafA(L2V)_{Tth} was supplemented with 10 % glycerol, concentrated to ca. 1.5 mg/ml in an Amicon ultrafiltration chamber (Amicon, Beverly, USA) using a 3 kDa cut-off membrane and applied on a MonoQ 5/5 anion exchange column at a flow rate of 1 ml/min using the Buffer A. The gradient table used was the following:

Step	Time (min)	Flow (ml/min)	Buffer A (%)	Buffer B (%)	Slope
Initial	0	1	100	0	*
Washing	35	1	100	0	6
Salt Gradient	55	1	0	100	6
Re-equilibration	65	1	100	0	1
Stop flow	85	0	100	0	6

DafA(L2V)_{Tth} does not bind to the MonoQ column and is found in the flow through. DafA(L2V)_{Tth} fractions were pooled, concentrated to ca. 1 mg/ml and extensively dialyzed (4 hours and over-night at 4°C) against Storage Buffer. After dialysis, the protein was centrifuged to remove the aggregates and concentrated to 0.7-0.9 mg/ml. The protein was again centrifuged (30 minutes, 40000 rpm, 4°C) to eliminate the aggregates, its final concentration measured and stored at -80°C in small aliquots. Following this protocol, a protein yield of more than 4 mg/l cell culture with more than 99 % purity as judged by SDS-PAGE was obtained.

The cysteine mutants of DafA(L2V)_{Tth} was purified following the same protocol except that all the buffers contained 5 mM 2-mercaptoethanol as reducing agent.

- Lysis Buffer: 50 mM HEPES/NaOH pH 7.5, 100 mM KCl, 5 mM EDTA, 1 mM PMSF, protease inhibitors (1 pill/50 ml buffer)
- Washing Buffer: Lysis Buffer supplemented with 1 M urea and 10 % glycerol
- Extraction Buffer: Lysis Buffer supplemented with 4 M urea and 10 % glycerol
- GF-Buffer: 50 mM HEPES/NaOH pH 7.5, 100 mM KCl, 5 mM MgCl₂, 2 mM EDTA, 4 M urea
- Buffer A: 50 mM HEPES/NaOH pH 7.5, 100 mM KCl, 5 mM MgCl₂, 2 mM EDTA, 4 M urea, 10 % glycerol
- Buffer B: 50 mM HEPES/NaOH pH 7.5, 1 M KCl, 5 mM MgCl₂, 2 mM EDTA, 4 M urea, 10 % glycerol
- Storage Buffer: 20 mM HEPES/NaOH pH 7.5, 50 mM KCl, 1 mM MgCl₂ and 10% glycerol

Purification of the DnaK_{Tth}-DnaJ_{Tth}-DafA(L2V)_{Tth} complex

The purification of DnaK_{Tth}-DnaJ_{Tth}-DafA(L2V)_{Tth} complex was based on a purification protocol previously described (Klostermeier et al., 1999). Several modifications of the initial protocol were made in order to improve the quality of the final product.

The *E. coli* cell pellet was re-suspended in AE-Buffer A (Anion Exchange Buffer A) in the presence of protease inhibitors and disrupted using a microfluidizer (Microfluidics, Newton, Mass, USA) at a pressure of 600 kPa. The cell lysate was centrifuged for 30 minutes at 35000 rpm and 4°C in a Beckman Ti-45 rotor. The supernatant was collected and applied on an over-night equilibrated EMD-DEAE Sepharose column (Merck, Darmstadt) using AE-Buffer A at a flow rate of 6 ml/min. After the baseline recovery the column was washed with 30 mM NaCl (97 % AE-Buffer A and 3 % AE-Buffer B) at a flow of 2 ml/min.

The complex was eluted from the EMD-DEAE column using a salt gradient in two steps: i) from 30 mM to 250 mM NaCl and ii) from 250 mM to 1 M NaCl. Each elution was carried out in a 1200 ml total volume at a flow rate of 6 ml/min. The fractions were pooled according to their purity and concentrated in an Amicon ultrafiltration chamber (3 kDa cut-off membrane).

The ammonium sulphate precipitation following the anion exchange chromatography was omitted and replaced by a heat denaturation step at 75°C for 30 minutes in order to denature the thermolabile host proteins. After heat treatment the denatured proteins were removed by centrifugation (30 minutes at 35000 rpm and 4°C in a Beckman Ti-45 rotor). After this heat treatment, the solution was centrifuged (35000 rpm, 30 minutes, 4°C, Beckman rotor Ti-45) and the supernatants were collected and concentrated to less than 10 ml using an Amicon chamber (3 kDa cut-off membrane).

Each pool was subjected to gel filtration chromatography using a Superdex S-200 column equilibrated in GF-Buffer (Gel Filtration Buffer). The elution was carried out at 2 ml/min flow rate. The fractions containing the complex were pooled and extensively dialyzed (4 hours and over-night at 4°C) against Dialysis Buffer. After dialysis, the protein was centrifuged to remove the eventual aggregates and highly concentrated. The protein was again centrifuged (30 minutes, 40000 rpm, 4°C), its final concentration measured and stored at -80°C in small aliquots.

- Anion Exchange Buffer A: 25 mM Tris/HCl pH 7.5, 3 mM MgCl₂, 1 mM DTE
- Anion Exchange Buffer B: 25 mM Tris/HCl pH 7.5, 3 mM MgCl₂, 1 mM DTE, 1 M NaCl
- GF-Buffer: 25 mM Tris/HCl pH 7.5, 3 mM MgCl₂, 100 mM Na₂SO₄
- Dialysis Buffer: 20 mM Tris/HCl pH 7.5, 25 mM NaCl, 1 mM MgCl₂

Purification of 70 S ribosomes from *T. thermophilus* HB27 cells

Thermus thermophilus strain HB27 was grown at 70°C under strong aeration in the corresponding medium (see 2.1.7) (Williams, 1992). Cells were harvested and stored at -80°C until use. All buffers used were at 4°C and contained 6 mM 2-mercaptoethanol unless indicated otherwise. The frozen cells were disrupted by grinding with 2 times the cell mass of alumina and then resuspended in Buffer A. Alumina and cell debris were removed by centrifugation (30 minutes at 16000 g and 4°C; then twice for 15 minutes at 20000 g, 4°C). The supernatant was applied onto at least an equal volume of a cushion containing 1.1 M sucrose in Buffer B (Clemons, Jr. et al., 2001) and centrifuged at 148000 g for 15 hours. The pellet containing salt-washed 70 S ribosomes was briefly washed with Ribosomal Storage-Buffer and then resuspended in the same buffer. The ribosome solution was further clarified from eventual aggregates by centrifugation (20000 g, 30 minutes and then for 3 hours at 148000 g). The pellet was washed again and resuspended in a low volume of Ribosomal Storage-Buffer. The concentration of high salt washed 70 S ribosomes was calculated with the Equation 2-1:

$$1 \text{ OD}_{260\text{nm}} = 25 \text{ pmol ribosome}$$

Equation 2-1

- Buffer A: 20 mM HEPES/NaOH pH 7.5, 10.5 mM MgCl₂, 60 mM NH₄Cl, 0.5 mM EDTA, 0.1 mM PMSF
- Buffer B: 20 mM HEPES/NaOH pH 7.5, 1 M NH₄Cl, 10.5 mM MgCl₂, 0.5 mM EDTA
- Ribosomal Storage-Buffer: 20 mM HEPES/NaOH pH 7.5, 50 mM KCl, 100 mM NH₄Cl, 10.5 mM MgCl₂, and 0.5 mM EDTA

2.2.2.3 SDS-polyacrylamide gel electrophoresis (SDS-PAGE)

The separation of the proteins in order to estimate their purity or to determine their molecular weight was achieved by discontinuous polyacrylamide-gel electrophoresis based on the methods of Laemmli (for proteins other than DafA(L2V)_{Tth}) or Schagger and Jagow (for separation of DafA(L2V)_{Tth}) (Laemmli, 1970; Schagger and von Jagow, 1987). The following recipes were used for the preparation of the gels:

	<i>Tris/Glycine gel</i> (Laemmli, 1970)	<i>Tris/Tricine gel</i> (Schagger and von Jagow, 1987)
Stacking gel	4.5 % Acryamide, 0.12 % Bisacrylamide, 125 mM Tris/HCl pH 6.8, 0.06 % SDS (w/v), 50 µl 10 % APS/10 ml solution,	4.5 % Acryamide, 0.12 % Bisacrylamide, 0.8 M Tris/HCl pH 8.45, 0.3 % SDS (w/v), 50 µl 10 % APS/10 ml solution,

	5 μ l TEMED/10 ml solution	5 μ l TEMED/10 ml solution
Running gel	15 % Acryamide, 0.4 % Bisacrylamide, 375 mM Tris/HCl pH 8.8, 0.1 % SDS (w/v), 50 μ l 10 % APS/10 ml solution, 5 μ l TEMED/10 ml solution	16,5 % Acryamide, 0.44 % Bisacrylamide, 1 M Tris/HCl pH 8.45, 0.3 % SDS (w/v), 50 μ l 10 % APS/10 ml solution, 5 μ l TEMED/10 ml solution
Running Buffer	25 mM Tris, 192 mM Glycine, 0.01 % SDS (w/v)	Anode Buffer: 0.2 M Tris/HCl pH 8.9 Cathode Buffer: 0.1 M Tris/HCl pH 8.25, 0.1 M Tricine, 0.1 % SDS (w/v)

Before the electrophoresis the samples were mixed in a 1:3 ratio with 4 x Sample Buffer and incubated for 5-10 minute at 95°C. The Tris/Glycine gels were run in the Running Buffer at 40 mA in a Protean Minigel System II (BioRad, München). The Tris/Tricine gels were run under the same conditions but using the the two-running buffer system (Cathode Buffer inside of the electrode chamber, Anode Buffer outside). The Low Molecular Weight Calibration Kit (Pharmacia) and the Polypeptide SDS-PAGE Molecular Weight Standards (BioRad) were used as molecular weight marker. After electrophoresis the gels were incubated for ca. 20 minutes with the Staining Solution and then destained. For the fluorescent samples the gel was directly scanned with a FLA-5000 fluorescence imager (Fuji, Tokyo, Japan).

- 4 x Sample Buffer: 130 mM Tris/HCl pH 6.8, 200 mM DTE, 4 % SDS, 0.02 % (w/v) bromphenolblue, 40 % (v/v) glycerol
- Staining Solution: 25 % (v/v) isopropanol, 10 % (v/v) acetic acid, 0.1 % (w/v) Coomassie Blue-R250, 0.01% (w/v) Coomassie Blue-G250
- Destaining Solution: 20 % (v/v) acetic acid, 10 % (v/v) ethanol

2.2.2.4 Native gel electrophoresis

Native gel electrophoresis was carried out using native gels containing various concentrations of acrylamide/bis-acrylamide and 375 mM Tris/HCl pH 8.8. The gels were run in the 1x Native Running Buffer at 20 mA in a Protean Minigel System II chamber (BioRad, München). Prior to the electrophoresis the samples were mixed in a 1:5 ratio with 4 x Native Sample Buffer. After electrophoresis the gels were incubated for ca. 20 minutes with the Staining Solution and then destained (see section 2.2.2.3). For the fluorescent samples the gel was directly scanned with a fluorescence imager (FLA-5000, Fuji, Japan).

- 6 x Native Sample Buffer: 150 mM Tris/HCl pH 6.8, 0.25 % (w/v) bromphenolblue, 40 % (v/v) glycerol
- 10 x Native Running Buffer: 250 mM Tris, 1.92 M glycine, 10 mM EDTA, pH 8.5 (not adjusted)

2.2.2.5 Western Blot

Proteins separated by SDS-PAGE were electrotransferred to a PVDF membrane (Bio-Rad) for 20 minutes at 4 mA/cm² using a Biometra Blotter. Before transfer the gel was incubated in the Cathode Buffer and the membrane in the Anode Buffer. The membrane was blocked for 1 hour at room temperature in 1% blocking solution (Bio-Rad) diluted in TBS and incubated for 1 hour with polyclonal antibodies against DafA(L2V)_{Tth} in 0.5% blocking solution-TBS. Membranes were washed 3 x 10 minutes with TBS-Tween, incubated with goat anti-rabbit IgG-horseradish peroxidase (Promega) for 1 hour, washed again, and then the bands were visualized by chemiluminescence (BM Chemiluminescence Blotting Substrate (POD), Roche) or fluorescence (ECF western blotting reagent, Amersham).

- Cathode Buffer: 30 mM Tris, 300 mM ε-aminocaproic acid pH 8.8
- Anode Buffer: 300 mM Tris, 100 mM tricine pH 8.6
- TBS: 50 mM Tris, 150 mM NaCl pH 7.5
- TBS-Tween: TBS containing 0,1% Tween-20

2.2.2.6 Labeling of cysteine-DafA(L2V)_{Tth} mutants with fluorophores

The labeling of various cysteine mutants of DafA(L2V)_{Tth} with Alexa Fluor 488-C₅-Maleimide, IANBD-ester (2-(methyl(7-nitro-4-benzofurazanyl) amino)ethyl ester) and IAEDANS-ester (1-Naphthalenesulfonic acid, 5-((2-((iodoacetyl)amino)ethyl) amino)-ester) (Molecular Probes, Eugene, USA) was carried out conform to the manufacturer's recommendations in Labeling Buffer. Typically, 1-2 mg protein was labeled using a 5 to 10-fold excess dye over the protein concentration. After over night incubation at 4°C, excess dye was removed by ultrafiltration in an Amicon chamber (Amicon, Beverly, USA) using a 3 kDa cut off membrane. This washing step was carried out with the Labeling Buffer supplemented with 5 mM DTE. The presence of 4 M urea in the Washing Buffer is necessary to prevent aggregation of the protein during ultrafiltration. A NAP-5 desalting column (Amersham) was used to remove urea from the sample using the Storage Buffer. The concentration of the labeled proteins was calculated after subtraction of the dye's contribution from the protein absorption at 280 nm (for the calculated extinction coefficients see section 2.2.3.2). Labeling efficiency was calculated using the Equation 2-2. The labeling efficiency calculated as shown before was varying from 60 % to 100 %.

$$A_x / \epsilon \times \text{MW of protein} / \text{mg/ml} = \text{moles of dye} / \text{moles of protein}$$

Equation 2-2

A_x the absorbance of the dye at the absorption maximum wavelength

ϵ molar extinction coefficient of the dye at the absorption maximum wavelength

- Labeling Buffer: 50 mM HEPES/NaOH pH 7.5, 150 mM KCl, 5 mM MgCl₂, 2 mM EDTA, 2 mM sodium ascorbate, 4 M urea, 10 % glycerol
- Washing Buffer: 50 mM HEPES/NaOH pH 7.5, 150 mM KCl, 5 mM MgCl₂, 2 mM EDTA, 4 M urea, 10 % glycerol
- Storage Buffer: 20 mM HEPES/NaOH pH 7.5, 100 mM KCl, 2 mM MgCl₂, 5 mM DTE, 10 % glycerol

2.2.2.7 Sucrose cushion assay

DafA(L2V)_{Tth} or DafA(L2V)S14C_{Tth}-Alexa488 mutant were incubated with the *T. thermophilus* 70 S ribosomes for the indicated times and temperature in the Ribosome Interaction Buffer. The mixture was then layered onto a 2-fold volume of 30 % (w/v) sucrose in the interaction buffer and centrifuged for 70 min at 75000 rpm (~ 80000 g) in a TLA-100 rotor (Beckman, CA, USA). The supernatants were collected and the ribosomal pellets were briefly washed with the same buffer. Both the supernatant and the ribosomal pellet were TCA-precipitated before applying on 16.5 % Tris-Tricine denaturing gels. Only half of the total sample volume was applied on the gel. The gels were then subjected to western blotting using rabbit-anti DafA(L2V)_{Tth} antibodies or to fluoroimaging in the case of fluorescent labeled DafA(L2V)S14C_{Tth} using a FLA-5000 fluorescence scanner (Fuji, Tokyo, Japan). For the visualization of fluorescent protein on FLA-5000 scanner a laser with an excitation at 473 nm and a cut-off filter of 510 nm were used.

- Ribosome Interaction Buffer: 20 mM HEPES/NaOH pH 7.5, 60 mM KCl, 10 mM MgCl₂, 4 mM 2-mercaptoethanol, 10 % glycerol

2.2.2.8 Analysis of fluorescent complexes by analytical gel filtration (HPLC)

Analytical gel filtration experiments were carried out on a Superdex S-200 HR10/30 (Amersham) columns using a high performance liquid chromatography system (Waters, Milford, USA). The excitation and emission wavelengths were 493 nm and 516 nm, respectively. The samples were incubated for indicated times and temperatures in Ribosome Interaction Buffer (see 2.2.2.7). The elution was carried out at room temperature a flow rate of 0.5 ml/min or 0.75 ml/min. Before applying on the column the samples were briefly centrifuged for removal of eventual aggregates.

- Elution Buffer: 50 mM HEPES/NaOH pH 7.5, 100 mM NaCl, 12 mM MgCl₂, 2 mM EDTA, 4 mM 2-mercaptoethanol

2.2.3 Spectroscopic methods

2.2.3.1 Absorption spectroscopy

Absorption spectra necessary for determination of the protein and nucleic acid concentration were obtained using a DU 650- Spectrophotometer (Beckman, Palo Alto, USA). For the chaperone activity measurements an iEMS Reader (Labsystems, Helsinki, Finland) for micro-titer plates (8 x 12) was used.

2.2.3.2 Determination of the protein concentration

The concentration of the proteins in the presence of nucleotides or nucleic acids was determined using the method of Ehresmann (Ehresman et al., 1973) by measuring the absorption at 228.5 nm and 234.5 nm in a 1 ml quartz cuvette. The protein concentration was calculated using the following equation:

$$c = (A_{228.5} - A_{234.5}) / 3.14$$

Equation 2-3

$A_{228.5}$ absorption at 228.5 nm

$A_{234.5}$ absorption at 234.5 nm

c protein concentration in mg/ml

For the highly purified DafA(L2V)_{Th} variants the concentration was determined using the Lambert-Beer equation (Equation 2-4) and the calculated extinction coefficients (9530 M⁻¹cm⁻¹ for tryptophane mutants and 15220 M⁻¹cm⁻¹ for DafA(L2V)_{Th} and the other mutants).

$$c = A \cdot \epsilon \cdot l$$

Equation 2-4

A absorption at 280 nm

ϵ extinction coefficient of the protein at 280 nm (M⁻¹cm⁻¹)

l path length of the sample (cm)

c concentration (M)

2.2.3.3 Fluorescence spectroscopy

The fluorescence spectroscopy measurements were performed using an Aminco Bowman 8100 Fluorimeter (SLM, Urbana, USA), a FluoroMax-II (Spex Industries, Edison, NJ, USA) or a FluoroMax-III Spectrofluorimeter (Jobin Yvon, Edison, NJ, USA) and using 1 ml quartz cuvettes or 100 μ l black quartz cuvette.

The emission spectra were taken by exciting the fluorophore at its maximum absorption value. The settings of the instruments (integration time, resolution, and bandwidth) were variable due to their different characteristics. The settings together with the buffers used for the measurements are shown individually for each experiment in the Results section.

In order to obtain the midpoint of the GdmCl-induced denaturation of DafA(L2V)_{Tth}, the maximum fluorescence in the tryptophane emission spectra was plotted against the concentration of denaturant. The curve obtained was fitted with a nonlinear regression following the equation (Santoro and Bolen, 1988):

$$y_{\text{obs}} = \frac{(y_n^0 + m_n \cdot [\text{GdmCl}]) + (y_u^0 + m_u \cdot [\text{GdmCl}]) \cdot e^{-\frac{\Delta G_{\text{stab}}^0 - m \cdot [\text{GdmCl}]}{R \cdot T}}}{1 + e^{-\frac{\Delta G_{\text{stab}}^0 - m \cdot [\text{GdmCl}]}{R \cdot T}}}$$

Equation 2-5

y_{obs}	fluorescence of the native protein
$[\text{GdmCl}]$	concentration of GdmCl in M
y_n^0	intercept of the pre-transition baseline (native protein) at 0 M GdmCl
m_n	slope of the pre-transition baseline
y_u^0	intercept of the post-transition baseline (unfolded protein) at 0 M GdmCl
m_u	slope of the post-transition baseline
ΔG_{stab}^0	free enthalpy, measure of the conformational stability of the protein in 0 M GdmCl (in kJ/mol)
m	cooperativity parameter, measure of the dependence of ΔG_{stab}^0 on denaturant concentration (in kJ/mol·M)

The parameters obtained from the fit are: y_n^0 , m_n , y_u^0 , m_u , ΔG_{stab}^0 and m .

The concentration of GdmCl at the midpoint of the transition ($[\text{GdmCl}]_M$) is given by equation:

$$[\text{GdmCl}]_M = \frac{\Delta G_{\text{stab}}^0}{m}$$

Equation 2-6

2.2.3.4 Fluorescence anisotropy

Fluorescence anisotropy experiments were carried out using a FluoroMax 3 (Jobin Yvon, Edison, USA) spectrofluorimeter with Spex polarizers. The proteins coupled with IAEDANS fluorophore were excited at 336 nm and the fluorescence emission was measured at 490 nm. Other parameters (integration time, resolution) are shown for each experiment in the Results section. The anisotropy values during time trace measurements were directly provided by the spectrofluorimeter software which converts the fluorescence emission intensities of the signal in anisotropy conform to the equation:

$$r = \frac{(F_{VV} - G \cdot F_{VH})}{(F_{VV} + 2G \cdot F_{VH})}$$

Equation 2-7

r	fluorescence anisotropy
F_{VV}	fluorescence intensity obtained at the vertical orientation of the excitation polarizer and vertical orientation of the emission polarizer
F_{VH}	fluorescence intensity obtained at the vertical orientation of the excitation polarizer and horizontal orientation of the emission polarizer
G	grating factor ($G(\lambda_{EM}) = F_{HV}/F_{HH}$) calculated automatically by the machine

2.2.3.5 α -Glucosidase assay: test of chaperone activity *in vitro*

The refolding of heat denatured α -glucosidase from *Bacillus stearothermophilus* by the DnaK-ClpB chaperone systems from *T. thermophilus* was followed in an activity assay (Beinker et al., 2002). The assay buffer contains para-nitrophenylglucosid which is a substrate of the enzyme. The enzymatic reaction leads to formation of para-nitrophenol which is can be detected at 405 nm.

0.2 μM α -glucosidase was incubated at 75°C for 10 minutes in Denaturation Buffer. After denaturation the thermophilic chaperones (1.6 μM DnaK_{Th}, 0.4 μM DnaJ_{Th}, 0.2 μM GrpE_{Th} and 1 μM ClpB_{Th}) or *E. coli* lysate containing co-expressed DnaK-ClpB chaperone systems were added and the mixture was incubated for 90 or 120 minutes at

55°C. After the 1/10 dilution of reaction mixture into the Assay Buffer, the activity of α -glucosidase was measured in a titer plate by following the absorption at 405 nm.

- Denaturation Buffer: 50 mM MOPS/NaOH pH 7.5, 150 mM KCl, 10 mM MgCl₂, 5 mM ATP, 2 mM DTE
- Assay Buffer: 50 mM KPi pH 6.8, 2 mM para-nitrophenilglucosid, 0.1 mg/ml BSA

2.2.3.6 Luminescence

Chaperone activity test *in vitro*: refolding of luciferase in a continuous assay

Luciferase catalyzes luciferin oxidation, an ATP-dependent reaction characterized by emission of light. The luminescence intensity is a direct measure of the luciferase activity. Luciferase assay has been described previously in Groemping et al. (Groemping et al., 2001). The assay was performed at 30°C in microtiterplates (White Cliniplate, Labsystem, Helsinki, Finland) coated with BSA (the plates were incubated with 1 mg/ml BSA solution for 30 minutes at room temperature).

Luciferase (Promega, Madison, USA) was incubated for 2 minutes at a concentration of 10 μ M in Unfolding Buffer and subsequently diluted 125-fold into Refolding Buffer. The refolding was measured continuously at 30°C using an Ascent Fluoroskan Fl spectrometer (Labsystems, Helsinki, Finland). The concentrations of chaperones used for the refolding of 0.08 μ M luciferase were: 3.2 μ M DnaK_{Tth}, 0.4 μ M GrpE_{Tth}, 1.6 μ M DnaJ_{Tth}. DafA(L2V)_{Tth} was added at a concentration of 2 μ M.

- Unfolding Buffer: 25 mM HEPES/NaOH pH 7.5, 50 mM KCl, 15 mM MgCl₂, 2 mM DTE, 1 mM ATP, 0.05 mg/ml BSA and 5 M GdmCl
- Refolding Buffer: 25 mM HEPES/NaOH pH 7.5, 50 mM KCl, 15 mM MgCl₂, 2 mM DTE, 1 mM ATP, 0.05 mg/ml BSA, 240 μ M CoenzymA
- Assay Buffer: 25 mM HEPES/NaOH pH 7.5, 50 mM KCl, 15 mM MgCl₂, 2 mM DTE, 1 mM ATP, 0.05 mg/ml BSA, 240 μ M coenzyme A and 0.1 mM luciferin

2.2.3.7 Nuclear magnetic resonance (NMR)

In order to evaluate the folding state of DafA(L2V)_{Tth} HSQC-NMR experiments were performed. HSQC-NMR (*Heteronuclear Single Quantum Coherence*) requires the ¹⁵N-labeling of the protein of interest. The ¹⁵N-HSQC is a 2D experiment with one ¹H frequency and one ¹⁵N frequency.

The HSQC-NMR studies were performed and analyzed by PD Dr. Peter Bayer.

For the production of ¹⁵N-labeled DafA(L2V)_{Tth} the BL21(DE3) strain transfected with pET-DafA(L2V)_{Tth} vector was grown on minimal medium enriched with ¹⁵N-ammonium chloride. The overexpression of ¹⁵N-labeled DafA(L2V)_{Tth} was induced as described in Table 2-5. The purification of the protein was carried out using the same protocol as for the unlabeled DafA(L2V)_{Tth}.

For one HSQC-NMR experiment ca. 80 μM ^{15}N -labeled DafA(L2V)_{Tth} in 20 mM HEPES/NaOH pH 7.5, 100 mM KCl, 1 mM MgCl₂, 10 % glycerol was used. A ^{15}N -HSQC experiment was recorded on a Varian INOVA 600 MHz spectrometer at 300 K for ca. 20 hours.

2.2.4 Calorimetry

2.2.4.1 Differential Scanning Calorimetry (DSC)

Thermal stability of DafA(L2V)_{Tth} was determined with the help of DSC using a Microcal VP-DSC Microcalorimeter (MicroCal, MA, USA). For the measurements the sample cell was filled with 1 mg/ml protein ($\sim 117 \mu\text{M}$) in the DSC buffer. The reference cell was filled with the degassed DSC buffer. As a control for the buffer the same measurement was done using only the buffer in both cells. The samples were heated from 25 to 120°C with a rate of 60°C/hour. The melting curve was corrected for the buffer effect and normalized for the protein concentration using the program MicroCal Origin 4.1 for DSC. After the subtraction of the baseline (the heat capacity is brought to zero) the data was fitted using a “non-2-state” model, which calculated the melting point T_m , the calorimetric enthalpy ΔH_{cal} , and the van't Hoff enthalpy ΔH_{vH} .

- DSC Buffer: 4 M urea, 50 mM HEPES/NaOH pH 7.5, 300 mM KCl, 1 mM MgCl₂

3 RESULTS

3.1 Biochemical and biophysical characterization of DafA(L2V)_{Tth} and DnaK_{Tth}-DnaJ_{Tth}-DafA(L2V)_{Tth} complex

3.1.1 Optimization of DafA(L2V)_{Tth} purification

DafA_{Tth} is a small acidic protein (pI 4.88) composed of only 78 amino acids (including the first methionine) and with a molecular weight of 8668 Da. Until present (see section 3.1.2.3), the production of wild type DafA_{Tth} in *E. coli* cells was not possible due to the presence of a leucine (Leu) residue at the N-terminus. After trimming of the N-terminal methionine (Met) during post-translational modification, this Leu residue remains exposed and, conform to the N-end-rule in bacteria (Tobias et al., 1991), induces protein degradation. The replacement of this Leu with a valine (Val) residue allowed to overcome this problem, the mutant DafA(L2V)_{Tth} could be overexpressed in *E. coli* in inclusion bodies (Klostermeier et al., 1999).

Purification from inclusion bodies represents a way of obtaining high amounts of partially pure protein. However, it brings the problem of protein refolding. The initial purification protocol for DafA(L2V)_{Tth} (Klostermeier et al., 1999) takes advantage of this feature of inclusion bodies. After solubilization of DafA(L2V)_{Tth} with 3 M urea and using only one chromatographic step (gel filtration on a Superdex S-75 column) a purity of ca. 95 % is obtained judging by SDS-PAGE (Figure 3-1A, lane 7). However, the absorption spectrum of DafA(L2V)_{Tth} after this gel filtration step exhibits a maximum at 260 nm instead of 280 nm indicating a high nucleotide or nucleic acid content (Figure 3-1B, open circles).

Several modifications were made to the original expression and purification protocol in order to improve the quality and the yield of the final protein obtained. A better overexpression of DafA(L2V)_{Tth} in *E. coli* cells was obtained when a lower concentration of IPTG was used (0.5 mM) and the induction time was extended to 18 hours (over-night induction) concomitant with lowering the induction temperature (28°C).

By increasing the concentration of urea used for DafA(L2V)_{Tth} extraction from inclusion bodies (Figure 3-1A, lane 6) from 3 M to 4 M and by prolonging the extraction time from 30 minutes to 60 minutes, the yield of solubilized protein was significantly improved. This change associated with the addition of 10 % glycerol in every step of purification (except the gel filtration) led to a final yield of ca. 4 mg protein/l cell culture. In comparison, the initial purification protocol provided only 1 mg protein/l cell culture.

Biochemical and biophysical analysis requires a high degree of purity for the protein of interest. Therefore, an important objective was to eliminate the contaminant absorbing at 260 nm from the $\text{DafA(L2V)}_{\text{Tth}}$ sample. It could be achieved with the help of the strong anion exchanger MonoQ (Figure 3-1A, lane 8). Interestingly, in the absence of urea $\text{DafA(L2V)}_{\text{Tth}}$ binds to the MonoQ matrix and it is eluted at a very high concentration of salt (ca. 0.9 M KCl). In the presence of urea the protein is eluted in the flow through in contrary to the 260 nm absorbing contaminant that binds to the column. After this purification step, a shift of the absorbance from 260 nm to 280 nm was observed (Figure 3-1B, closed circles) indicating removal of the contaminant.

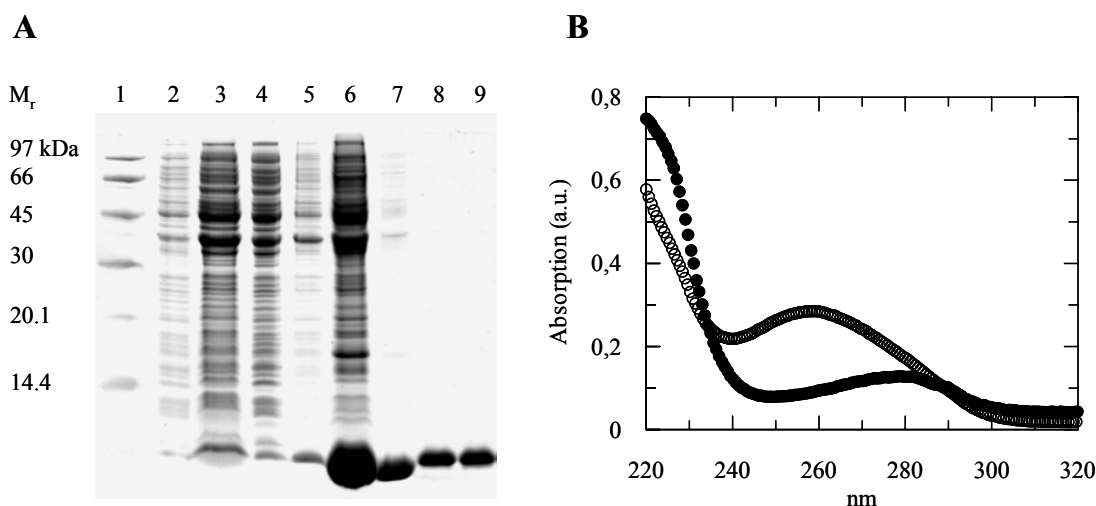


Figure 3-1: Improved purification strategy for $\text{DafA(L2V)}_{\text{Tth}}$. (A) *SDS-PAGE* for overexpression and purification of $\text{DafA(L2V)}_{\text{Tth}}$ (Coomassie staining). Lane 1, molecular weight marker; Lane 2, *E. coli* cells uninduced; Lane 3, *E. coli* cells overproducing $\text{DafA(L2V)}_{\text{Tth}}$ after over-night induction with 0.5 mM IPTG; Lane 4, cell lysate, soluble fraction; Lane 5, cell lysate, pellet; Lane 6, extraction of $\text{DafA(L2V)}_{\text{Tth}}$ from the pellet with 4M urea; Lane 7, gel filtration step; Lane 8, pool of MonoQ; Lane 9, final $\text{DafA(L2V)}_{\text{Tth}}$ sample. (B) Absorption spectrum of $\text{DafA(L2V)}_{\text{Tth}}$ after gel filtration and anion exchange steps. $\text{DafA(L2V)}_{\text{Tth}}$ after the gel filtration step displays an absorption maxima at 260 nm (○) which indicate the presence of nucleotides or nucleic acids within the protein sample. After using the MonoQ material, the maximum is shifted from 260 nm to 280 nm corresponding to $\text{DafA(L2V)}_{\text{Tth}}$ free of nucleic acids (●).

Following this improved protocol of $\text{DafA(L2V)}_{\text{Tth}}$ purification, it was possible to obtain a final protein purity higher than 99 % as indicated by Coomassie (Figure 3-1A, lane 9) and silver staining of the SDS-PAGE gels.

3.1.2 Optimization of $\text{DafA(L2V)}_{\text{Tth}}$ solubility

Although the overexpression and purification protocol described earlier has provided a high yield of very pure protein, the solubility of $\text{DafA(L2V)}_{\text{Tth}}$ was still unsatisfactory considering that $\text{DafA(L2V)}_{\text{Tth}}$ could be concentrated only to 0.8 mg/ml. Therefore, in order to improve the solubility of $\text{DafA(L2V)}_{\text{Tth}}$, various conditions have been tested starting with the overexpression conditions and ending with the addition of different compounds to the purified protein.

3.1.2.1 Modification of the overexpression conditions

It is known that by varying the IPTG concentration and/or induction times and/or lowering the induction temperature the solubility of proteins over-expressed in *E. coli* as inclusion bodies can be enhanced. Thus, in order to increase its solubility *in vivo*, DafA(L2V)_{Tth} was over-expressed in *E. coli* strain under conditions that implied lower IPTG concentration (between 0.02-0.5 mM), lower induction temperature (20-30°C) and longer induction times (4-18 hours), but none of these conditions have positively influenced DafA(L2V)_{Tth} solubility.

3.1.2.2 DafA(L2V)_{Tth} overexpression under osmotic shock

Organisms adapt to high external salinity by accumulating small organic compounds known as osmolytes, which equilibrate cellular osmotic pressure. Osmolytes can also act as “chemical chaperones” by increasing the stability of native proteins and assisting refolding of unfolded polypeptides (Samuel et al., 2000; Diamant et al., 2001). One of these osmoprotectants is glycine-betaine, a universal solute found in various prokaryotes including *E. coli*, animals, algae and salt-tolerant plants (Csonka, 1989).

Previous experience (Barth et al., 2000) showed that some recombinant proteins difficult to produce in a soluble form in *E. coli* may successfully be obtained in an active (soluble) form by cultivation of *E. coli* cells under osmotic shock and in the presence of osmolytes (glycine-betaine). Therefore, *E. coli* expressing DafA(L2V)_{Tth} was grown after IPTG induction under osmotic stress (4 % NaCl and 0.5 M sucrose) in a medium supplemented with various concentrations of glycine-betaine (10-100 mM). The results showed that DafA(L2V)_{Tth} is over-expressed under the conditions described, but an enhancement of solubility during its production in *E. coli* could not be observed.

3.1.2.3 Production of wild type DafA_{Tth} and of DafA(L2V)_{Tth} as fusion protein

Production of wild type DafA_{Tth}

The DafA(L2V)_{Tth} variant is able to form a heterotrimeric complex with DnaK_{Tth} and DnaJ_{Tth} similar to wild type DafA_{Tth} (Klostermeier et al., 1999). Although the replacement of the Leu₂ with a Val residue allowed for the stable production of DafA_{Tth} in *E. coli*, this change may affect its stability in terms of secondary and tertiary structure that would lead to formation of inclusion bodies.

Although production of wtDafA_{Tth} in *E. coli* was not successful due to the N-terminal Leu₂ (see 3.1.1), insertion of a second Met residue preceding this Leu was thought to aid overexpression of the wild type protein. With two Met residues at the N-end the wild type protein would be protected against proteolysis, the degradation-inducing Leu₂ being shielded by one Met still present after post-translational modifications. Following this reasoning wtDafA_{Tth} was obtained by site directed mutagenesis using the primers shown in Table 2-2. As seen in the Figure 3-2 wtDafA_{Tth} is produced in high yield at 37°C after

4 hours induction of the cells with 1 mM IPTG (lane 3). A similar expression yield was also obtained under different expression conditions (over night induction at 20°C, 0.5 mM IPTG).

The solubility tests showed that wtDafA_{Tth} is mainly found in the insoluble fraction (Figure 3-2, lanes 6, 7) and that only a very low percentage of the total protein is soluble (lanes 4, 5). A similar result was obtained independent of the expression conditions used. Nevertheless, the soluble fraction of the lysate was collected and concentrated to check for the stability of the protein obtained. This process led to precipitation of wtDafA_{Tth} and therefore the protein could not be used for further analysis.

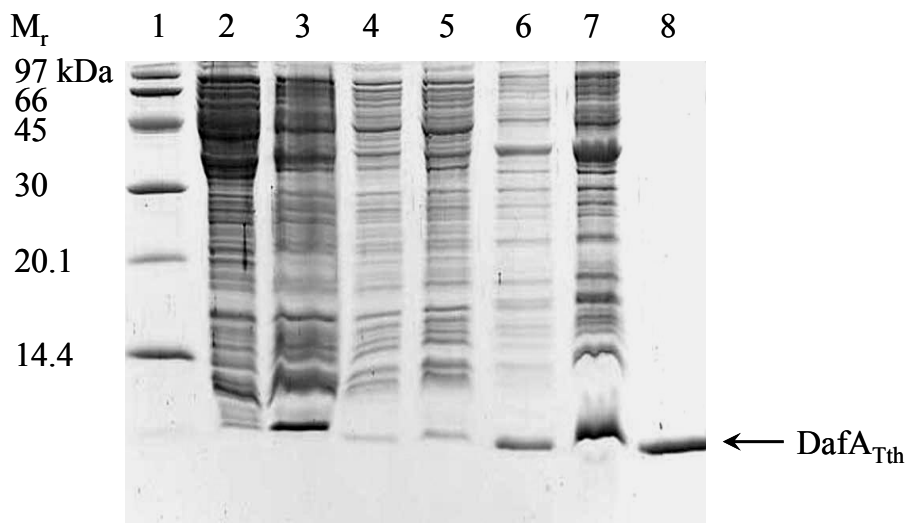


Figure 3-2. Overexpression of wtDafA_{Tth} in *E. coli*. wtDafA_{Tth} was over-expressed at 37°C for 4 hours after induction of the cells with 1 mM IPTG. Lane 1, molecular weight marker; Lane 2, uninduced cells; Lane 3, induced cells; Lane 4, 20 µl cell lysate, soluble fraction; Lane 5, 40 µl cell lysate, soluble fraction; Lane 6, 20 µl cell lysate, insoluble fraction; Lane 7, 40 µl cell lysate, insoluble fraction; Lane 8, standard DafA(L2V)_{Tth}.

Production of GST-DafA(L2V)_{Tth} fusion protein

Another strategy to optimize the solubility of DafA(L2V)_{Tth} was to express it as a fusion protein with glutathione-S-transferase (GST), a protein known to facilitate the soluble expression and purification of proteins.

The GST-DafA(L2V)_{Tth} fusion protein was over-expressed in *E. coli* in reasonable amounts (Figure 3-3, lane 3), but the presence of GST did not significantly improve DafA(L2V)_{Tth} solubility. When induced with 1 mM IPTG at 37°C for 4 hours, the fusion protein is mostly produced as inclusion bodies (Figure 3-3, lane 5) and only very low amounts were seen in the soluble fraction (lane 4). In order to enhance the yield of the soluble protein several other overexpression conditions have been tested. A minor increase of GST-DafA(L2V)_{Tth} expression yield was observed when lowering the induction temperature to 20°C (over night induction). This soluble fraction was subjected to affinity

chromatography for purification, but only few amounts of fusion protein could be collected due to aggregation processes occurring. Hence, even if the GST-fusion strategy showed some efficiency in solubilization of $\text{DafA(L2V)}_{\text{Tth}}$, it was not a successful way to produce considerable amounts of soluble protein.

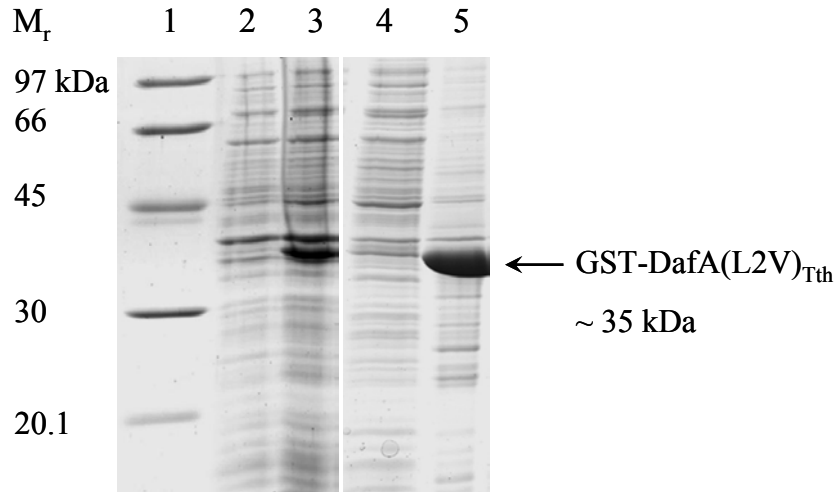


Figure 3-3: Overexpression of $\text{GST-DafA(L2V)}_{\text{Tth}}$ in *E. coli*. $\text{GST-DafA(L2V)}_{\text{Tth}}$ was over-expressed at 37°C for 4 hours after induction with 1 mM IPTG. Lane 1, molecular weight marker; Lane 2, uninduced cells; Lane 3, induced cells; Lane 4, cell lysate, soluble fraction; Lane 5, cell lysate, insoluble fraction.

Production of NusA- $\text{DafA(L2V)}_{\text{Tth}}$ fusion protein

NusA is a ca. 55 kDa protein constitutively expressed in *E. coli*. Studies based on a prediction model for the solubility of recombinant proteins expressed in *E. coli* have shown that NusA is one of the most efficient carrier proteins for production of soluble proteins in *E. coli* (Davis et al., 1999). Considering these findings, a vector containing *nusA* gene was used for the construction of a NusA- $\text{DafA(L2V)}_{\text{Tth}}$ fusion protein. The overexpression of the fusion protein in *E. coli* BL21(DE3) cells after induction with 1 mM IPTG for 3.5 hours was demonstrated by the appearance of a ca. 65 kDa band on a SDS-PAGE gel. Most importantly, more than 50 % of the total protein over-expressed was found in the soluble fraction (Figure 3-4, lane 4). Thus, the NusA fusion approach has incontestable the highest efficiency in production of a soluble $\text{DafA(L2V)}_{\text{Tth}}$ in *E. coli*. Nevertheless, it is not yet known whether after NusA cleavage $\text{DafA(L2V)}_{\text{Tth}}$ is maintaining its solubility. It might be also the case that $\text{DafA(L2V)}_{\text{Tth}}$ properties are conserved (formation of a complex with DnaK_{Tth} and DnaJ_{Tth}) under NusA-fusion protein form and thus no cleavage will be necessary. Further analyses are necessary to answer these questions.

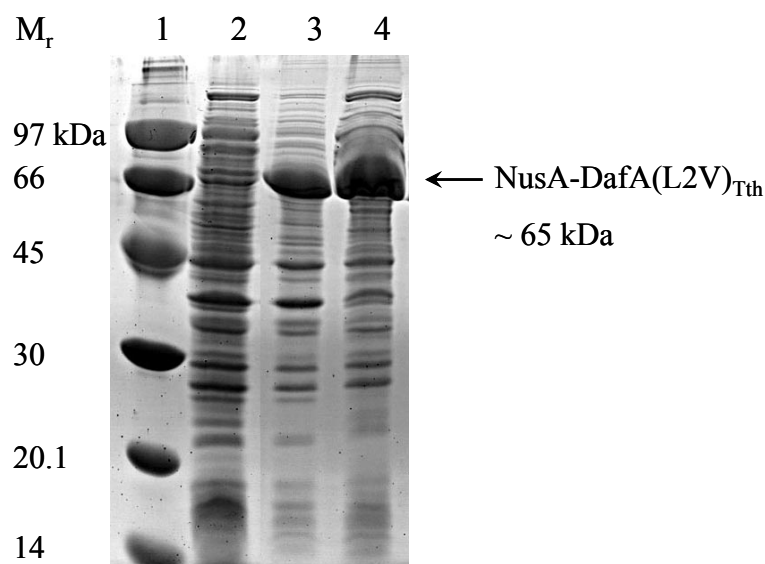


Figure 3-4: Overexpression of NusA-DafA(L2V)_{Tth} in *E. coli*. NusA-DafA(L2V)_{Tth} fusion protein was over-expressed at 37°C for 3.5 hours after induction with 1 mM IPTG. Lane 1, molecular weight marker; Lane 2, uninduced cells; Lane 3, induced cells insoluble fraction; Lane 4, induced cells, soluble fraction.

3.1.2.4 Addition of various compounds to the purified protein

The purified DafA(L2V)_{Tth} was supplemented with a variety of compounds in order to find conditions for an increased solubility and stability. The additives used are summarized in Table 3-1.

Table 3-1: Effect of various compounds on DafA(L2V)_{Tth} solubility

Compound added	Effect on solubility	Concentration increase
4 M urea	+	~ 2 x
6 mM CHAPS	+	~ 2 x
0.1 % Brij 58P	+	~ 2 x
1 M NDSB-195	+	~ 4 x
1 M NDSB-201	+	-
1 M NDSB-256	+	-
Various Salts	-	-

The concentration increase is shown only when it is considerable higher. NDSB = Non-Detergent Sulphobetaines.

Table 3-1 shows that NDSB-195 was the most effective additive from the pool of compounds analyzed. Non-detergent sulphobetains are small amphiphilic substances, which seem to have positive effects on protein solubility and protein refolding (Vuillard et al., 1995; Goldberg et al., 1995). NDSB-195 efficiency in stabilization of DafA(L2V)_{Tth} was concentration-dependent, an increase of protein concentration being obtained only at a concentration of 1 M.

3.1.3 Effect of chaotropic agents on DafA(L2V)_{Tth} structure analyzed by fluorescence spectroscopy

DafA(L2V)_{Tth} possesses intrinsic fluorescence due to two tryptophane and three tyrosine residues. Because of their increased hydrophobicity these residues are usually found in the inner regions of folded proteins. Tyrosine and especially tryptophane are very useful in monitoring the changes occurring in the tertiary structure of a protein because their fluorescence is highly dependent on the polarity of the environment. The fluorescence emission of a solvent exposed tryptophane within an unfolded protein will be close to 350 nm. In comparison, the fluorescence emission of a tryptophane buried in the interior of a folded protein is lower than 350 nm, directed toward 320 nm (hypsochromic effect).

When excited at 280 nm DafA(L2V)_{Tth} shows an emission maximum around 343 nm indicating tryptophane emission. Although the tyrosine is also excited at 280 nm, its emission is covered by the one of tryptophane, and therefore no maximum is observed at 305 nm.

An emission maximum at around 340 nm corresponds to the emission of an indole chromophore placed at the protein surface. It is assumed to be in contact with bound water and other polar groups (Ladokhin, 2000). Therefore the following possibilities for the topology of tryptophane residues in DafA(L2V)_{Tth} might be considered: one or both are exposed at the protein surface or one or both are situated in the interior of the protein, but surrounded by a rather polar environment. Unfolding studies using chaotropic agents might also offer valuable information about the arrangement of these residues within the DafA(L2V)_{Tth} structure.

The effect of chaotropic agents like urea and guanidinium hydrochloride (GdmCl) on the tertiary structure of highly purified DafA(L2V)_{Tth} was analyzed by measuring the change of tryptophane emission maximum. The fluorescence emission was measured after incubation of the protein (3 hours at room temperature) with increasing concentrations of urea or GdmCl (Figure 3-5). It can be seen that the two compounds have a different effect on DafA(L2V)_{Tth}, although both are considered to be protein denaturants. While the denaturing effect of GdmCl becomes apparent at a concentration higher than 3 M, the structural stability of the DafA(L2V)_{Tth} is barely affected by urea even at the maximal concentration. The reduction of the fluorescence signal caused by GdmCl denaturation is accompanied by a shift of the emission maximum, the completely denatured protein showing a maximum at 348 nm. This slight shift of 5 nm is the result of further exposure of both tryptophane residues to the solvent indicating that at least one of them is embedded inside the structure.

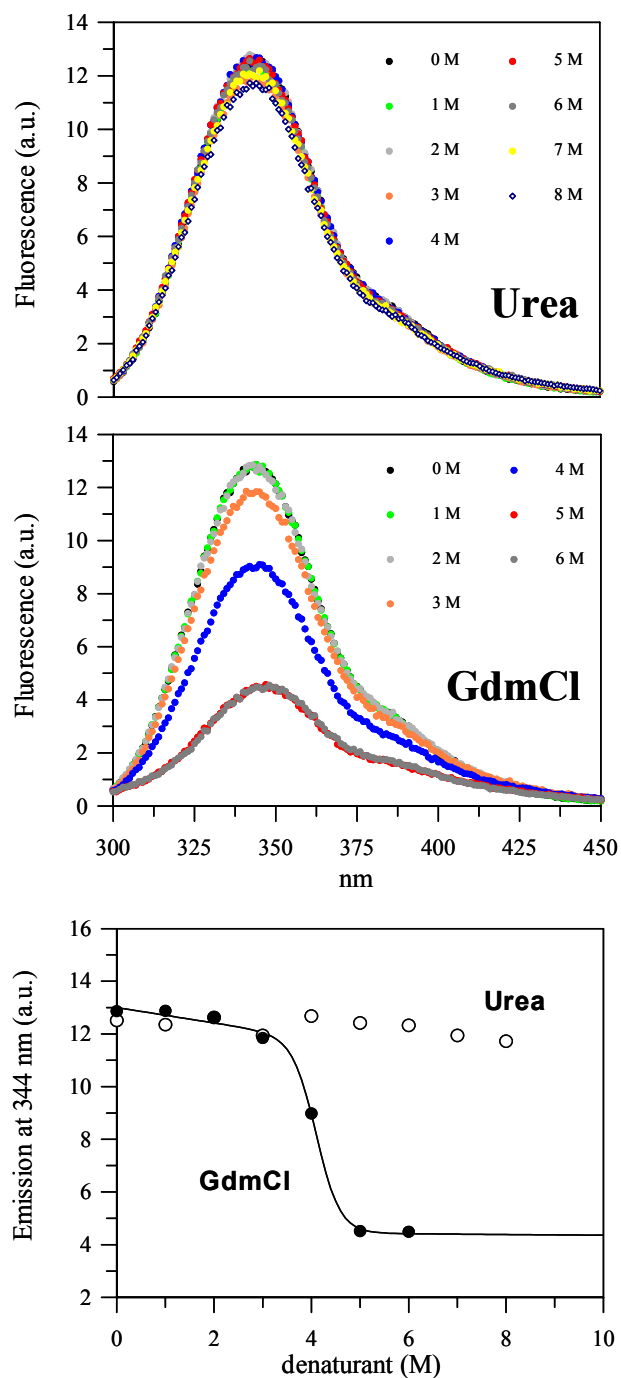


Figure 3-5: Emission spectra of DafA(L2V)_{Tth} in the presence of chaotropic agents. The upper and central panels show the emission spectra of 5 μ M DafA(L2V)_{Tth} incubated for 3 hours at room temperature with increasing concentration of urea or guanidinium hydrochloride. The lower panel presents the denaturation curves obtained by plotting the maximum fluorescence emission (343 nm) against the concentration of denaturant. The lower panel shows also the non-linear fit for the GdmCl-induced transition using equation **Equation 2-5**. The spectra were taken at 25°C in a buffer containing 50 mM HEPES/NaOH pH 7.5, 100 mM KCl, 5 mM MgCl₂ and 2 mM EDTA using an Aminco Bowman 8100 (SLM, Illinois, USA). Excitation/Emission: 280/350 nm with corresponding bandwidths of 1/16 nm. Integration time: 0.1 seconds.

Figure 3-5 lower panel shows the plotting of maximum fluorescence emission of the samples for both urea and GdmCl denaturation. GdmCl-induced transition was fitted with the equation Equation 2-5 (Santoro and Bolen, 1988). The value obtained for the free enthalpy of stabilization (ΔG_{stab}^0) was close to 42 kJ/mol. This value is in agreement to the average value for the energy of stabilization of medium size globular proteins which is on the order of 50 kJ/mol. Using Equation 2-6 a value of 4.1 M GdmCl was obtained for the midpoint of the transition from native to denatured state.

Although urea can solubilize inclusion bodies containing DafA(L2V)_{Tth} this process is obviously not associated with unfolding of the protein as it is indicated by the emission spectra. Therefore urea should not be considered a denaturant but rather a solubilizing agent for DafA(L2V)_{Tth}. This property of urea was taken in consideration when performing further experiments with DafA(L2V)_{Tth} (see 3.1.2.4, 3.1.5).

3.1.4 Stability of DnaK_{Tth}-DnaJ_{Tth}-DafA(L2V)_{Tth} complex in urea

The stability towards urea is not only characteristic for DafA(L2V)_{Tth}, but also for the whole group of proteins belonging to the DnaK_{Tth} chaperone system (Klostermeier, 1998). These proteins also share the same sensitivity to the denaturing effect of guanidinium hydrochloride.

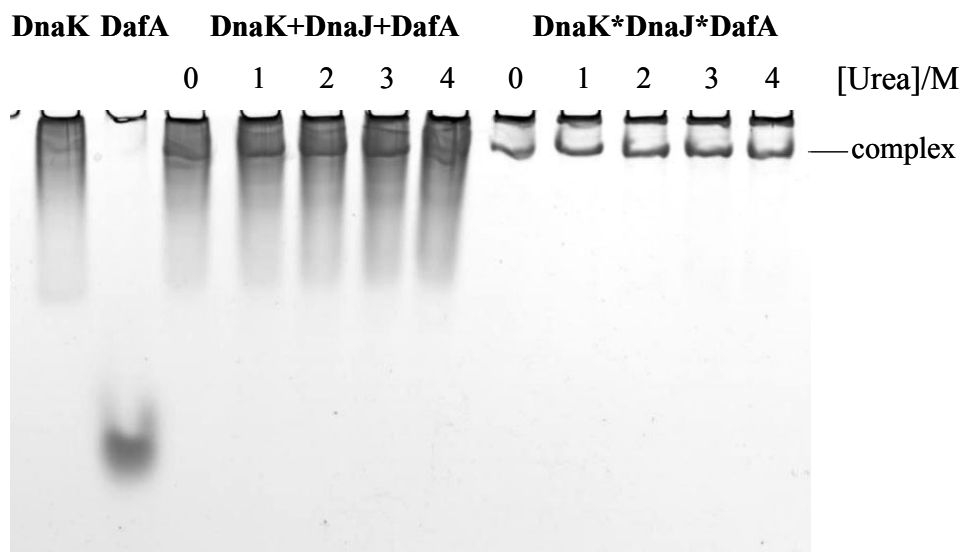


Figure 3-6: Effect of urea on DnaK_{Tth}-DnaJ_{Tth}-DafA(L2V)_{Tth} complex visualized by native PAGE. DnaK_{Tth}, DnaJ_{Tth} and DafA(L2V)_{Tth} were mixed in an equimolar ratio (10 μ M each) and incubated for 1 hour at room temperature in the presence of urea (0-4 M). 10 μ M of purified complex was incubated with urea under the same conditions. The samples were applied on an 8 % polyacrylamide native gel and the bands were stained with Coomassie. 10 μ M of DnaK_{Tth} and DafA(L2V)_{Tth} were applied as controls. DnaJ_{Tth} cannot be visible on the gel due to its basic pH. DafA represents the DafA(L2V)_{Tth} variant. DnaK+DnaJ+DafA is the complex formed by incubation of the components. DnaK*DnaJ*DafA is the purified complex.

In order to test whether urea affects the interaction between DafA(L2V)_{Tth} and its two partners, binding experiments were performed in the presence of 1 M to 4 M urea.

Also, the complex over-expressed and purified as a whole ensemble from *E. coli* was treated with urea and its dissociation was tested. The isolated proteins were incubated in an equimolar ratio in the presence of urea. Additionally, the purified complex was treated under the same conditions. The samples were then subjected to native PAGE and the association of the components or dissociation of the complex was visualized by Coomassie staining.

The results presented in the Figure 3-6 show that, in a concentration range of 1-4 M, urea does not have a significant influence on either the formation of the complex from individual components or on the disassociation of the purified complex. Under the conditions tested all three proteins are stable and form the complex.

3.1.5 Thermal stability of DafA(L2V)_{Th} analyzed by DSC

Originating from a thermophilic organism, DafA(L2V)_{Th} in principle is expected to show enhanced stability at increased temperatures, similar to the other members of the DnaK_{Th} chaperone system (Klostermeier et al., 1998; Groemping and Reinstein, 2001). It was possible to determine the melting point and other thermodynamic parameters of DafA(L2V)_{Th} from thermal denaturation curves using *Differential Scanning Calorimetry* (DSC).

In a DSC experiment the heat capacity of the protein solution is measured at constant pressure. The energy absorption at protein unfolding is calculated by comparing the protein sample with a buffer sample treated under identical conditions. The output of a DSC experiment is a curve obtained by plotting the heat capacity versus temperature. Each peak of the curve represents transitions from one state (e.g. native) to another (e.g. denatured) and the maximum of the peak represents the melting temperature (transition) of one particular protein. The modification of the baseline before and after denaturation of the protein represents the difference in the heat capacity between the native state and the denatured one.

A relevant DSC experiment for DafA(L2V)_{Th} was possible only when the protein was concentrated to 1 mg/ml using 4 M urea. As tryptophane fluorescence and native PAGE shows (see above) urea is not destabilizing the secondary and tertiary structure of DafA(L2V)_{Th} and it is considered to be a solubilizing agent for this protein.

The thermal unfolding of DafA(L2V)_{Th} is shown in Figure 3-7. The protein was heated from 25°C to 120°C with a rate of 60°C/hour. Two thermal transitions can be observed, one with a maximum at ca. 89°C and the second one with a maximum at ca. 110°C (see scan 1). Thus, DafA(L2V)_{Th} is a thermostable protein.

After the first heat denaturation, the sample was cooled rapidly, and a second scan (under the same conditions as the first scan) was performed to test for reversibility of the process. For a “clean” thermodynamically controlled folding the curve after the first run and the one obtained after recooling of the sample must be identical. In case of

DafA(L2V)_{Tth} only ca. 80 % of the initial protein molecules are refolded. The enlargement of the first transition width visible on the left side of the peak is a clear sign for irreversible denaturation of a fraction of DafA(L2V)_{Tth} molecules. Nevertheless, despite this loss of protein through irreversible aggregation, the denaturation of DafA(L2V)_{Tth} is approximately reversible and therefore, the thermodynamic parameters of unfolding were calculated using the Microcal-Origin for DSC software.

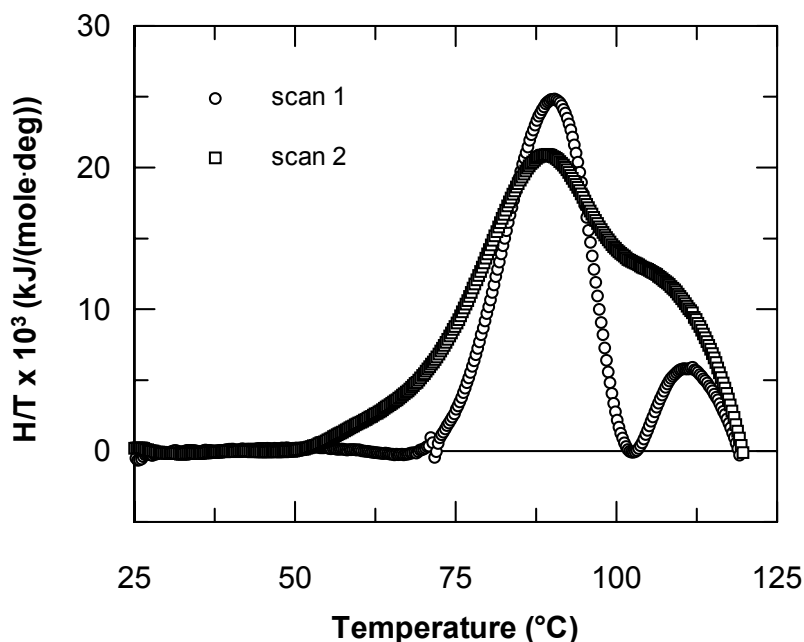


Figure 3-7: Thermal unfolding of DafA(L2V)_{Tth}. 1 mg/ml (~117 μ M) DafA(L2V)_{Tth} in 4 M urea, 50 mM HEPES/NaOH pH 7.5, 300 mM KCl, 1 mM MgCl₂ was heated twice from 25 to 120°C with a rate of 60°C/hour. The second scan was taken after the protein solution was cooled down to 25°C. The buffer effect and the baseline were extracted from the protein signal. The heat capacity (H/T) was normalized to the protein concentration.

Table 3-2 shows the values for the thermodynamic parameters obtained after fitting the curve of the first scan with a “non-2-state” model considering that two transitions take place corresponding to three folding states of DafA(L2V)_{Tth}. Briefly, this model takes in consideration that the protein denaturation occurs in more than one step (from native state to denatured state). Usually globular proteins follow the unfolding pattern characterized by a “two state” model. Such proteins have only one structural domain, the whole protein behaving as a unit during unfolding (unfolding transition is cooperative) (Leharne and Chowdry, 1998).

The “non-2-state” model fit provided the following thermodynamic parameters for each transition of DafA(L2V)_{Tth} unfolding: the melting point, T_m (when 50 % of the molecules are unfolded), the calorimetric enthalpy, H_{cal} , and the van't Hoff enthalpy, H_{vH} . The calorimetric enthalpy is a direct measure of the enthalpy of the unfolding process. It represents the area under the transition peak (variation in the absorbed heat per mole) and

is concentration dependent. On the other hand, the van't Hoff enthalpy is not a direct measure of the unfolding enthalpy, it is independent of the concentration and determined by the shape of the unfolding curve (variation in the absorbed heat per unfolding unit)

Table 3-2: Thermodynamic parameters for DafA(L2V)_{Tth} thermal denaturation

T_{m1} (°C)	$H_{cal1} \cdot 10^5$ (kJ/mol)	$H_{vH1} \cdot 10^5$ (kJ/mol)	T_{m2} (°C)	$H_{cal2} \cdot 10^5$ (kJ/mol)	$H_{vH2} \cdot 10^5$ (kJ/mol)
89.80	3.6	3.11	110.0	1.05	2.81

T_m = melting point; H_{cal} = calorimetric enthalpy (area under the peak, concentration dependent); H_{vH} = van't Hoff enthalpy (shape of the denaturation curve, concentration independent)

The ratio between the van't Hoff enthalpy (H_{vH}) and the calorimetric enthalpy (H_{cal}) is a valuable measure of the transition's cooperativity. The H_{vH}/H_{cal} ratio corresponding to the first transition is close to unity (thus $H_{vH} \approx H_{cal}$). Since this value is characteristic for cooperative transition during which denaturation takes place in a single step without any intermediates accumulating, the observed transition has to be attributed to the unfolding of the DafA(L2V)_{Tth} monomers. For the second transition (110°C), the value of H_{vH}/H_{cal} ratio is larger than unity indicating that there might be intermolecular interactions such as changes in the state of oligomerization (including aggregation) (Leharné and Chowdry, 1998). Consequently, the observed transition might correspond to monomerization or denaturation of DafA(L2V)_{Tth} oligomers. Although DafA(L2V)_{Tth} is prone to aggregation, it can be assumed that this transition is the result of the disassembly/denaturation of DafA(L2V)_{Tth} oligomers rather than of DafA(L2V)_{Tth} aggregates formation, because a signal from aggregated molecules would be expected at the beginning of the spectrum (the lowest thermal stability).

Interestingly, the H_{vH}/H_{cal} ratio for the second transition is close to a value of three. This indicates that there are three cooperative unfolding units per monomer protein (Privalov and Potekhin, 1986). Since DafA(L2V)_{Tth} is too small to be a multi-domain protein, the value obtained for the second transition might indicate the presence of DafA(L2V)_{Tth} trimers. Although it is difficult to establish the oligomerization state of DafA(L2V)_{Tth} due to the aggregate formation, analytical ultrafiltration experiments (equilibrium centrifugation; in collaboration with Dr. Urbanke, Medizinische Hochschule, Hannover) suggested that DafA(L2V)_{Tth} monomers might associate to form a higher order oligomer (trimer or tetramer). Therefore, the possibility that the second transition corresponds to monomerization or denaturation of DafA(L2V)_{Tth} trimers is conceivable. Further DSC experiments using various DafA(L2V)_{Tth} concentrations might give a clear answer as long as oligomerization is a concentration-dependent process.

3.1.6 Inhibitory effect of DafA(L2V)_{Tth} on luciferase refolding assisted by DnaK_{Tth} chaperone system

3.1.6.1 Luciferase as a model substrate

Luciferase is a one of the model protein substrate widely used for analysis the DnaK chaperone system from *E. coli* (Schroder et al., 1993; Szabo et al., 1994; Buchberger et al., 1996; Lu and Cyr, 1998; Souren et al., 1999). Luciferase catalyzes the transformation of luciferin to oxyluciferin, a reaction energetically sustained by ATP. This process is accompanied by emission of light which is a direct measure of luciferase activity (DeLuca, 1976). Thus, the emitted light is also a direct measure of refolding yield in the chaperone refolding assays. However, luciferase is very sensitive to temperature. In the refolding assays, the refolding efficiency of luciferase is determined also by the temperature at which the experiments are performed. Even at 30°C luciferase is denatured at longer incubation times. Also, the luciferase refolding is dependent on the ratio of chaperones used in the refolding assay. The concentrations of thermophilic chaperones used here were experimentally determined to be optimal for an efficient refolding (Groemping et al., 2001). Another disadvantage of this protein substrate-model is the decay of luminescence in time due to product inhibition (Figure 3-8). This effect is correlated to the amount of native and active luciferase.

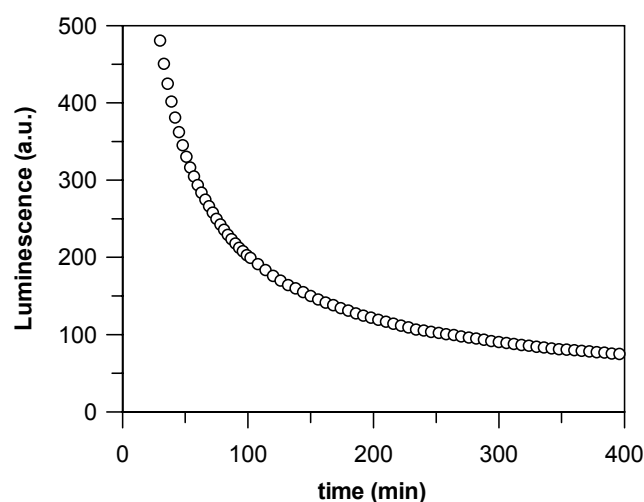


Figure 3-8: Chemical conversion of luciferin by luciferase in continuous assay. 0.8 μ M native luciferase was diluted 10-fold in assay buffer (25 mM HEPES/NaOH, pH 7.5, 50 mM KCl, 15 mM MgCl₂, 1 mM ATP, 2 mM DTE, 240 μ M coenzyme A, 0.05 mg/ml BSA, 0.1 mM luciferin) and the luminescence was monitored in a continuous assay.

3.1.6.2 Effect of DafA(L2V)_{Tth} on luciferase refolding

The effect of DafA(L2V)_{Tth} on luciferase refolding was initially observed by Dr. Yvonne Groemping (Groemping Y., 2000). The experiments and data presented here are based on these findings.

Studies with fluorescent model peptides have indicated that binding of DafA(L2V)_{Tth} and substrate proteins to DnaK_{Tth}-DnaJ_{Tth} chaperones may be competitive (Klostermeier et al., 1999). The finding of a model-protein substrate that would bring new evidences to sustain this hypothesis was an important requirement. Luciferase model is therefore a very useful tool that measure directly the influence of DafA(L2V)_{Tth} on the refolding activity of DnaK_{Tth} chaperone system. The thermophilic system, though originating from an organism that lives at about 75°C, is fully functional at 30°C in a continuous luciferase refolding assay (Groemping et al., 2001). The refolding of GdmCl-denatured luciferase assisted by DnaK_{Tth} chaperone system and the influence of DafA(L2V)_{Tth} on this process are shown in Figure 3-9.

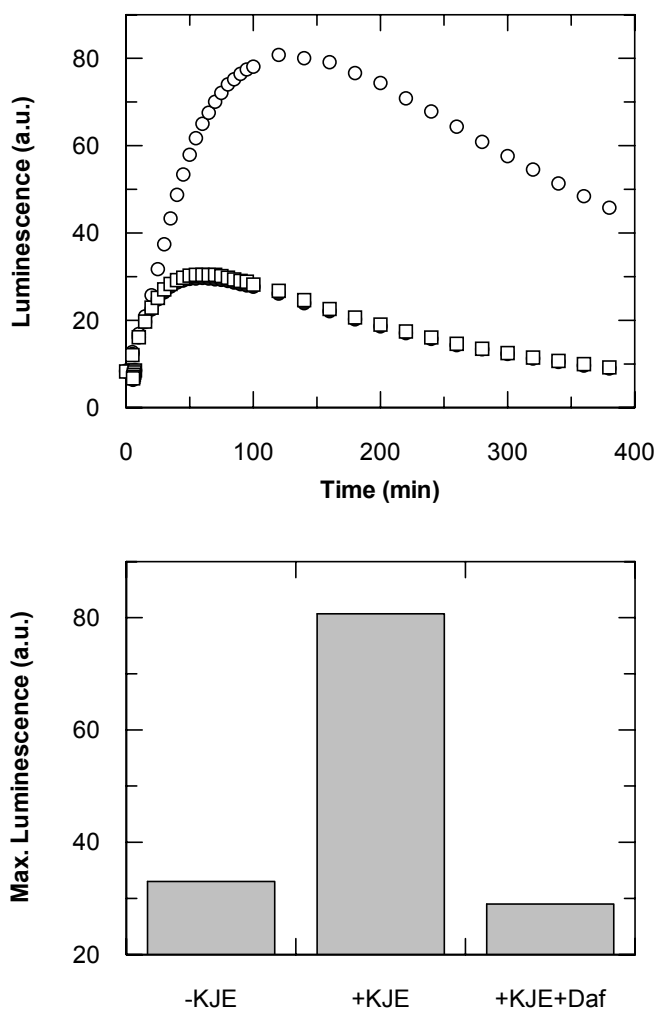


Figure 3-9: Influence of DafA(L2V)_{Tth} on luciferase refolding. After denaturation (final concentration 0.08 μM) in a buffer containing 5 M GdmCl, luciferase (□) was incubated in assay buffer (25 mM HEPES/NaOH, pH 7.5, 50 mM KCl, 15 mM MgCl₂, 1 mM ATP, 2 mM DTE, 240 μM coenzyme A, 0.05 mg/ml BSA, 0.1 mM luciferin) with 3.2 μM DnaK_{Tth}, 0.4 μM DnaJ_{Tth} and 0.2 μM GrpE_{Tth} in the absence (○) or in the presence (●) of 2 μM DafA(L2V)_{Tth}. The continuous assay was performed at 30°C. The upper panel shows the raw data and the lower panel shows the maximum luminescence obtained for various samples. The maximum luminescence is a direct measure of the luciferase refolding yield. KJE represents the mixture of DnaK_{Tth}, DnaJ_{Tth} and GrpE_{Tth}.

The addition of DafA(L2V)_{Tth} to the refolding mixture has dramatic consequences on the luciferase renaturation. Groemping Y. showed in a luciferase refolding experiment that the luciferase refolding is decreasing with increasing DafA(L2V)_{Tth} concentration (Groemping Y., 2000). The presence of a 25-fold excess of DafA(L2V)_{Tth} over the concentration of denatured luciferase in the refolding mixture leads to a reactivation yield close to nil. This inhibitory effect of DafA(L2V)_{Tth} is obvious in Figure 3-9. In this experiment DafA(L2V)_{Tth} was added to the mixture prior to denatured luciferase. Whereas in the presence of DnaK_{Tth} chaperone system the luciferase activity after ca. 100 minutes is considerable, it is similar to the one of denatured luciferase in the presence of DafA(L2V)_{Tth}. This is an indication that DafA(L2V)_{Tth} suppresses the association of the substrate. Although DafA(L2V)_{Tth} is essential to mediate the interaction of DnaJ_{Tth} and DnaK_{Tth}, it is not part of the active chaperone system.

3.1.7 Cysteine mutants engineering

All proteins belonging to the DnaK chaperone system from *Thermus thermophilus* are deficient in cysteine residues. This makes them excellent candidates for fluorescent labeling at a specific cysteine residue, which can be engineered by site directed mutagenesis. Using this approach several cysteine mutants of DafA(L2V)_{Tth} have been constructed, expressed in *E. coli* and purified. Various positions were selected for mutagenesis in order to cover the entire sequence of the protein. The position and the mutated amino acids are presented in the Figure 3-10.

The functional integrity of the cysteine mutants was verified by analyzing their ability to form a complex with DnaK_{Tth} and DnaJ_{Tth} in native gel electrophoresis. The results showed that incubation of the proteins under native conditions leads to the appearance of a band characteristic for the heterotrimeric complex. Also, the addition of mutant proteins to the luciferase assay (in the conditions described above) showed the same inhibitory effect on luciferase refolding as DafA(L2V)_{Tth}. Both results show that none of the various point mutations altered the functional properties of DafA(L2V)_{Tth} and the mutants were therefore used for further experiments.



Figure 3-10: The engineered DafA(L2V)_{Tth} point mutants. The bold letters with an asterisk represents the amino acids replaced with a cysteine residue and subsequently labeled with various fluorophores. The position of the selected mutations was correlated with the predicted secondary structure of DafA(L2V)_{Tth} using GOR IV method (C, random coiled; H, α -helix; E, extended strand). Cylinders are representing the α -helixes (H).

3.1.8 Dynamics of DnaK_{Tth}-DnaJ_{Tth}-DafA(L2V)_{Tth} complex formation at equilibrium

One of the features of the DnaK_{Tth}-DnaJ_{Tth}-DafA(L2V)_{Tth} complex is its increased stability as a result of the high affinity existent between the three partners. The affinity constant was initially determined by measuring the heat release upon complex formation using isothermal titration calorimetry (ITC). From these measurements an apparent dissociation constant (K_D) of ca. 33 nM was obtained for the formation of the ternary complex (Klostermeier et al., 1999). However, this dissociation constant does not represent a true K_D value. With the help of the fluorescently labeled cysteine mutants it was now possible to obtain a more accurate K_D for the complex association. These fluorescence measurements not only allowed the determination of the affinity constant, but also the rates constants for the formation and dissociation of the complex at equilibrium.

For the fluorescence experiments the variant DafA(L2V)S14C_{Tth} was used after its covalent coupling with the fluorescent dye IANBD-ester. Although NBD is not the most desirable fluorophore (low photostability, low extinction coefficient), its fluorescence properties are very sensitive to the environmental changes. Because it was expected that binding of DafA(L2V)S14C_{Tth} to DnaK_{Tth} and DnaJ_{Tth} will lead to such environmental changes (hydrophobicity increase), we took advantage of this feature of NBD in analyzing the complex formation.

As seen in Figure 3-11 the fluorescent signal of the NBD-labeled DafA(L2V)S14C_{Tth} sample is decreasing slowly in time due to the photo-bleaching of the fluorophore and the slow aggregation of the protein (black dots). Addition of both DnaK_{Tth} and DnaJ_{Tth} brings a significant increase in the signal amplitude as a result of complex formation (blue dots). It is noticeable that the addition of only one interaction partner (DnaK_{Tth}-green or DnaJ_{Tth}-red) to the labeled protein does not have a considerable influence on the fluorescence indicating no binary complexes formation. However, a stabilization of the signal after addition of DnaK_{Tth} or DnaJ_{Tth} can be observed, with more pronounced increase in case of DnaJ_{Tth}. This might be the result of weak interactions occurring between two partners, which finally facilitate the rapid association of the complex in the presence of the third partner.

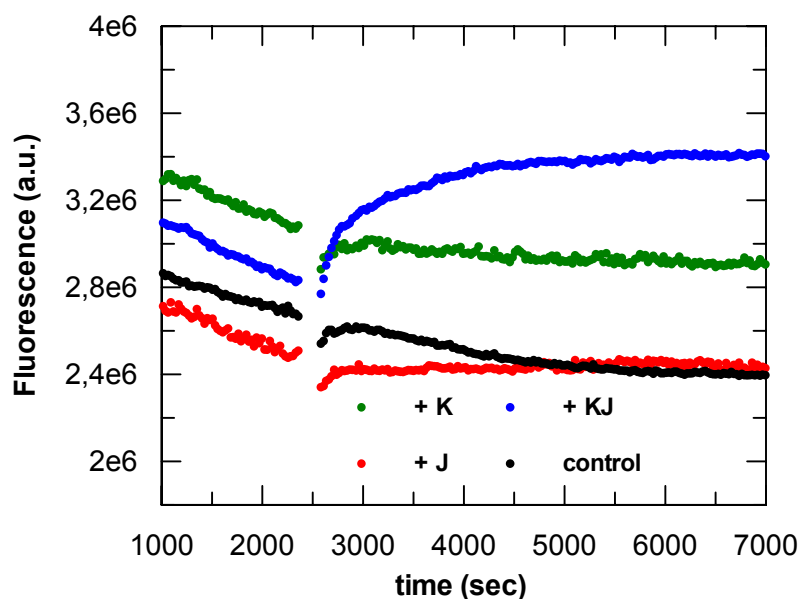


Figure 3-11: Interaction between DafA(L2V)S14C_{Tth}-NBD with DnaK_{Tth} and DnaJ_{Tth} (fluorescence raw data). 0.2 μ M DafA(L2V)S14C_{Tth}-NBD (control) were mixed with 0.4 μ M DnaK_{Tth} (+ K) or 0.4 μ M DnaJ_{Tth} (+ J) or 0.4 μ M of each (+ KJ). The measurements were done at 25°C in 50 mM Tris/HCl pH 7.5, 100 mM KCl, 2 mM EDTA, 10 % glycerol and 0.2 mM CHAPS using a FluoroMax 2 spectrophotometer. Excitation/Emission: 495/545 nm with corresponding bandwidths of 1/2 nm. Integration time: 5 seconds.

Because a direct measurement of the association rate constant k_{on} is not possible, it was calculated using the apparent association rate constant k_{obs} that can be determined experimentally. In order to calculate k_{on} from the measured k_{obs} it was necessary to consider DnaK_{Tth} and DnaJ_{Tth} as being a single “ligand” for DafA(L2V)S14C_{Tth} under pseudo-first order reaction conditions (see 7.1.1, Equation 7-3). The apparent association rate constant was experimentally measured by keeping the concentration of NBD-labeled DafA(L2V)S14C_{Tth} constant and varying the concentrations of DnaK_{Tth} and DnaJ_{Tth} added. As shown in Figure 3-12A the curves obtained could be fitted with a simple exponential equation. From this fit an apparent association constant was obtained for each concentration of DnaK_{Tth}-DnaJ_{Tth} used (Figure 3-12B). By plotting the apparent association constants against the concentration of the added proteins and using a linear regression equation an association rate constant k_{on} (slope) of $9.3 \cdot 10^3 \text{ M}^{-1} \text{ s}^{-1}$ and a dissociation rate constant k_{off} (intercept) of $1.3 \cdot 10^{-3} \text{ s}^{-1}$ were obtained (linear regression equation $k_{obs} = k_{on} \cdot [\text{Ligand}] + k_{off}$).

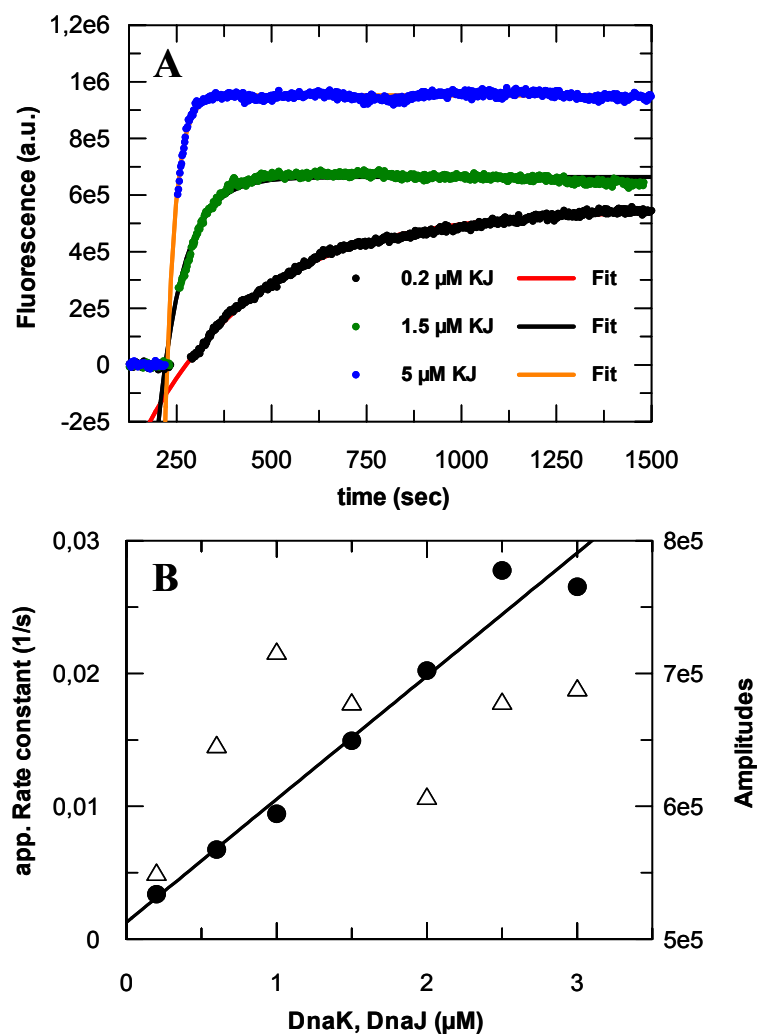


Figure 3-12: Association of DafA(L2V)S14C_{Tth}-NBD to DnaK_{Tth} and DnaJ_{Tth}. (A) Example of increase in fluorescence after addition of various concentrations of DnaK_{Tth} and DnaJ_{Tth} to DafA(L2V)S14C_{Tth}-NBD. 0.3 μM DafA(L2V)S14C_{Tth}-NBD were mixed with different concentrations of DnaK_{Tth} and DnaJ_{Tth} under the same conditions as in Figure 3-11. After subtraction of the control (see Figure 3-11) the curves were fitted with a simple exponential equation. (B) Complex formation. The apparent rate constants k_{obs} (●) for the complex formation were obtained as shown in (A) and plotted against the concentration of DnaK_{Tth} and DnaJ_{Tth} added. After fitting with a linear regression equation an association constant $k_{on} = 9.3 \cdot 10^3 \text{ M}^{-1} \text{ s}^{-1}$ (slope) and a dissociation constant $k_{off} = 1.3 \cdot 10^{-3} \text{ s}^{-1}$ (intercept) were obtained. The amplitudes for each measurement are also shown (△).

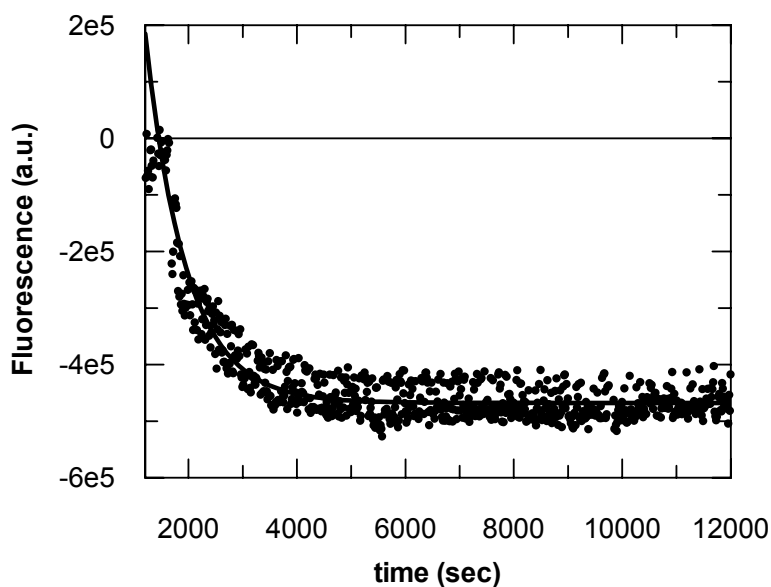


Figure 3-13: Dissociation of DafA(L2V)S14C_{Tth} from DafA(L2V)S14C_{Tth}-NBD*DnaK_{Tth}*DnaJ_{Tth} complex. The proteins were incubated in a 1:1:1 ratio (0.3 μ M of each). After the equilibrium was reached, 3 μ M of DafA(L2V)_{Tth} was added. The curve obtained was fitted with a simple exponential equation that gave a dissociation rate constant $k_{off} = 0.0013 \text{ s}^{-1}$.

Although the described approach can be successfully used for the accurate determination of the association rate constant, it is less accurate with respect to the dissociation constant. Hence, for a more accurate estimation of the ternary complex dissociation rate constant, displacement experiments were carried out as shown in Figure 3-13. From the fitting of the dissociation curve with a simple exponential equation a value of $1.3 \cdot 10^{-3} \text{ s}^{-1}$ was obtained for k_{off} , which is identical with the k_{off} value obtained *via* measuring the k_{obs} .

Since the affinity constant is the ratio between complex dissociation rate constant and the association rate constant (see 7.1, Equation 7-4) it was now possible to obtain an accurate K_D for the formation of the ternary complex, which has a value of ca. 140 nM.

3.1.9 Structural analysis of DafA(L2V)_{Tth} using HSQC-NMR spectroscopy

In order to obtain more information about DafA_{Tth} function, structural studies were carried out using the DafA(L2V)_{Tth} variant. Due to its low molecular weight, DafA(L2V)_{Tth} is a good candidate for NMR experiments. DafA(L2V)_{Tth} was ¹⁵N-labeled and prepared as described in the Methods section, and subjected to two-dimensional HSQC-NMR. These NMR experiments were performed in collaboration with Dr. Peter Bayer.

In Figure 3-14 the HSQC-NMR resulting spectrum of DafA(L2V)_{Tth} is shown. Each resonance signal found in the plot results from an amide group of the protein. DafA(L2V)_{Tth} is comprised of 78 amino acids including one proline residue. Prolines do not appear in the spectrum due to the lack of an NH proton. Also, due to fast exchange, the

amide group signal of the N-terminal residue is not visible. Additional two signals belonging to the indole NH groups of the two tryptophanes can be also observed. Taking all this into account a total of 78 NH signals should be found in DafA(L2V)_{Tth} spectrum. However only ~ 50 residues are detected under the conditions used (ca. 20 hours of spectrum recording).

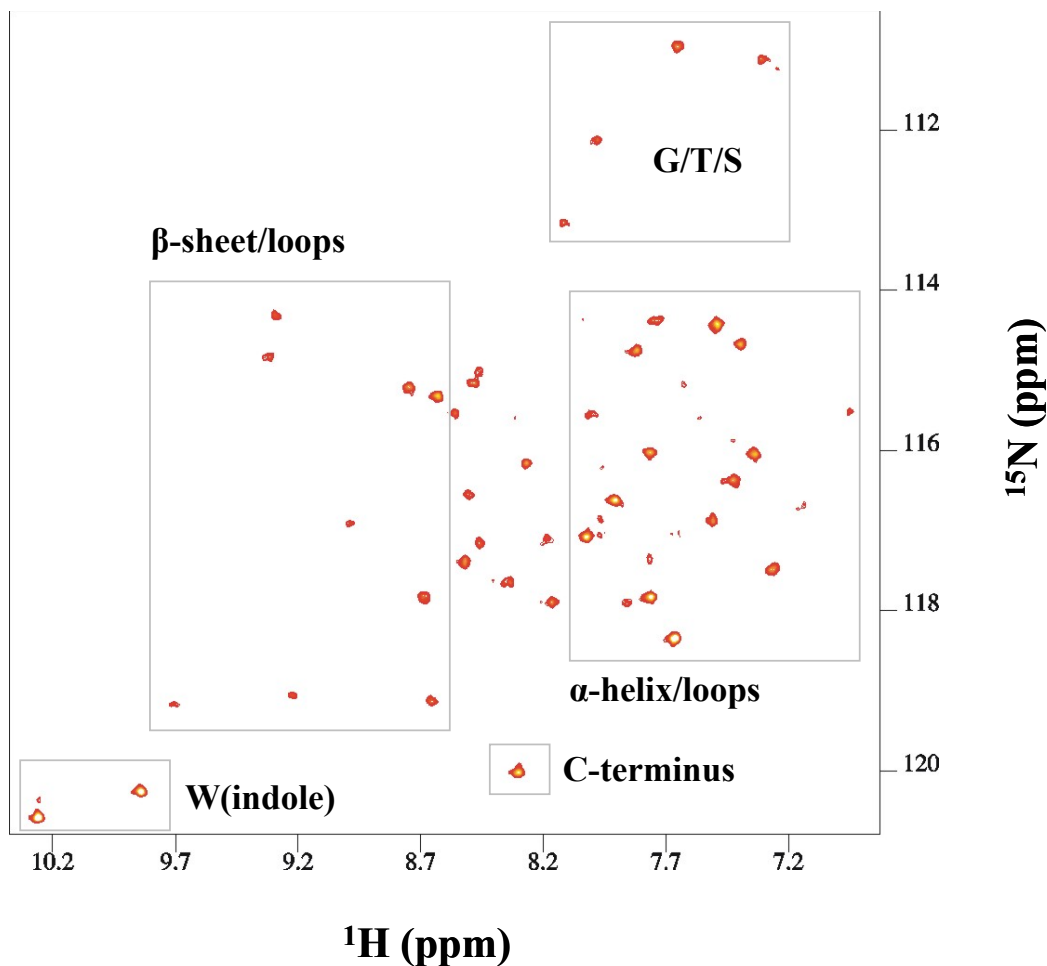


Figure 3-14: HSQC-NMR spectrum of DafA(L2V)_{Tth}. DafA(L2V)_{Tth} was labeled with ^{15}N by growing the DafA(L2V)_{Tth} producing cells in a minimum medium containing ^{15}N -ammonium chloride. The labeled protein was used at a concentration of 80 μM . The spectrum was recorded for ca. 20 hours. The boxes show signals that could be assigned to certain residues or to secondary structure elements.

The distribution (dispersion along both frequency axes) of the amide group signals indicates a folded state of the protein. Studies carried out by Wüthrich and Wishart (Wuethrich, 1986; Wishart et al., 1995) have shown that the chemical shifts of resonances of random coil peptides or unfolded proteins in HSQC spectrum have very low dispersion and are found between 8 and 8.4 ppm at the hydrogen frequency axis. Shifts to lower or higher ppm values are found for structured or at least partly folded molecules. However, exactly such shifts of resonances are found in the HSQC spectrum of DafA(L2V)_{Tth}. They

are characteristic for proteins comprising helical elements, beta-strands and loop regions (see boxes in Figure 3-14).

An additional indication for the folded state of DafA(L2V)_{Tth} is the shift of one of the indole NH groups to ppm values of about 9.8. A tryptophane residue, which exhibits its side chain to the surface or is located in an unfolded region (e.g. flexible N-, C-termini) has a shift of about 10.2 ppm. This shift can be also observed here suggesting that one of the tryptophane residues is exposed to the surface of the protein. The other tryptophane of DafA(L2V)_{Tth} is placed in the hydrophobic core or the side chain is partly embedded in the structure. This result is in agreement with the DafA(L2V)_{Tth} emission spectra obtained for the tryptophane fluorescence (see 3.1.3).

Although this study clearly shows that DafA(L2V)_{Tth} comprises secondary structure elements, a determination of its conformation is not straightforward. In order to obtain a higher resolution, and thus the complete number of amino acids, it was necessary to increase the concentration of DafA(L2V)_{Tth}. Several solubilizing agents have been used for this purpose (see 3.1.2.4) since DafA(L2V)_{Tth} alone can hardly be concentrated to 1 mg/ml. Though an increase in the protein concentration was observed in few cases (urea, Brij, CHAPS, NDSBs), the homogeneity of the sample was not satisfactory for the NMR measurements, DafA(L2V)_{Tth} associating into higher order oligomers (or aggregates). The monomer population, important for the quality of the NMR data, could not be enhanced to an adequate level. Also, it has to be noticed that the protein stability (stored at -80°C) was decreasing with time, the best spectrum being obtained only with the freshly prepared protein.

3.1.10 Analysis of various DafA(L2V)_{Tth} mutants

3.1.10.1 Tryptophane mutagenesis and its effect on DafA(L2V)_{Tth} properties

Fluorescence emission characteristics

DafA(L2V)_{Tth} amino acid sequence comprises two tryptophane residues (W7 and W41). Tryptophane emission spectra of DafA(L2V)_{Tth} (see 3.1.3) suggest that these residues are not embedded deep in the structure since the emission maximum is found around 343 nm. However, at least one of these residues must be placed in a less polar region of the protein since guanidinium chloride denaturation leads to a small but visible shift of the emission maximum to a wavelength closer to the pure tryptophane maxima (350 nm).

The information obtained from the tryptophane emission spectra is sustained by the results obtained from HSQC-NMR experiments (see 3.1.9). The NMR spectrum of ¹⁵N-DafA(L2V)_{Tth} had shown that one tryptophane residue is found in the interior of the structure while the other one is found unprotected at the surface of the protein.

Because none of these experiments could determine which tryptophane residue is placed inside and which outside within DafA(L2V)_{Tth} structure, each residue was consecutively replaced with a cysteine residue using site directed mutagenesis. Although cysteine is not the first candidate for replacing a tryptophane residue (usually the mutation Trp/Phe is performed), it was chosen due to the possibility of subsequent labeling with fluorescent probes.

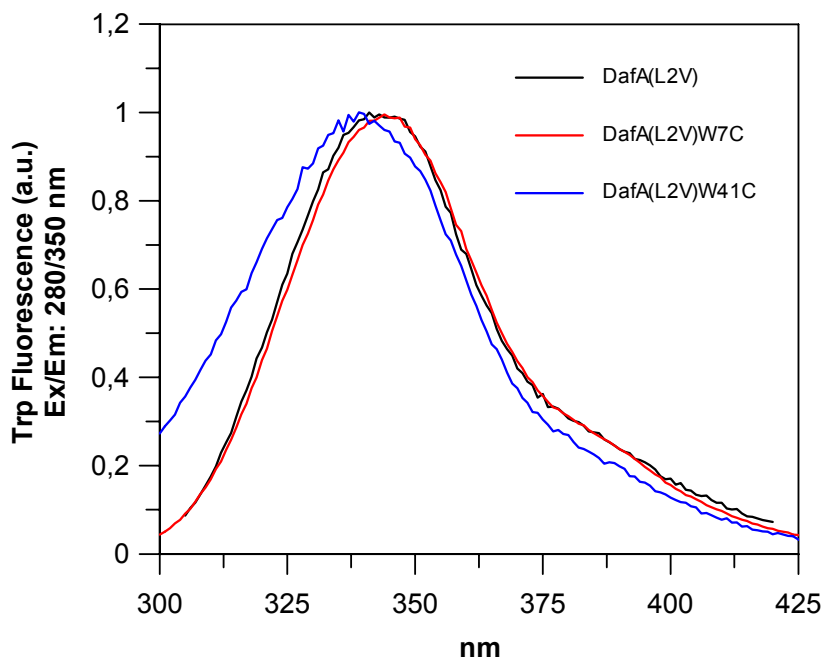


Figure 3-15: Emission spectra of DafA(L2V)_{Tth} tryptophane mutants. The tryptophane emission spectra of 5 μ M DafA(L2V)_{Tth}, DafA(L2V)W6C_{Tth} or DafA(L2V)W40C_{Tth} in 50 mM Tris/HCl pH 7.5, 100 mM KCl, 5 mM MgCl₂, 2 mM EDTA and 2 mM DTE were measured at 25°C using an Aminco Bowman 8100 (SLM, Illinois, USA). Excitation/Emission: 280/350 nm with corresponding bandwidths of 1/16 nm. Integration time: 0.1 seconds.

The emission spectrum of each tryptophane mutant in comparison with DafA(L2V)_{Tth} tryptophane emission is shown in Figure 3-15. The emission scans were taken after excitation of the samples at 280 nm. At this wavelength both tryptophane and tyrosine residues are excited. Similar to the DafA(L2V)_{Tth} variant, none of the tryptophane mutants showed a shoulder at 305 nm that is characteristic for tyrosine emission maximum, although three tyrosine residues are present.

Comparing the spectra of the mutants with the one of DafA(L2V)_{Tth} it is noticeable that they have slightly different emission characteristics. The spectrum obtained for the mutant DafA(L2V)W7C_{Tth} is almost identical to the one of DafA(L2V)_{Tth}. However, a small shift of the emission maximum to higher wavelength is observed. In contrast, the emission maximum of DafA(L2V)W41C_{Tth} is slightly shifted to a lower wavelength compared to the one of DafA(L2V)_{Tth}. Additionally, the spectrum of DafA(L2V)W41C_{Tth} is somewhat wider than the other two proteins (~51 nm compared to 45 nm for

DafA(L2V)W41C_{Tth} and DafA(L2V)_{Tth} when fluorescence intensities are measured at the half width of the spectrum).

From the difference in the emission spectra of those three proteins the following considerations can be made regarding the arrangement of the two tryptophane residues within the DafA(L2V)_{Tth} structure. Tryptophane W7 is most likely the residue buried in the interior of the protein, since, upon its replacement, the emission maximum is slightly shifted to a wavelength closer to the one of free tryptophane. This emission corresponds to the remaining tryptophane residue (W41). Thus, W41 must be the residue exposed on the protein surface. On the other hand, the mutation W41C affects the emission maximum in the opposite direction. The blue shift of the emission maximum at the replacement of W41 indicates again that this residue is found in an unprotected area on the protein surface. The W7 residue still present within DafA(L2V)W41C_{Tth} structure has a maximum closer to a wavelength characteristic for a tryptophane surrounded by a somehow less polar environment. This shows that W7 is embedded into DafA(L2V)_{Tth} structure.

Interaction with DnaK_{Tth} and DnaJ_{Tth}

Very often tryptophane residues are important, if not essential, for a correct folding or for a specific function of proteins. To check whether the replacement of the tryptophane residues does or does not affect DafA(L2V)_{Tth} properties, its ability to form a ternary complex together with DnaK_{Tth} and DnaJ_{Tth} was assessed in native-PAGE electrophoresis.

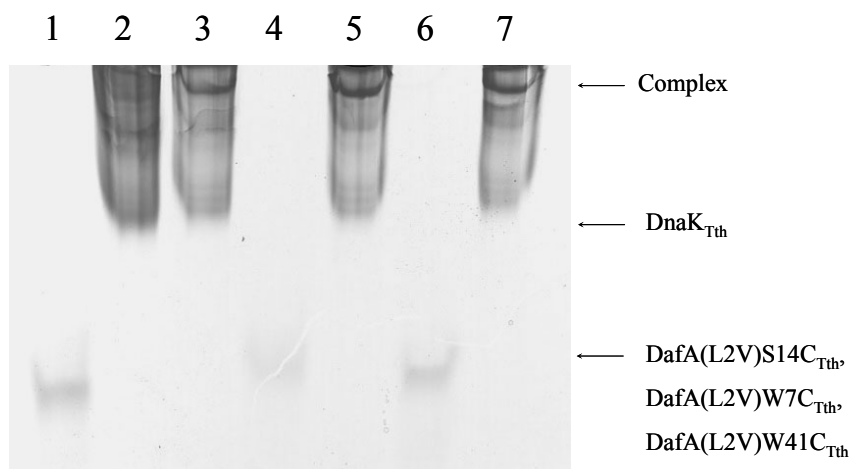


Figure 3-16: Binding of DafA(L2V)_{Tth} tryptophane mutants to DnaK_{Tth} and DnaJ_{Tth} in native-PAGE electrophoresis. 10 μM DafA(L2V)W7C_{Tth} or DafA(L2V)W41C_{Tth} were incubated with 10 μM DnaK_{Tth} and 10 μM DnaJ_{Tth} over night at room temperature. The samples were then applied on a 6 % polyacrylamide native gel. 10 μM DafA(L2V)S14C_{Tth} was used as a control for the complex formation. After gel electrophoresis the proteins were Coomassie-stained. Lane 1, DafA(L2V)W7C_{Tth} control; lane 2: DnaK_{Tth} control; lane 3: DafA(L2V)W7C_{Tth}-DnaK_{Tth}-DnaJ_{Tth} complex; lane 4: DafA(L2V)S14C_{Tth} control; lane 5: DafA(L2V)S14C_{Tth}-DnaK_{Tth}-DnaJ_{Tth} complex; lane 6: DafA(L2V)W41C_{Tth} control; lane 7: DafA(L2V)W41C_{Tth}-DnaK_{Tth}-DnaJ_{Tth} complex.

Incubation of either DafA(L2V)W7C_{Tth} or DafA(L2V)W41C_{Tth} with DnaK_{Tth} and DnaJ_{Tth} leads to the appearance of a band characteristic for the 300 kDa DnaK_{Tth}-DnaJ_{Tth}-DafA(L2V)_{Tth} complex (Figure 3-16). The corresponding bands are migrating at the same height as a control sample represented by the DafA(L2V)S14C_{Tth}-DnaK_{Tth}-DnaJ_{Tth} complex. This is an indication that for both tryptophane mutants the stoichiometry of the components (1:1:1) is preserved.

Because none of the tryptophane mutations is affecting the ability of DafA(L2V)_{Tth} to bind to DnaK_{Tth} and DnaJ_{Tth}, it is fair to assume that these residues are not essential for the interaction between DafA_{Tth} and its two partners. Nevertheless, these mutations might affect the affinity constant for the complex formation (see 3.1.8). In an attempt to check for such affinity changes, each W/C mutant was labeled with IANBD dye. Due to the low efficiency of labeling (~ 5 %), the signal-to-noise ration was not suitable for accurate experiments. Nonetheless, even under these conditions, the formation of the complex and the displacement of the labeled protein by DafA(L2V)_{Tth} could be observed. The change of the fluorescence signal upon complex formation suggest that both tryptophane residues are located at the contact surface either between DafA(L2V)_{Tth} and its two partners or between the DafA(L2V)_{Tth} monomers within the complex.

3.1.10.2 Other cysteine mutants

A number of cysteine mutants were constructed (see 3.1.7) in order to obtain more information about the ternary complex formation and to facilitate functional studies involving DafA(L2V)_{Tth}. The mutations were aimed to cover the entire DafA(L2V)_{Tth} sequence.

The mutants obtained after replacing F31, M51 and A69 residues with a cysteine were labeled with IANBD dye and their ability to interact with DnaK_{Tth} and DnaJ_{Tth} was assessed. Except DafA(L2V)M51C_{Tth} which could not be labeled, these mutants have shown relatively good efficiencies of labeling (more than 60 %).

The labeled proteins were used for fluorescence measurements to test for DnaK_{Tth}-DnaJ_{Tth}-DafA(L2V)_{Tth} complex formation in a similar manner as for the NBD-labeled DafA(L2V)S14C_{Tth} variant. None of these NBD-labeled proteins showed a modification in the fluorescence emission upon addition of DnaK_{Tth} and DnaJ_{Tth}. This result indicates either that the assembly of the ternary complex is perturbed, or that the solvent accessibility of the NBD attached is unaltered when the complex is formed.

To test for the possibility that the ternary complex formation is affected in the case of the DafA(L2V)F31C_{Tth} and DafA(L2V)A69C_{Tth} mutants, native-PAGE electrophoresis experiments have been performed with unlabeled and NBD-labeled proteins. In both cases complex assembly was observed. Thus, neither do the mutations affect binding, nor does NBD interfere with binding of DafA(L2V)_{Tth} variants to DnaK_{Tth} and DnaJ_{Tth}. Therefore,

the lack of emission changes observed during fluorescence measurements is the result of an unaltered solvent accessibility of NBD attached to the proteins.

The observations presented here lead to the conclusion that F31 and A69 residues are not positioned at the interfaces between DafA(L2V)_{Tth} and its two interaction partners or at the interaction sites of DafA(L2V)_{Tth} monomers in the interior of the complex.

3.2 Functional analysis of DafA_{Tth}

3.2.1 Identification of new potential interaction partners of DafA(L2V)_{Tth}

The co-elution of DafA(L2V)_{Tth} with a 260 nm-absorbing molecule was the first indication that DafA_{Tth}'s mediating role in DnaK_{Tth}-DnaJ_{Tth} interaction might be not the sole function of this protein. Since DafA_{Tth} does not share high homology with proteins of known function, a way to obtain more information about another potential role of DafA_{Tth} was to use its primary sequence and the bioinformatics tools available on the internet. Considering the output of the secondary structure prediction program based on GOR method (Garnier J et al., 1996) DafA_{Tth} has a helix-loop-helix secondary structure (Figure 3-10), which is a feature of many DNA/RNA-binding proteins. On the other hand, prediction of the tertiary structure using the 3D-PSSM method (Kelley et al., 2000) also suggests that the fold of DafA_{Tth} might be the one of a DNA- or RNA-binding protein (Figure 3-17).

Fold	Superfamily	Family
=====	=====	=====
SAM domain-like	DNA repair protein Rad51, N-terminal	DNA repair protein Rad51, N-terminal
DNA/RNA-binding 3-helical bundle	"Winged helix" DNA-binding domain	mu transposase, DNA-binding domain
Cytochrome c	Cytochrome c	Two-domain cytochrome c
S15/NS1 RNA-binding domain	S15/NS1 RNA-binding domain	N-terminal, RNA-binding domain
Anti-LPS factor/recA domain	RecA protein, C-terminal domain	RecA protein, C-terminal domain
TetR/NARL DNA-binding domain	TetR/NARL DNA-binding domain	Tetracyclin repressor (Tet-repressor)
RuvA C-terminal domain-like	N-terminal domain of phosphate	N-terminal domain of phosphate
Long alpha-hairpin	Effector domain of the protein	Effector domain of the protein
DNA/RNA-binding 3-helical bundle	"Winged helix" DNA-binding domain	Replication terminator protein
DNA/RNA-binding 3-helical bundle	Homeodomain-like	AraC type transcriptional activator
Cytochrome c	Cytochrome c	monodomain cytochrome c
DNA/RNA-binding 3-helical bundle	"Winged helix" DNA-binding domain	Biotin repressor, N-terminal
DNA/RNA-binding 3-helical bundle	Ribosomal protein L11, C-terminal	Ribosomal protein L11, C-terminal

Figure 3-17: Fold Recognition Results-Sequences alignment using 3D-PSSM Method (Kelley et al., 2000). Results are sorted by E-value, most confident assignment first.

Another line of experiments was based on the low homology existent between the N-terminal region of HspR from *S. coelicolor* (21 % of DafA_{Tth} amino acid sequence is identical with the one of HspR_{Sco}, see alignment in Table 3-3) (Motohashi et al., 1996). HspR is a regulatory protein that modulates negatively the transcription of the dnaK_{Sco} operon (Bucca et al., 1997). Moreover, HspR_{Sco} and DafA_{Tth} share the same genetic localization within the dnaK operon (Figure 3-18).

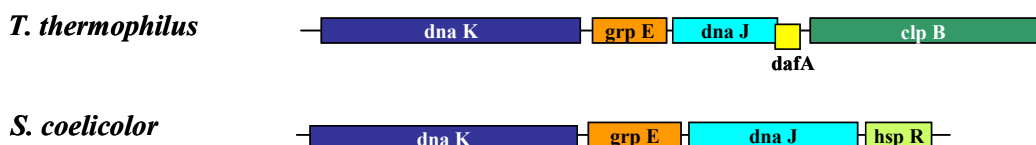


Figure 3-18: Comparison between organization of dnaK gene cluster from *T. thermophilus* and *S. coelicolor*. The dnaK operon is similarly organized in both species except for clpB gene which is located differently in *S. coelicolor*. In *T. thermophilus* dafA gene occupies the same position as hspR in *S. coelicolor*.

HspR_{SCO} on the other hand displays high similarity to the MerR family of eubacterial transcriptional regulators (Bucca et al., 1995). The MerR family is a group of transcriptional activators with similar N-terminal helix-turn-helix DNA-binding domain and C-terminal effector binding regions that are specific to the effector recognized (Brown et al., 2003). The sequence alignment performed for DafA_{Th}, HspR_{SCO} and several MerR family members (Table 3-3) had shown that the whole DafA_{Th} amino acid sequence shows also reduced homology with the DNA-binding domain of the MerR family. This result was considered also during the search for potential binding partners of DafA_{Th}.

Table 3-3: Sequence alignment of various MerR transcription regulators, HspR_{SCO} and DafA_{Th} using ClustalW software (Thompson et al., 1994)

MerR <i>H. influenzae</i>	-----MKIGALAKALGCTVETIRYYEQQLIPPPKRTSGNFRQYN	40
MerR <i>A. fulgidus</i>	-----MKKKDR-----YTISELAREFEISTRITIRYYEIGLLNPE-RTPGNORIFS	45
MerR <i>D. radiodurans</i>	MTTPSKSTAPTDEAGSDLTFYTTAELAREAGVTRRTVMHYAEIGLLPPDQVTASGRVLYA	60
MerR <i>B. subtilis</i>	-----MLLYSISKAAEKTSISSYTLRYYEKIGLLPPPKRKNNGRRFYT	43
MerR <i>C. acetobutylicum</i>	-----MYYTISEVSKKINVSPhTLRFYAKEGLMPFVERSKSGIRMFK	42
MerR <i>A. aeolicus</i>	-----MKRKAAYTIGVVAKMYNIHPQTLRLYEREGLLKPS-RSEGNRLYT	46
HspR <i>S. coelicolor</i>	---MDGRRRNPYELTETPVYVISVAAQLSGLHPQTLRQYDRLGLVSPD-RTAGRRRYS	56
DafA <i>T. thermophilus</i>	-----MLARSGWLSLEALS-EYGLSLAAVRAVVEIGFVEP--LEVGGAWYFR	44
MerR <i>H. influenzae</i>	EEHLQRLSFICNC-RNLDISLSEIKSLLNLENA-----SKQQAEEINRVLDKHIKEV	91
MerR <i>A. fulgidus</i>	RKDRAKLKLIRG-RRLGFSLLEIREMTEMVDV-AG----EPEQIRLTLKYGEKKLKEI	98
MerR <i>D. radiodurans</i>	PYSRLRLDLIDL-RALGMTLEESRDVMTLRRATHAPDGTYRRDWWREDVPLSDEQLQRL	119
MerR <i>B. subtilis</i>	ETDIQFMLFLKSL-KETGMSLEDINEFVKDGCILEKIN--SDVKSQQLSPSINKRIEIL	99
MerR <i>C. acetobutylicum</i>	DEDLESLEFIECL-KKSGMSIKDKIFMNCMQ-----GDETIDQRLNMFRRQQQERV	93
MerR <i>A. aeolicus</i>	DEDLERLEFIFLFTRELGNLAGVDIILNLKEQ-----MEQMQRKIDQLMEFT	94
HspR <i>S. coelicolor</i>	ARDIELLRQVQQLSQDEGINLAGIKRIIELENQ-----VAELQARAAELAAALDGA	107
DafA <i>T. thermophilus</i>	EEDLLRMAKERIRKDLGANLIGAAALVVEILERT-----	78
MerR <i>H. influenzae</i>	ATRIHELALHRMKLIELREKTVSNDEDPMKLLLQHSVGFVRLK-----	135
MerR <i>A. fulgidus</i>	EEKIRELELLKEDLLNREMLVKRLEELEKGS-----	130
MerR <i>D. radiodurans</i>	QTRLHVLNSAYERQKDNLARFDRWLTKRFVATRDSLIINGLNG-----	162
MerR <i>B. subtilis</i>	TKHLEKMEIKKRELEEVISTTKGKLDYYSILKEEVENK-----	138
MerR <i>C. acetobutylicum</i>	IKQIAELKETLDLIKWKYETAQAAGTCDIHTSLKLEDIPETIRNLKENMGKMYCHK	152
MerR <i>A. aeolicus</i>	QNELSKLQG-EAYQRAIVKVPKTKVMKFEVIVSRQKKSDEEE-----	136
HspR <i>S. coelicolor</i>	ATAMRQREAAVHASYRRDLVPYQEVQQTSAVVWRPSPRRGQSSD-----	151
DafA <i>T. thermophilus</i>	-----	

H. influenzae: *Haemophilus influenzae*; *A. fulgidus*: *Archaeoglobus fulgidus*; *D. radiodurans*: *Deinococcus radiodurans*; *B. subtilis*: *Bacillus subtilis*; *C. acetobutylicum*: *Clostridium acetobutylicum*; *A. aeolicus*: *Aquifey aeoliticus*; *S. coelicolor*: *Streptomices coelicolor*; *T. thermophilus*: *Thermus thermophilus*. The amino acids colored in: red (AVFPMILW) = small + hydrophobic (incl. aromatic except Y); blue (DE) = acidic; magenta (RHK) = basic; green (STYHCNGQ) = hydroxyl + amine + basic (except Q).

3.2.1.1 Co-elution of DafA(L2V)_{Th} with RNA molecules during purification

To identify the nature of the 260 nm high absorbing component that co-elutes with DafA(L2V)_{Th} in gel filtration, this fraction was purified using classical protocols for

nucleotides and nucleic acid purification. The eventuality that this component could be RNA was considered and therefore precautions were taken (RNase-free conditions) to avoid its degradation during isolation from DafA(L2V)_{Tth} sample. However, during DafA(L2V)_{Tth} purification these RNase-free conditions were not considered and therefore degradation processes might have occurred during protein purification.

The purified component was initially tested by analytical HPLC in order to check whether it is a nucleotide. The outcome of this analysis showed a very broad and undefined pattern of peaks that excluded the simple nucleotide nature of the DafA(L2V)_{Tth} co-eluting component. Thus, assuming that it might be a polynucleotide or a larger nucleic acid molecule, it was analyzed *via* nucleic acid urea-denaturing polyacrylamide gels. As seen in Figure 3-19 (-RNaseA lane) the component co-eluted with DafA(L2V)_{Tth} has indeed nucleic acid origin since it can be stained with ethidium bromide. The gel does not show a single band but a broad pattern of bands of various lengths. It could not be excluded with certainty that the large number of bands is the result of degradation of a single nucleic acid molecule during DafA(L2V)_{Tth} purification.

In order to identify its nature (RNA or DNA molecules?) the nucleic acids were treated with nucleases prior to electrophoresis. Figure 3-19, lane + RNaseA shows that incubation with RNaseA leads to disappearance of the bands indicating that the nucleic acids co-purified with DafA(L2V)_{Tth} during gel filtration step are RNA molecules. This result was the first indication that DafA(L2V)_{Tth} could have nucleic acid binding properties.

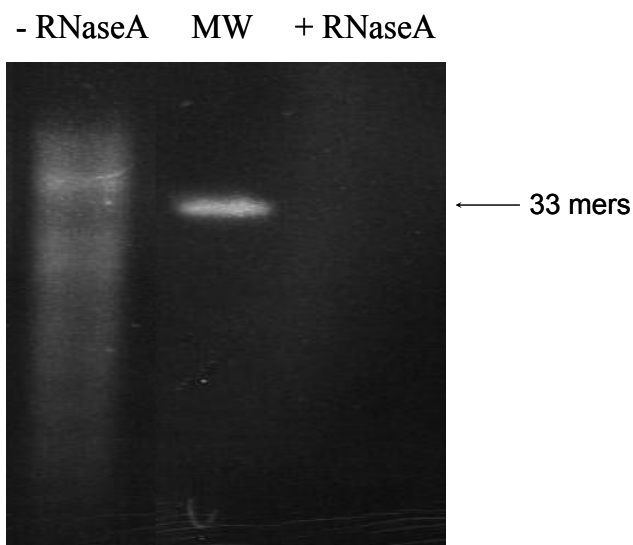


Figure 3-19: RNaseA treatment of a nucleic acid-containing fraction of DafA(L2V)_{Tth} obtained after gel filtration. The component with high absorption at 260 nm was purified and applied on a 20 % urea denaturing gel for nucleic acids. In the absence of RNaseA (-RNaseA lane) a broad pattern of bands was visible with ethidium bromide staining. RNaseA digestion of this sample (+RNaseA lane) leads to their disappearance from the gel. For a rough approximation of the RNAs length a 33-mer RNA molecule was used as a molecular weight marker (MW).

3.2.1.2 Binding of DafA(L2V)_{Tth} to a heterologous RNA

It was previously shown that DafA(L2V)_{Tth}, and consequently the wild type protein, could have RNA-binding properties. Since several attempts to identify the RNA sequences co-eluted with DafA(L2V)_{Tth} were not successful, the potential binding of the protein to various available RNA molecules was tested. One of the RNA molecules used is a 33-mer pseudoknot RNA (pkRNA), which is an aptamer specifically recognized by the HIV-1 reverse transcriptase (RTase) (Jaeger et al., 1998). In order to test whether the pkRNA is recognized also by DafA(L2V)_{Tth} it was radiolabeled using [γ -³²P]ATP and subjected to binding experiments. The influence of DafA(L2V)_{Tth} on the ³²P-pkRNA migration in a native gel was analyzed in a gel shift assay (Figure 3-20).

Due to the sensitivity of the radioactive method, the ³²P-pkRNA used was in nM range (30 nM). HIV-1 RTase (kindly provided by Dr. Tobias Restle), being a specific binder for the pkRNA, was used as positive control for retardation of the radioactive band in the gel shift assay (Figure 3-20A lanes 6-7 and B lane 3). As seen in Figure 3-20A, at reasonable concentrations of DafA(L2V)_{Tth} (50 nM, 0.5 μ M and 1 μ M corresponding to lanes 3, 4 and 5) no shift of the ³²P-pkRNA band could be observed after over night incubation at room temperature. It is important to mention that DafA(L2V)_{Tth} used for these experiments was not the RNA-free DafA(L2V)_{Tth}, but a sample obtained prior to optimization of the purification protocol. Thus, a potential binding of pkRNA by DafA(L2V)_{Tth} was in fact followed in the presence of possible competitor RNAs. To increase the chances of a pkRNA- DafA(L2V)_{Tth} interaction, the concentration of protein was increased to 60 μ M (2000-fold increase). Under these conditions the presence of contaminating RNases in DafA(L2V)_{Tth} sample was also tested.

As shown in Figure 3-20 (A and B, lane 2) the presence of DafA(L2V)_{Tth} in excess led to a clear shift of the ³²P-pkRNA band, which might be an indication for pkRNA-DafA(L2V)_{Tth} complex formation. Also, the ³²P-pkRNA seems to suffer a low extend of degradation in the same sample. Therefore, to check if the band shift is not in fact the result of the RNA binding by a contaminating RNase, two different concentrations of DafA(L2V)_{Tth} were applied as controls on the same gel and subsequently stained with Coomassie (B, lane 5-6). The result shows that the shifted ³²P-pkRNA band is migrating at the same level with the one corresponding to DafA(L2V)_{Tth}. This shows that the pkRNA retardation is caused by DafA(L2V)_{Tth}. On the other hand, a contaminating RNase present in the sample would probably digest almost the entire RNA during the incubation conditions. In B, lane 4 is shown, as an example, the degrading effect of 30 nM RNaseA on pkRNA incubated under the same conditions.

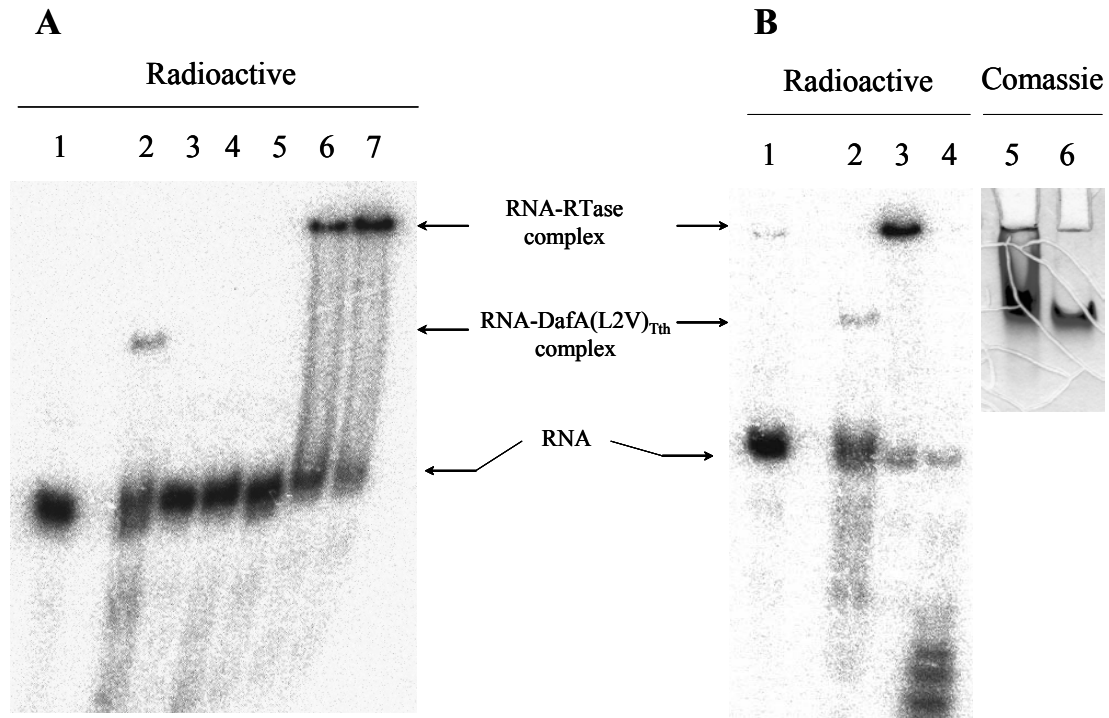


Figure 3-20: 33-mer pseudoknot RNA retarded by DafA(L2V)_{Tth} in gel shift assay. (A) 30 nM of radiolabeled 33-mer pseudoknot RNA (lane 1) were incubated in 50 mM Tris/HCl pH 7.5, 100 mM KCl, 5 mM MgCl₂, 2 mM EDTA and 2 mM DTE over night at room temperature with various concentration of DafA(L2V)_{Tth} (60 μM, 50 nM, 0.5 μM and 1 μM DafA(L2V)_{Tth} corresponding to lanes 2, 3, 4 and 5). As a positive control for binding it was used HIV-1 reverse transcriptase (RTase) (0.5 μM, lane 6 and 1 μM, lane 7). The samples were migrated in a 20 % polyacrylamide native gel. (B) The same experiment as in (A) using only 60 μM DafA(L2V)_{Tth} (lane 2) and 1 μM RTase (lane 3) for incubation with ³²P-RNA (lane 1). In lane 4 the RNA was incubated in the same conditions with 30 nM RNaseA. Lanes 5-6 shows the controls for DafA(L2V)_{Tth} (60 μM in lane 5 and 2.5 μM in lane 6) migrated in the same gel and stained with Coomassie.

In conclusion, the result presented here shows that DafA(L2V)_{Tth} is able to bind the 33 mers pkRNA, but the affinity constant for the complex formation is extremely low. However, this data corroborates the hypothesis that DafA(L2V)_{Tth} might be an RNA-binding protein or a nucleic acid-binding protein in general.

3.2.1.3 Binding of DafA(L2V)_{Tth} to the 70 S ribosomes from *T. thermophilus*

The hypothesis that DafA_{Tth} might have a regulatory function at a transcriptional level was investigated in various *in vitro* assays using DafA(L2V)_{Tth} variant and several potential interaction partners.

As described previously, the amino acid sequence of DafA(L2V)_{Tth} shows some similarities with the one of HspR_{SCO} and, to a lower extent, with sequences of MerR proteins (see 3.2.1). All MerR-family members and HspR_{SCO} are transcriptional regulators which modulate (positively or negatively) the synthesis of proteins important for cell survival under stress conditions (heat, oxidative, heavy metals, antibiotics induces stress). They act at the operator regions of the regulated genes by binding to specific inverted repeats sequences.

In order to test whether DafA_{Tth} is also recognizing regulatory elements found in the promoter region of dnaK_{Tth} operon, several DNA sequences were chosen as candidates for DafA(L2V)_{Tth} binding. These sequences are represented by a promoter segment of dnaK_{Tth} operon (including -35 and -10 cassettes) and some inverted repeats located up-stream of the same promoter. The results obtained from various experiments (native-PAGE electrophoresis, filter binding assay involving radioactive labeled DNA, fluorescence spectroscopy using fluorescently labeled DafA(L2V)_{Tth}) indicated that none of these molecules interact with DafA(L2V)_{Tth} under the conditions studied.

Given the fact that these approaches did not confirm the hypothesis of a transcriptional regulatory role of DafA_{Tth}, the possibility that it might be involved in translational control was also considered. Thus, 70 S ribosomal particles from *T. thermophilus* were purified and a potential interaction existent between DafA(L2V)_{Tth} and the translational machinery was tested.

DafA(L2V)_{Tth} binds *in vitro* to the 70 S ribosomes in sucrose cushion assay

The sucrose cushion assay is a tool that offers direct information about a potential binding event between ribosomes and a particular interaction partner. When subjected to a centrifugal field the ribosomes will be the first molecules pelleted in a sucrose cushion due to their huge molecular weight. If the protein of interest stably associates with the ribosomes before the ultracentrifugation step it will be found also in the ribosomal pellet (Figure 3-21).

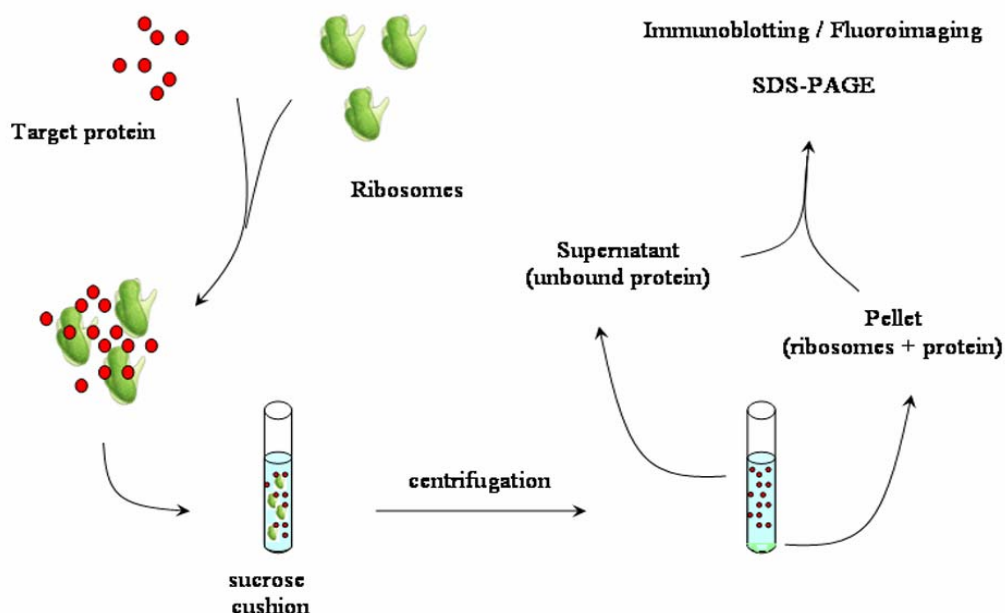


Figure 3-21: Sucrose cushion assay - schematic representation. The target protein (here, DafA(L2V)_{Tth}) is incubated with the ribosomes and the mixture is then applied on a sucrose cushion (usually 20 % sucrose). The tubes are centrifuged to allow the recovering of the ribosomes. After centrifugation the two fractions (supernatant and pellet) are separated and subjected to different detection assays. The complex formation between the ribosomes and the target protein is followed by detecting the protein in the ribosomal pellet.

Because DafA(L2V)_{Tth} is prone to aggregation it was necessary to establish ultracentrifugation conditions in which its precipitation does not interfere with ribosome-DafA(L2V)_{Tth} complex formation. These conditions were obtained by raising the sucrose concentration from 20 % to 30 % sucrose and by using two-fold volumes of sucrose over the volume of sample.

These experiments were performed using either DafA(L2V)_{Tth} followed by immunoblotting detection or using the Alexa488-labeled DafA(L2V)S14C_{Tth} mutant and subsequent fluoroimaging analysis, which provided an easier and faster evaluation of the data. Prior to ultracentrifugation the components were incubated for 15 minutes at 30°C or at 70°C, a temperature closer to the optimal growth conditions of *T. thermophilus*.

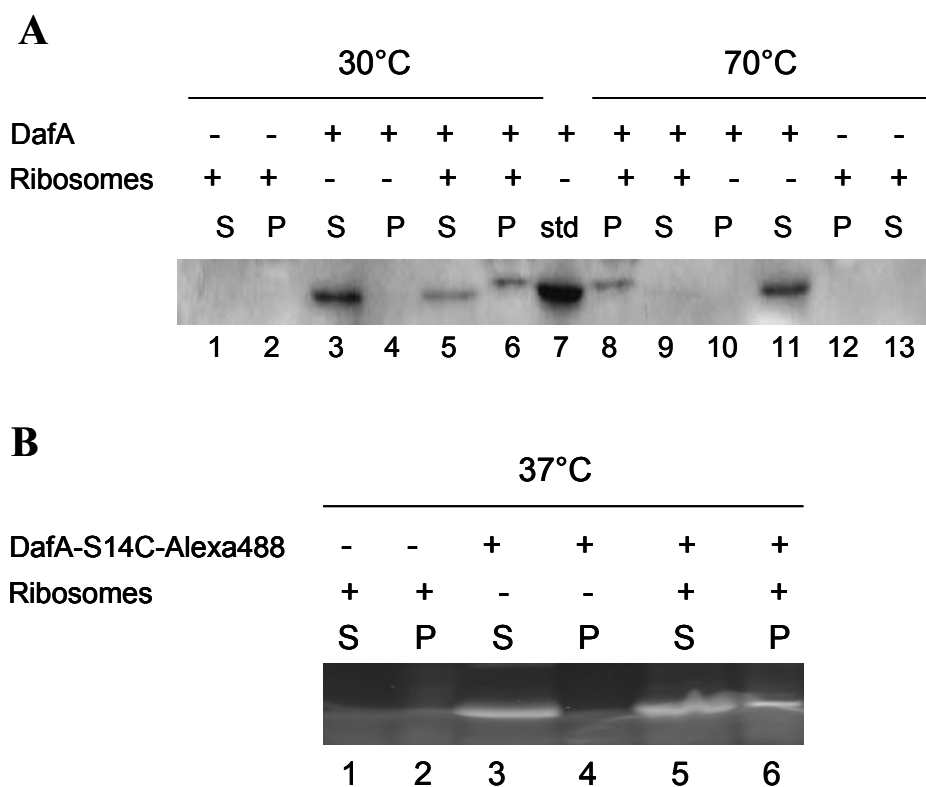


Figure 3-22: Binding of DafA(L2V)_{Tth} to the 70 S ribosomes in sucrose cushion assay. (A) *Immunoblotting*. 30 μ M DafA(L2V)_{Tth} was incubated at 30°C or 70°C with 2 μ M 70 S ribosomes for 15 minutes and applied on two volumes of 30 % sucrose cushion followed by ultracentrifugation to re-isolate the ribosomal particles. Equal volumes of supernatants (S) and ribosomal pellets (P) were separated by SDS-PAGE and subjected to western blotting using rabbit anti-DafA(L2V)_{Tth} antibodies. 2 μ M DafA(L2V)_{Tth} were applied as a standard (std). (B) *Fluoroimaging*. Alexa488 labeled DafA(L2V)S14C_{Tth} at final concentration of 5 μ M was incubated 15 minutes with 1 μ M 70 S ribosomes at 37°C. After ultracentrifugation on 30 % sucrose cushion the pellets (P) and the supernatants (S) were applied on SDS-PAGE. The fluorescence of the bands was detected directly from the gel using a Fuji FLA-5000 fluorescence scanner.

As seen in Figure 3-22, in both immunoblotting (A) and fluoroimaging (B) approaches, in the absence of ribosomes DafA(L2V)_{Tth} is found only in the soluble fraction (Figure 3-22A, lanes 3 and 11; Figure 3-22B, lane 3) while in the samples containing both

components DafA(L2V)_{Tth} is also found in the pellets together with the ribosomes (Figure 3-22A, lanes 6 and 8; Figure 3-22B, lanes 6). This is a clear indication that 70 S ribosome-DafA(L2V)_{Tth} complexes were formed either after incubation at 30°C or at 70°C. Surprisingly, the interaction seems to be temperature independent *in vitro* given that incubation of the components at 30°C or at 70°C does not show significant changes in the intensity of the bands corresponding to the ribosomal pellets (Figure 3-22A, lanes 6 and 8). This temperature independence was already observed for the DnaK_{Tth} system during luciferase refolding, the thermophilic chaperone machinery being fully functional at 30°C (Groemping et al., 2001).

There is a very faint DafA(L2V)_{Tth} band in the lane corresponding to the supernatant fraction derived from ribosome plus DafA(L2V)_{Tth} (Figure 3-22A, lane 9). This is not associated with an amplified signal in the corresponding pellet lane that could indicate a higher degree of binding. It is only the result of the protein loss during manipulation prior to SDS-PAGE.

DafA(L2V)_{Tth} binds *in vitro* to the 70 S ribosomes in analytical gel filtration

Analytical gel filtration experiments using the Alexa488-labeled DafA(L2V)S14C_{Tth} mutant were performed in order to analyze further the complex formation between DafA(L2V)_{Tth} and the 70 S ribosomes. During these experiments, the formation of the ribosome-DafA(L2V)S14C_{Tth} complex was monitored via fluorescence emission of the ribosomal peak obtained in the absence or in the presence of the fluorescent protein. Due to their very high molecular weight, ribosomes are not separated on a Superdex S-200 gel filtration column, but are found in the exclusion volume instead.

Figure 3-23A shows the elution profiles characteristic for the analytical gel filtration experiment. The first peak corresponds to 70 S ribosomes and 70 S ribosome-DafA(L2V)S14C_{Tth} complex and appears roughly at an elution volume of 8 ml. Interestingly, a fluorescence signal at this elution volume was also detected for a ribosome only sample (Figure 3-23A, black line). The reason for this is not an intrinsic fluorescence of the ribosomes but the occurrence of light scattering due to the very large size of these molecules.

The addition of a 5-fold excess of DafA(L2V)S14C_{Tth}-Alexa488 over the ribosome and incubation for 15 minutes at 30°C leads to an almost 8-fold increase in the fluorescence emission of the ribosomes which is an indication for complex formation (Figure 3-23A, red).

The specificity of this interaction was probed by incubation of the two components in the presence of a 10-fold excess of unlabeled protein (DafA(L2V)_{Tth}) over the concentration of the labeled one (Figure 3-23A, blue). Under these conditions the amplitude of the fluorescent signal of the ribosome-DafA(L2V)S14C_{Tth}-Alexa488 complex is decreasing drastically to a signal that is very close to the ribosomes-only sample.

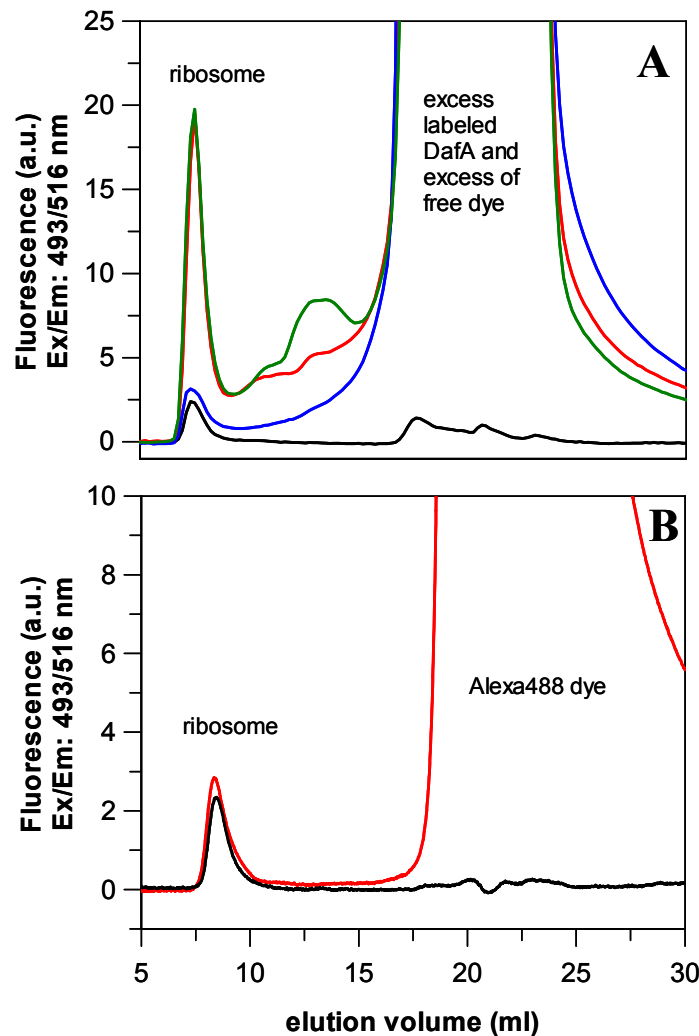


Figure 3-23: Interaction of DafA(L2V)S14C_{Tth}-Alexa488 with *T. thermophilus* 70 S ribosomes assayed by analytical gel filtration. (A) Binding of Alexa488-labeled DafA(L2V)S14C_{Tth} to the ribosomes and its displacement by an excess of unlabeled protein. 1 μ M ribosomes (—) were incubated with 5 μ M labeled protein for 15 min at 30°C in the absence (—) or in the presence (—) of a 10-fold excess of unlabeled protein. The influence of large RNA impurities present in the samples was analyzed by incubation of the ribosomes with DafA(L2V)S14C_{Tth}-Alexa488 in the presence of RNaseA (—). The samples were briefly centrifuged and then applied to a Superdex S-200 analytical gel filtration column at a flow rate of 0.75 ml/min. (B) Incubation of ribosomes with an excess of Alexa488 dye. 0.5 μ M 70 S ribosomes (—) were incubated for 15 minutes at 30°C with 50-fold excess Alexa488-maleimide (—) and subjected to analytical gel filtration on a Superdex S-200 column at a flow rate of 0.5 ml/min. Excitation/Emission wavelengths: 493/516 nm.

Despite the fact that the RNA-binding properties of DafA(L2V)_{Tth} have not been clarified yet, the possibility that residual RNA present in the ribosomal stock solution could lead to artifacts was taken into account. Therefore it was necessary to test whether the fluorescence of the ribosomal peak is not caused by an interaction between DafA(L2V)S14C_{Tth}-Alexa488 and some contaminating RNA molecules. To check for this possibility, the labeled protein was incubated with 70 S ribosomes in the same condition, but in the presence of RNaseA. If DafA(L2V)S14C_{Tth}-Alexa488 would form a complex

with a large RNA molecule, then it would be expected that the presence of RNaseA will interfere with the complex assembly by digesting the RNA. However this is not the case (Figure 3-23A, green) since the presence of RNaseA during incubation of the labeled protein with 70 S ribosomes does not modify the fluorescence signal originating from ribosome-DafA(L2V)S14C_{Tth}-Alexa488 complex formation.

It was noticed that an intense and broad peak appears at higher retention times. This corresponds to the excess of labeled protein and also to some residual Alexa488 dye which could not be completely removed during purification procedure. To check whether the increase of ribosome fluorescence in the presence of labeled protein is not caused by an unspecific interaction between the ribosomes and the free dye, the 70 S ribosomes were incubated with a 50-fold excess of Alexa488 dye under the same conditions described above. As seen in Figure 3-23B there is no significant shift of the ribosome fluorescence even in the presence of such excess of dye. Thus, the higher fluorescence signal obtained in the presence of DafA(L2V)S14C_{Tth}-Alexa488 derives from complex formation between the two components and not from unspecific binding of the free dye.

Taken together, the gel filtration and sucrose cushion results lead to the conclusion that thermophilic 70 S ribosome represents the new interaction partner of DafA_{Tth}. The association of this complex might have important, if not essential, consequences on the regulation of the heat shock response at a transcriptional level.

3.2.2 Analysis of 70 S ribosome-DafA(L2V)_{Tth} complex in correlation with DnaK_{Tth}-DnaJ_{Tth}-DafA(L2V)_{Tth}

By using both analytical gel filtration and sucrose cushion approaches, it was tested whether DafA(L2V)S14C_{Tth}-Alexa488 is recruiting DnaK_{Tth} and DnaJ_{Tth} to the translational machinery. A specific association of DnaK and DnaJ proteins was previously observed in *Saccharomyces cerevisiae* where Ssb, a Hsp70 chaperone, assemble together with zuotin, a DnaJ-like chaperone (Yan et al., 1998), and Ssz, another Hsp70 family member, into a “ribosome-associated complex” (RAC) that functions “on” the ribosome (Gautschi et al., 2001; Gautschi et al., 2002).

The results of the gel filtration experiments are illustrated in Figure 3-24. With a Superdex S-200 gel filtration column the two complexes are very well distinguished. The ribosome-DafA(L2V)S14C_{Tth}-Alexa488 complex, with its huge molecular weight, appears at 8 ml elution volume followed by the DnaK_{Tth}-DnaJ_{Tth}-DafA(L2V)S14C_{Tth}-Alexa488 complex at 11 ml. Addition of DnaK_{Tth} and DnaJ_{Tth} to a preformed ribosome-DafA(L2V)S14C_{Tth}-Alexa488 complexes leads to a significant fluorescence decrease of the ribosome peak (Figure 3-24A) indicating that ribosomes and DnaK_{Tth}/DnaJ_{Tth} are competing for DafA(L2V)S14C_{Tth}-Alexa488 binding.

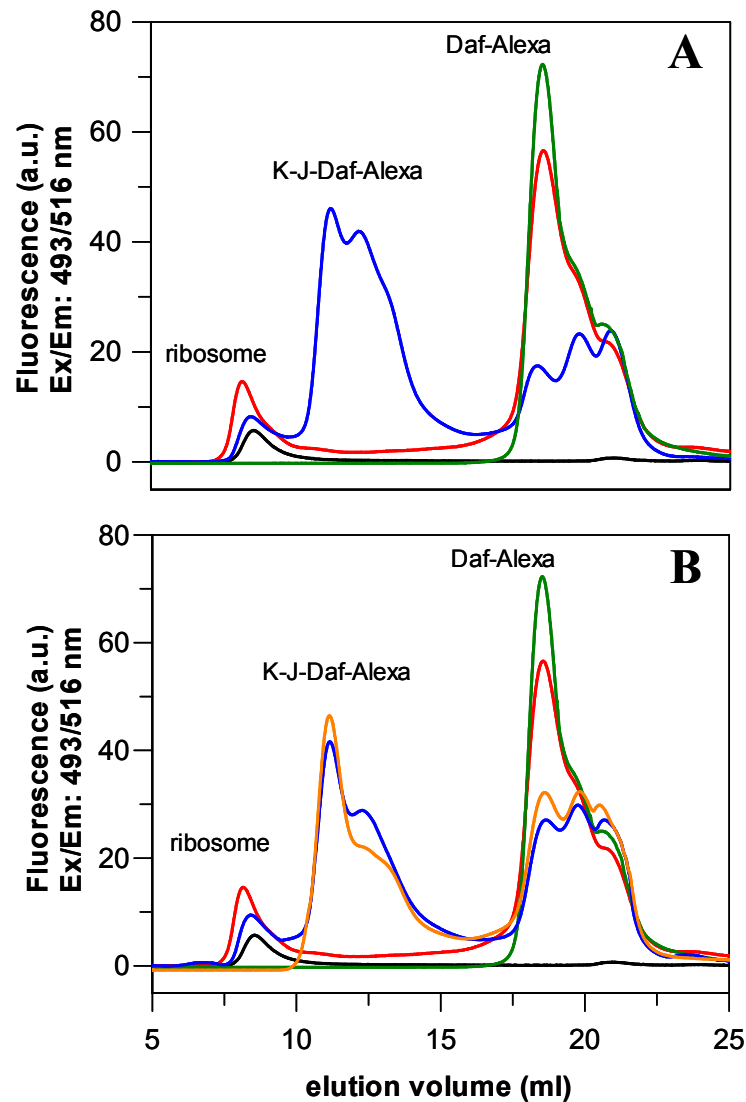


Figure 3-24: DnaK_{Tth} and DnaJ_{Tth} compete with 70 S ribosomes for DafA(L2V)S14C_{Tth}-Alexa488 binding. (A) Recruitment of ribosome-bound DafA(L2V)S14C_{Tth}-Alexa488 by DnaK_{Tth} and DnaJ_{Tth}. 0.5 μ M DafA(L2V)S14C_{Tth}-Alexa488 was incubated with 1 μ M ribosomes at 37°C (—). After one hour incubation time DnaK_{Tth} and DnaJ_{Tth} were added at a three-fold excess and the mixture was re-incubated under the same conditions (—). Ribosomes only (black) and DafA(L2V)S14C_{Tth}-Alexa488 only (—) samples were treated accordingly and used as controls. (B) Recruitment of DafA(L2V)S14C_{Tth}-Alexa from DnaK_{Tth}-DnaJ_{Tth}-DafA(L2V)S14C_{Tth}-Alexa complex by the 70 S ribosomes. 0.5 μ M labeled DafA(L2V)S14C_{Tth} (—) was incubated with equimolar concentrations of DnaK_{Tth} and DnaJ_{Tth} (—). After incubation of the three components for one hour at 37°C ribosomes were added to a final concentration of 1 μ M (—). The resulting spectra were compared to samples containing ribosomes only (—) and the ribosomes-DafA(L2V)S14C_{Tth}-Alexa488 complex (—) samples.

To test for reversibility, the same experiment was performed, but the components were added in an inverted order (the 70 S ribosomes were added subsequent to the formation of DnaK_{Tth}-DnaJ_{Tth}-DafA(L2V)S14C_{Tth}-Alexa488 complex). The outcome of this experiment (Figure 3-24B) is similar to the result presented in Figure 3-24A. This time the fluorescence of DnaK_{Tth}-DnaJ_{Tth}-DafA(L2V)S14C_{Tth}-Alexa488 decreases in favor of the ribosome-DafA(L2V)S14C_{Tth}-Alexa488 complex.

A similar result was obtained in a sucrose cushion experiment (Figure 3-25). Here the concentration of the components was slightly modified to ensure that DafA(L2V)S14C_{Tth}-Alexa488 was still detectable even after inevitable loss of protein during experimental manipulation.

It was observed that the addition of DnaK_{Tth} and DnaJ_{Tth} to the already formed ribosome-DafA(L2V)S14C_{Tth}-Alexa488 complex (lanes 7, 8) leads to a fluorescence reduction in the ribosomal pellet (lane 8) when compared to the same fraction of ribosome DafA(L2V)S14C_{Tth}-Alexa488 sample (lane 6). Similarly, at the addition of ribosomes to the preformed DnaK_{Tth}-DnaJ_{Tth}-DafA(L2V)S14C_{Tth}-Alexa488 complex (lanes 9, 10), a faint but visible band is detected in the ribosomal pellet (lane 10). It is important to note that only half of the samples were applied to SDS-PAGE and therefore resulted in a weak fluorescence signal observed in the pellets (corresponding only to 0.25 μ M ribosomes). Remarkably, the ribosome-DafA(L2V)S14C_{Tth}-Alexa488 complex is still formed even in the presence of a 10-fold excess DnaK_{Tth} and DnaJ_{Tth} over the ribosome concentration (Figure 5C, lane 8, 10), indicating that the interaction of DafA(L2V)S14C_{Tth} with the ribosomes is significantly tighter than the interaction with DnaK_{Tth} and DnaJ_{Tth}.

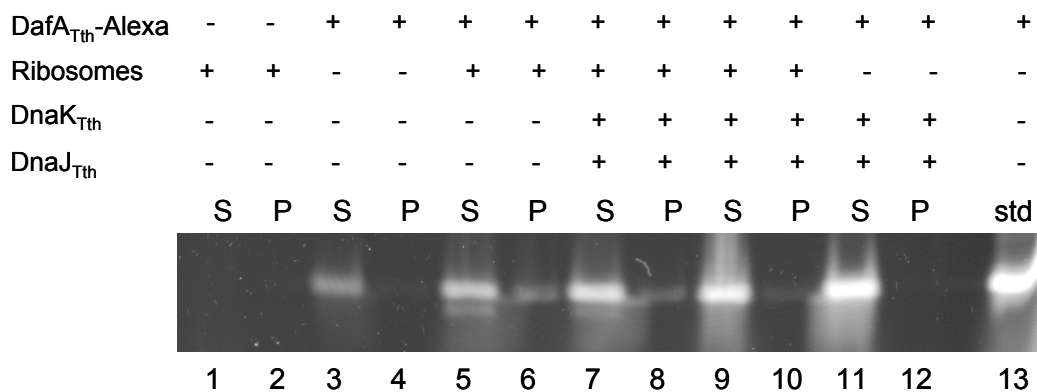


Figure 3-25: Competition between DnaK_{Tth}-DnaJ_{Tth} and 70 S ribosomes for DafA(L2V)S14C_{Tth}-Alexa488 binding in sucrose cushion assay. DafA(L2V)S14C_{Tth}-Alexa488 at a concentration of 2 μ M was incubated with 0.5 μ M 70 S ribosomes (lanes 5, 6). After one hour at 30°C, 5 μ M DnaK_{Tth} and 5 μ M DnaJ_{Tth} were added and the sample was incubated for another hour (lanes 7, 8). In lanes 9 and 10 the order of addition was inverted (first DnaK_{Tth} and DnaJ_{Tth}, then the ribosomes). The control samples are represented by ribosome only (lanes 1 and 2), DafA(L2V)S14C_{Tth}-Alexa488 only (lanes 3 and 4), the DnaK_{Tth}-DnaJ_{Tth}-DafA(L2V)S14C_{Tth}-Alexa488 complex (lanes 11 and 12) and a DafA(L2V)S14C_{Tth}-Alexa488 sample, which was not subjected to sucrose cushion and used as standard (std, lane 13).

Both gel filtration and sucrose cushion results show that DafA(L2V)_{Tth} does not mediate association of DnaK_{Tth} and DnaJ_{Tth} to the 70 S ribosomes. In contrast, the formation of the two complexes rather represents a competitive process *in vitro*. DafA(L2V)_{Tth} can be exchanged between DnaK_{Tth} and DnaJ_{Tth} on one hand and 70 S ribosomes on the other hand.

The DnaK_{Tth}-DnaJ_{Tth}-DafA_{Tth} complex comprises three copies from each protein species (Motohashi et al., 1996). In both analytical gel filtration and sucrose cushion assay, the fluorescence signal derived from the DnaK_{Tth}-DnaJ_{Tth}-DafA(L2V)S14C_{Tth}-Alexa488 complex is higher than the one corresponding to ribosome-DafA(L2V)S14C_{Tth}-Alexa488 complex. Although determination of the ribosome-DafA(L2V)S14C_{Tth}-Alexa488 complex stoichiometry is not straightforward, comparing the fluorescence intensities of these two complexes, it can be estimated that DafA(L2V)S14C_{Tth}-Alexa488 is bound to the 70 S ribosomes as a monomer rather than a trimer as it is in DnaK_{Tth}-DnaJ_{Tth}-DafA(L2V)S14C_{Tth}-Alexa488 complex. This estimation assumes however that the fluorescence intensities of DafA(L2V)S14C_{Tth}-Alexa488 in both complexes are comparable.

3.2.3 DafA(L2V)_{Tth} binding to 70 S ribosomes from *T. thermophilus* and *E. coli*: fluorescence anisotropy studies

In order to determine the affinity and rate constants for the association of DafA(L2V)_{Tth} with 70 S ribosome, several cysteine mutants of DafA(L2V)_{Tth} (S14C, V27C, F31C and A69C) were covalently labeled with IAEDANS (Molecular Probes, Eugene, USA) and their interaction with the ribosomes was assessed via fluorescence anisotropy.

The fluorophore IAEDANS is recommended for anisotropy measurements due to the long lifetime of the excited state (ca. 20 ns, compare to 4 ns of Alexa Fluor 488). A characterization of the ribosome-DafA(L2V)_{Tth} complex formation is not possible using the fluorescence intensity approach due to the scatter of light caused by the ribosomes with their huge molecular mass.

Fluorescence anisotropy measurements provide information on the mobility of fluorescent molecules, which is dependent on their molecular mass. Therefore, the anisotropy measurements should discriminate between the free fluorescently-labeled DafA(L2V)_{Tth} and the one either complexed with the ribosomes or with DnaK_{Tth} and DnaJ_{Tth}.

The physical basis of fluorescence anisotropy assays is the selective excitation of the fluorescent molecules with their absorption transition vectors aligned parallel to the electric vector of linearly polarized light. For dyes attached to small, rapidly rotating molecules, the initially photoselected orientation becomes randomized prior to emission, resulting in low fluorescence anisotropy. On the contrary, the orientation of fluorophores bound to a large, slowly rotating molecule, will not change rapidly between excitation and emission which will lead to an increase in fluorescence anisotropy. Therefore, fluorescence anisotropy provides a direct readout of the extent of binding between a fluorescently labeled molecule (proteins, nucleic acids) and its partners.

In a fluorescent anisotropy experiment the degree of polarization is determined from measurements of fluorescence intensities parallel and perpendicular with respect to the plane of linearly polarized excitation light, and is expressed in terms of anisotropy:

$$r = \frac{(F_{\parallel} - F_{\perp})}{(F_{\parallel} + 2F_{\perp})}$$

Equation 3-1

F_{\parallel} fluorescence intensity parallel to the excitation plan

F_{\perp} fluorescence intensity perpendicular to the excitation plan

The dependence of fluorescence anisotropy on molecular mobility is described by the Perrin equation:

$$r = \frac{r_0}{1 + \tau/\theta}$$

Equation 3-2

r_0 fundamental anisotropy of the dye in the absence of rotation diffusion

τ life time of the dye excited state

θ rotation correlation time of the dye or dye-conjugate (ca. 10 ns for a 25 kDa protein)

The theoretical values for anisotropy are ranging between -0.33 and 0.5, but in practice they are rarely obtained. Usually, in bioanalytical applications the minimal limit is 0.01 whereas the maximum value is about 0.3.

The dependence of rotation correlation time of the molecular weight is described by the equation:

$$\theta = \frac{\eta M}{RT} (v + h)$$

Equation 3-3

η viscosity of the solution

R gas constant ($8.31 \text{ J K}^{-1} \text{ mol}^{-1}$)

T temperature (in K)

- v specific volume of the protein
- h hydration

3.2.3.1 Interaction of DafA(L2V)_{Tth} with *T. thermophilus* 70 S ribosomes in comparison with DnaK_{Tth}-DnaJ_{Tth}-DafA(L2V)_{Tth} complex association

In Figure 3-26 it is shown the modification of fluorescence anisotropy of several AEDANS-labeled DafA(L2V)_{Tth} cysteine mutants upon addition of thermophilic 70 S ribosomes (Figure 3-26A) or addition of DnaK_{Tth} and DnaJ_{Tth} (Figure 3-26B). When either ribosomes or DnaK_{Tth}/DnaJ_{Tth} are added to the labeled proteins the fluorescence anisotropy increases. This change in anisotropy is the result of increased molecular weight of AEDANS labeled-DafA(L2V)_{Tth} mutants due to the association with the ribosomes on one hand, or with DnaK_{Tth} and DnaJ_{Tth} on the other hand.

Although the modification of anisotropy can be noticed in all cases, the degree of change is dependent on which of four cysteine variants was used. DafA(L2V)S14C_{Tth}-AEDANS and DafA(L2V)V27C_{Tth}-AEDANS seems to be tight binders either when complexed with the ribosomes (Figure 3-26A) or with DnaK_{Tth} and DnaJ_{Tth} (Figure 3-26B), whereas DafA(L2V)F31C_{Tth}-AEDANS and DafA(L2V)A69C_{Tth}-AEDANS variants show lower extend of binding in both systems.

Despite the fact that the association of labeled DafA(L2V)_{Tth} mutants with the ribosomes is apparent, the displacement of fluorescent protein by unlabeled one is not observed. More, the addition of a high excess (12.8 μM) of DafA(L2V)_{Tth} leads to a further increase of the anisotropy (Figure 3-26A). This behavior is again dependent on the mutant use. A similar result was obtained at the addition of an excess unlabeled protein (4.5 μM) to the complex formed with DnaK_{Tth} and DnaJ_{Tth} (Figure 3-26B).

The explanation for the increased anisotropy upon unlabeled DafA(L2V)_{Tth} addition is found in the Figure 3-27. The displacement of labeled DafA(L2V)_{Tth} from the complexes is impaired by the association (due to oligomerization or aggregation processes) between labeled and unlabeled protein present in excess. This effect is as higher as the excess of unlabeled DafA(L2V)_{Tth} is increased (see Figure 3-26A, compare addition of 2.6 μM DafA(L2V)_{Tth} with 12.8 μM).

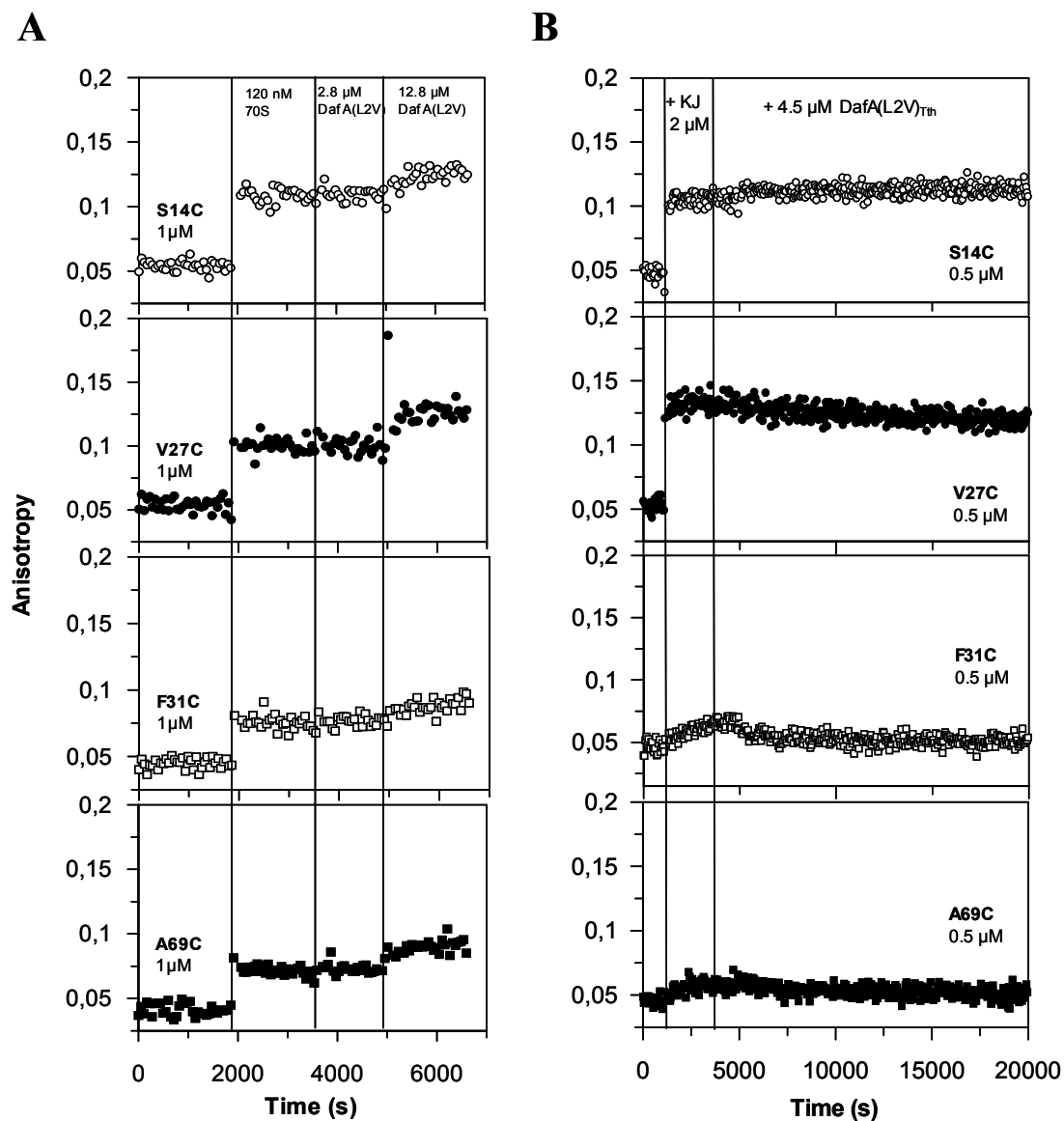


Figure 3-26: Fluorescence anisotropy measurements. (A) Interaction of various AEDANS-labeled *DafA(L2V)*_{Th} mutants with *T. thermophilus* 70 S ribosomes. 1 μM from each AEDANS-labeled cysteine variant was incubated with 120 nM 70 S ribosomes at 25°C in 50 mM HEPES/NaOH pH 7.5, 100 mM KCl, 20 mM MgCl₂, 5 mM DTE and 10 % glycerol and the anisotropy changes were measured. Excess of *DafA(L2V)*_{Th} (2.8 μM and subsequent, 12.8 μM) was added to each sample in order to displace the labeled proteins from the ribosomes. The measurements were made using FluoroMax 3 spectrofluorimeter (Jobin Yvon, Edison, USA) with Spex polarizers. Excitation/Emission: 336/490 nm with corresponding slits: 5/10 nm; integration time: 0.5 sec. (B) Interaction of various AEDANS-labeled *DafA(L2V)*_{Th} mutants with *DnaK*_{Th} and *DnaJ*_{Th}. 0.5 μM from each AEDANS-labeled cysteine variant was incubated with 2 μM *DnaK*_{Th} and 2 μM *DnaJ*_{Th} at 25°C in 50 mM HEPES/NaOH pH 7.5, 100 mM KCl, 5 mM MgCl₂, 5 mM DTE and 10 % glycerol and the anisotropy changes were measured. 4.5 μM *DafA(L2V)*_{Th} was added for displacement of the labeled proteins from the ternary complex. Settings FluoroMax 3: excitation/emission: 336/490 nm with slits: 5/10 nm; integration time: 0.1 sec.

A fraction from the total anisotropy change observed may also be caused by the local motion of the fluorophore about its point of attachment to the protein. Also it may be due to movement of part of the labeled protein. If the fluorophore becomes more rigid after

association of the labeled protein with its partners it might indicate that this region is directly involved in the interaction. In this view, by comparing the amplitude of anisotropy changing upon addition of ribosomes or DnaK_{Tth}/DnaJ_{Tth} to each AEDANS-labeled DafA(L2V)_{Tth} mutant, several assumption regarding the position of the mutated amino acids might be made. Since DafA(L2V)S14C_{Tth}-AEDANS and DafA(L2V)V27C_{Tth}-AEDANS show the highest degree of polarization in both systems (ribosomes or DnaK_{Tth}/DnaJ_{Tth} added), it might be probable that the amino acids S14 and V27 are localized at the interface between the interaction partners. Fluorescence measurements using NBD-labeled DafA(L2V)S14C_{Tth} (see 3.1.8) are in agreement with this supposition since the NBD fluorescence highly increases upon addition of DnaK_{Tth} and DnaJ_{Tth} which is correlated with an increase in the hydrophobicity of the NBD environment. Similar fluorescence measurements have revealed that DafA(L2V)F31C_{Tth}-NBD and DafA(L2V)A69C_{Tth}-NBD variants do not show any modification of the NBD fluorescence upon DnaK_{Tth}/DnaJ_{Tth} addition, though the complex formation occurs (see 3.1.10.2).

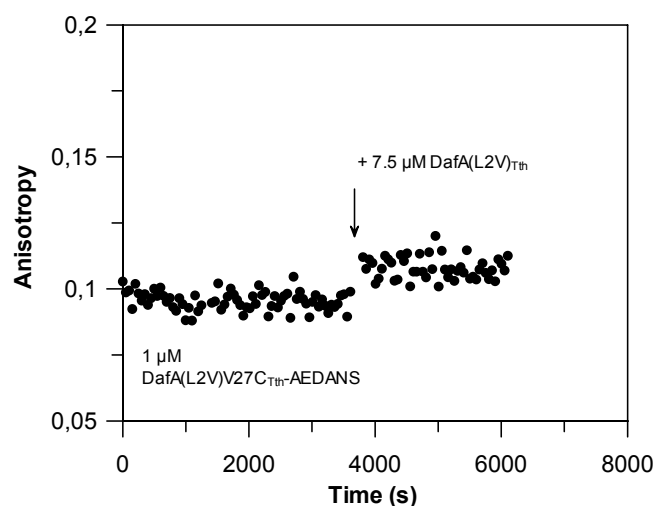


Figure 3-27: Self-association of DafA(L2V)_{Tth} during fluorescence anisotropy measurements. 1 μ M DafA(L2V)V27C-AEDANS was mixed with 7.5 μ M DafA(L2V)_{Tth} at 25°C in 50 mM HEPES/NaOH pH 7.5, 100 mM KCl, 5 mM MgCl₂, 5 mM DTE and 10 % glycerol and the anisotropy change was measured. The measurements were made using FluoroMax 3 spectrofluorimeter (Jobin Yvon, Edison, USA) with Spex polarizers. Excitation/Emission: 336/490 nm with corresponding slits: 5/10 nm; integration time: 0.2 sec.

Due to the self-association of DafA(L2V)_{Tth} molecules, a further analysis of the complex formation between DafA(L2V)_{Tth} and the 70 S ribosomes is not appropriate under the conditions used. A solution to this problem would be to determine the rotational correlation time (see Equation 3-3) for each species present in the solution (free labeled DafA(L2V)_{Tth}, the one complexed with the ribosomes and DafA(L2V)_{Tth} oligomers) in a time-resolved fluorescence anisotropy experiment.

3.2.3.2 Binding of DafA(L2V)_{Tth} to the 70 S ribosomes in the presence of Trigger Factor from *T. thermophilus*

Despite the unsatisfactory results obtained for the ribosome-DafA(L2V)_{Tth} complex formation during anisotropy experiments, this approach was further used in the attempt to identify the DafA(L2V)_{Tth} binding site on the ribosome. These experiments were based on the availability of thermophilic Trigger Factor (kindly provided by Dr. Elke Deuerling, ZMBH Heidelberg), a ribosome-associated chaperone intensely studied in *E. coli* (Stoller et al., 1995; Hesterkamp and Bukau, 1996; Deuerling et al., 1999). Trigger factor (TF) is a peptidyl-prolyl-cis-trans isomerase bound to the ribosome in a 1:1 ratio. Its function is to assist the folding of nascent polypeptide chains. The binding site of Trigger Factor on the ribosome was relatively recently identified in *E. coli* (Kramer et al., 2002). TF docking site on the ribosome is situated at the exit of the peptide tunnel in the ribosome. Taking into account this fact, it was tested whether DafA(L2V)_{Tth} and TF_{Tth} would share the same binding site or whether their binding sites on the ribosome are overlapping.

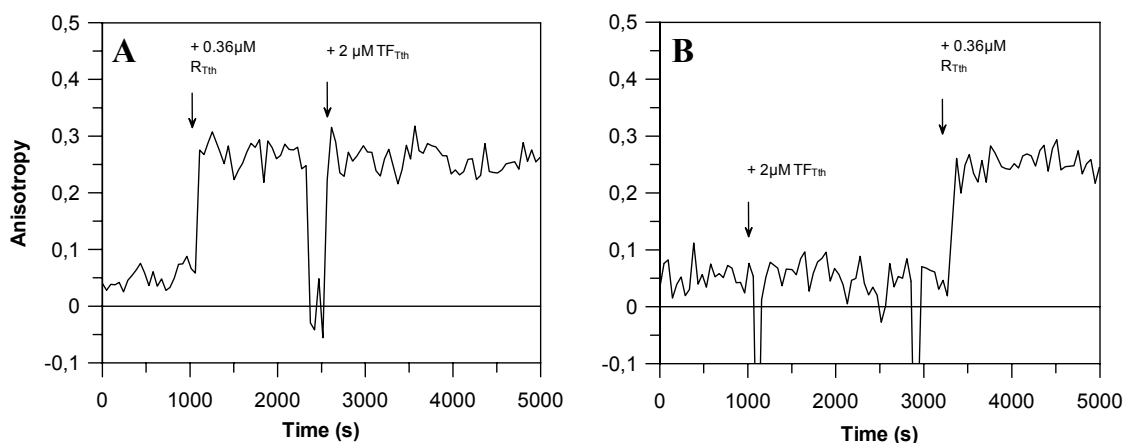


Figure 3-28: Influence of Trigger Factor on DafA(L2V)_{Tth} binding to the 70 S ribosomes (fluorescence anisotropy). (A) 0.5 μM DafA(L2V)V27C-AEDANS was incubated with 0.36 μM 70 S ribosomes (R_{Tth}) at 25°C in 50 mM HEPES/NaOH pH 7.5, 100 mM KCl, 20 mM MgCl₂, 5 mM DTE and 10 % glycerol. After the formation of the complex, 2 μM Trigger Factor (TF_{Tth}) was added to the mixture. (B) 0.5 μM DafA(L2V)V27C-AEDANS was incubated with 0.36 μM 70 S ribosomes in the presence of 2 μM Trigger Factor. The anisotropy measurements were made using FluoroMax 3 spectrofluorimeter (Jobin Yvon, Edison, USA) with Spex polarizers. Excitation/Emission: 336/490 nm with corresponding slits: 5/10 nm; integration time: 0.1 sec.

The influence of TF_{Tth} on DafA(L2V)_{Tth} binding to the 70 S ribosomes is shown in Figure 3-28. In fluorescence anisotropy measurements, it was tested whether TF_{Tth} is able to displace AEDANS-labeled DafA(L2V)V27C_{Tth} variant from the complex formed with the ribosome (Figure 3-28A) or whether the binding of the fluorescent protein to the ribosome is affected by the presence of TF_{Tth} in excess (Figure 3-28B).

Figure 3-28A shows that at a ribosome:DafA(L2V)V27C_{Tth}-AEDANS ratio closed to 1:1 (0.5 μM labeled protein, 0.36 μM 70 S ribosomes) the anisotropy increases significantly. At the addition of ribosomes the anisotropy value almost reaches the

maximum limit of about 0.3 units (see 3.2.3.1). This shows that the majority of the fluorescent molecules are associated with the ribosomes suggesting that DafA(L2V)_{Tth} is bound as a monomer to the 70 S ribosomal particle. The addition of 2 μM TF_{Tth} to the ribosome-DafA(L2V)V27C_{Tth}-AEDANS complex does not modify the fluorescence anisotropy. If TF_{Tth} would displace DafA(L2V)V27C_{Tth}-AEDANS from its complex with the ribosome, a decrease in the anisotropy would be expected. However this is not the case, suggesting that DafA(L2V)_{Tth} and TF_{Tth} have different binding site on the ribosome.

Similarly, Figure 3-28B shows that the presence of 2 μM TF_{Tth} prior ribosomes addition does not affect the binding of DafA(L2V)V27C_{Tth}-AEDANS to the ribosomes. Also, this experiment shows that DafA(L2V)V27C_{Tth}-AEDANS does not associate with TF_{Tth}.

To conclude, as far as these experiments show, the docking site of DafA(L2V)_{Tth} on the ribosome is different from the one of TF_{Tth}. The possibility that their ribosomal binding site are overlapping is also excluded.

3.2.3.3 Interaction of DafA(L2V)_{Tth} with the 70 S ribosomes from *E. coli*

In order to test whether DafA(L2V)_{Tth} is able to interact also with ribosomal particles from other prokaryotic organisms, the ability of AEDANS-labeled DafA(L2V)V27C_{Tth} variant to bind to the 70 S ribosomes from *E. coli* (kindly provided by Dr. Elke Deuerling, ZMBH, Heidelberg) was assessed in fluorescence anisotropy measurements.

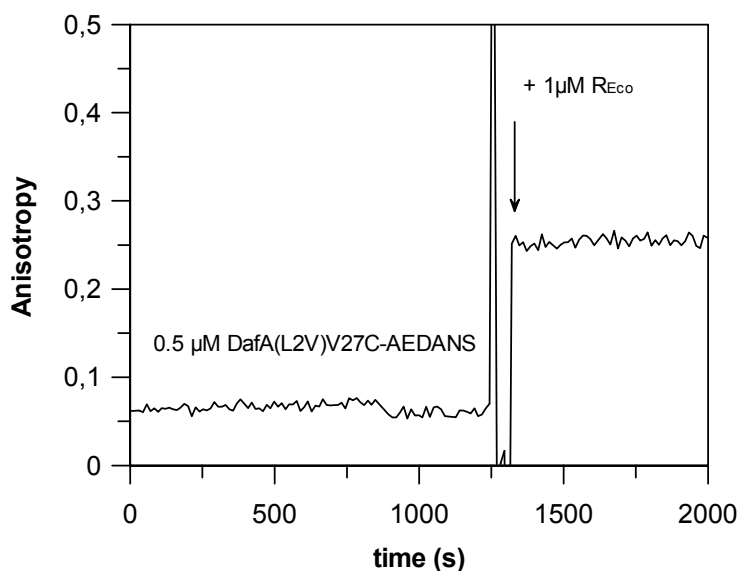


Figure 3-29: Binding of DafA(L2V)V27C_{Tth}-AEDANS to the 70 S ribosomes from *E. coli*. 0.5 μM DafA(L2V)V27C_{Tth}-AEDANS was mixed with 1 μM 70 S ribosomes from *E. coli* (R_{Eco}) at 20°C in 50 mM HEPES/NaOH pH 7.5, 100 mM KCl, 20 mM MgCl₂, 5 mM DTE and 10 % glycerol and the anisotropy changes were measured. The anisotropy measurements were made using FluoroMax 3 spectrofluorimeter (Jobin Yvon, Edison, USA) with Spex polarizers. Excitation/Emission: 336/490 nm with corresponding slits: 5/10 nm; integration time: 0.5 sec.

As seen in Figure 3-29 addition of 1 μM of *E. coli* 70 S ribosomes to 0.5 μM DafA(L2V)V27C_{Th}-AEDANS leads to a considerable increase in the anisotropy signal. This result shows that DafA(L2V)_{Th} is able to bind also to the *E. coli* ribosomes. Similarly to the DafA(L2V)V27C_{Th}-AEDANS association with the thermophilic ribosomes, here the anisotropy in the presence of the *E. coli* ribosomes is close to the maximum value of 0.3 (the high concentration of the *E. coli* ribosome stock allowed for addition of an excess of ribosomes over the concentration of labeled protein). This indicated that almost all free DafA(L2V)V27C_{Th}-AEDANS is associated with the *E. coli* ribosomes, which leads to the assumption that the stoichiometry of the partners is 1:1.

Although from the species specificity point of view the binding of DafA(L2V)_{Th} to the *E. coli* 70 S ribosomes would appear surprising, the results presented here show that the binding site of DafA(L2V)_{Th} on the 70 S ribosome is not a particularity of the thermophilic ribosome and it might suggest that a functional homologue for DafA(L2V)_{Th} exist also in *E. coli*.

3.3 *In vitro* refolding studies using *E. coli* cell lysate containing co-expressed DnaK, DnaJ, GrpE and ClpB chaperones from *T. thermophilus*

3.3.1 Co-expression of DnaK_{Th} and ClpB_{Th} chaperone systems in *E. coli*

The molecular chaperone DnaK together with its co-chaperones, DnaJ and GrpE, is able to refold denatured proteins and prevent protein aggregation. However, the reactivation efficiency of this system is limited when denatured proteins form large aggregates (Diamant et al., 2000). In this case, the protein reactivation occurs when the DnaK chaperone system co-operates with the ClpB system in an ATP-dependent manner (Parsell et al., 1994; Motohashi et al., 1999; Goloubinoff et al., 1999). Schlee et al. have recently shown that DnaK and ClpB from *T. thermophilus* form a weak complex (Schlee et al., 2004).

The collaboration between DnaK and ClpB in reactivation of protein aggregates has important implications from the biotechnological point of view. Development of an optimized refolding method for insoluble recombinant proteins has been the subject of many publications. Similarly, the establishment of an *in vitro* refolding procedure aimed to reactivate recombinant proteins expressed in insoluble form in *E. coli* using thermophilic DnaK and ClpB chaperone systems was here considered. The difference between this approach and classical *in vitro* renaturation experiments consists in the fact that all members of DnaK chaperone system and ClpB chaperone are co-expressed in *E. coli*. The advantage of this approach is straightforward. The thermal stability shown by the thermophilic chaperones allows for an easy and fast separation of these molecules by a

heat treatment (70-75°C). Moreover, co-expression of the thermophilic chaperones within the same cell could be further used for *in vivo* renaturation of insoluble recombinant proteins.

For the co-expression of DnaK_{Tth}, DnaJ_{Tth}, GrpE_{Tth} and ClpB_{Tth} in *E. coli*, BL21(DE3) competent cells were transformed with a vector containing the dnaK_{Tth} operon (kindly provided by Dr. Ralf Seidel) that includes all genes with the exception of *dafA* gene. Due to its inhibitory effect on chaperone assisted refolding, the removal of *dafA* gene was a requirement for the studies presented here.

Production of all four thermophilic chaperones in *E. coli* is presented in Figure 3-30. The Coomassie staining of the heat treated (70°C, 20 minutes) *E. coli* lysate applied on a SDS-PAGE shows that the overexpression is predominant for DnaK_{Tth}, while the presence of the other thermophilic chaperones cannot be detect in this way. Nonetheless, the western blotting analysis reveals also the production of the other chaperones, though not in the same amount as DnaK_{Tth}. The western blotting also shows that DafA(L2V)_{Tth} is not expressed indicating that its gene was successfully removed from the dnaK operon.

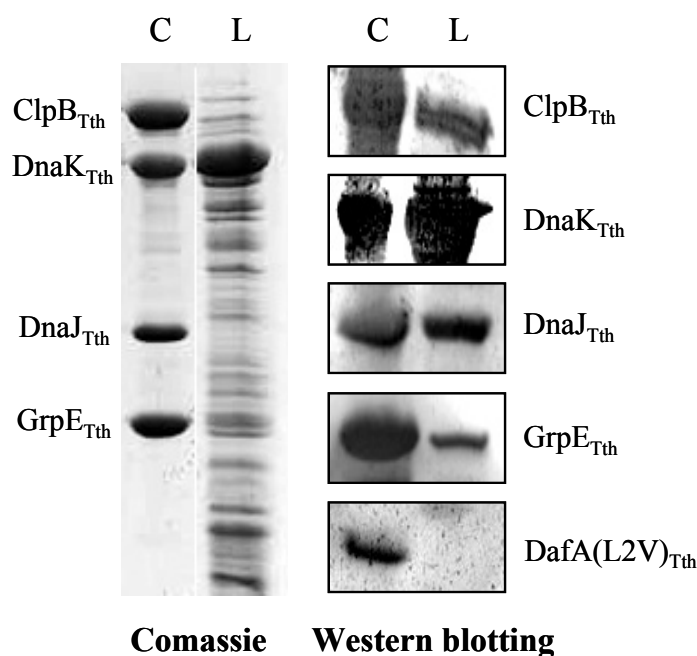


Figure 3-30: Co-expression of the thermophilic DnaK, DnaJ, GrpE and ClpB in *E. coli*. Left panel shows the total *E. coli* lysate containing co-expressed chaperones that was applied on a SDS-PAGE gel and subsequent stained with Coomassie. The lysate (L) was previously incubated at 70°C for 20 minutes and the aggregated proteins were removed by centrifugation. The total amount of protein applied on lane is ~ 50 µg. 5 µg of DnaK_{Tth}, DnaJ_{Tth}, GrpE_{Tth} and ClpB_{Tth} were used as control (C). In the right panel the co-expression of the chaperones was detected using monoclonal anti-rabbit antibodies developed against pure proteins. The lysate was tested also for the expression of DafA(L2V)_{Tth}.

3.3.2 Refolding of model substrates using *E. coli* cells lysate co-expressing DnaK_{Tth}, DnaJ_{Tth}, GrpE_{Tth} and ClpB_{Tth}

3.3.2.1 Model substrates

The model substrates used during *in vitro* refolding studies were the firefly luciferase (see 3.1.6.1) and α -glucosidase from *B. stearothermophilus*. α -Glucosidase used here is originating from an organism which has an optimal growth temperature between 50-55°C. It was previously described to be a substrate protein for the thermophilic system (Motohashi et al., 1999). It is a monomeric 65 kDa enzyme that catalyzes the hydrolysis of p-nitrophenyl- α -D-glucopyranosid. One of the products, p-nitrophenol, can be spectroscopically detected (405 nm) and therefore, the reactivation of α -glucosidase by the DnaK_{Tth}-ClpB_{Tth} systems can be easily followed. The α -glucosidase assay used here was established by P. Beinker (Beinker et al., 2002). By incubation for 10 minutes at 75°C the enzyme is losing the activity and a spontaneously recovery of this activity is not observed (as in luciferase case). Almost 40 % of the initial enzymatic activity of α -glucosidase can be recovered during incubation of denatured molecules with DnaK_{Tth}-ClpB_{Tth} system at 55°C.

3.3.2.2 Effect of lysate on the activity of native substrates and on chaperone assisted refolding

As it can be seen further, the analysis of the refolding activity of *E. coli* lysate containing DnaK_{Tth} and ClpB_{Tth} chaperone systems was concentrated more on the luciferase refolding than α -glucosidase refolding. The advantage of luciferase assay is that the effect of the lysate can be directly and continuously monitored during the refolding period. On the other hand, α -glucosidase assay is less dependent on various perturbation (no product inhibition during the measurement, higher stability etc.). Therefore, the α -glucosidase approach was preferred when luciferase assay was considered to be too sensitive at the experimental conditions used.

In order to test the refolding activity of *E. coli* lysate containing DnaK_{Tth}-ClpB_{Tth} chaperone systems, it was first necessary to check the potential effect of the lysate on native substrate proteins. This control experiment for luciferase assay is presented in Figure 3-31 (left panel). To ensure that the influence of the *E. coli* proteins on luciferase is as low as possible, the lysate was first heat denatured at 70°C for 30 minutes and the denatured host proteins were removed by centrifugation. Surprisingly, the result obtained shows that in the presence of various amounts of lysate (corresponding to various concentration of total protein) the activity of native luciferase decays extremely fast to a value close to nil.

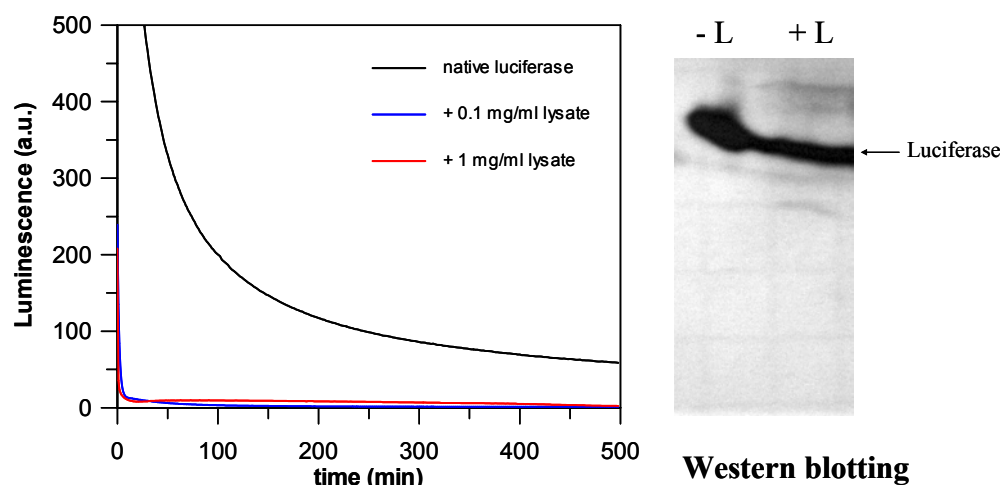


Figure 3-31: Effect of *E. coli* lysate containing co-expressed DnaK_{Th} and ClpB_{Th} chaperone systems on native luciferase. The left panel shows the activity of native luciferase during luciferase assay at the addition of 0.1 mg/ml total protein in lysate (5 μ l lysate/250 μ l total volume sample) and 1 mg/ml (50 μ l/250 μ l). The lysate was initially heat denatured at 70°C for 30 minutes and the denatured host proteins were removed by centrifugation. Right panel shows the western blotting for luciferase degradation in the absence (-L) and in the presence (+L) of lysate (total protein concentration is 4 mg/ml) using rabbit anti-luciferase antibodies (Promega). The lysate buffer is 50 mM Tris/HCl pH 8, 2 mM EDTA and “Complete” protease inhibitors (1 pill/30 ml total volume).

To check for the luciferase degradation in the presence of the lysate, the native enzyme was incubated at room temperature for 25 minutes with lysate (4mg/ml total protein) and then its integrity was assessed by western blotting. As seen in Figure 3-31 (right panel) the luciferase band is not altered and thus, the activity decay during luciferase assay is not caused by a degradation process. Rather, this is the inhibitory effect of a component present in the lysate (eg. proteins, small molecules).

As discussed before, α -glucosidase is a more robust enzyme when compared with luciferase. Therefore, a potential reactivation effect of the lysate was measured in an α -glucosidase refolding experiment (Figure 3-32). The reactivation yield obtained at the addition of purified thermophilic DnaK, DnaJ, GrpE and ClpB chaperones (at concentrations of 1.6, 0.4, 0.2 and 1 μ M) was set up to 100%. The outcome of the experiment showed that a concentration of 0.8 mg/ml total protein in the lysate didn't lead to an increase in the refolding yield. Moreover, when the same amount of lysate was present together with the purified chaperones, the refolding yield is dropping significantly. This shows that the lysate affects also the chaperone activity of purified chaperones. Addition of excess of pure chaperones does not really overcome this problem, although a small increase in the reactivation yield is observed after doubling or tripling the chaperone concentration (Figure 3-32).

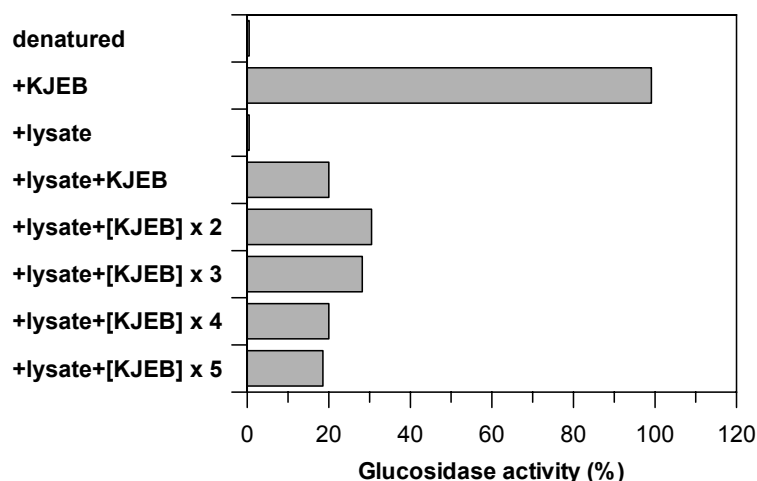


Figure 3-32: Effect of *E. coli* lysate containing co-expressed DnaK_{Tth}-ClpB_{Tth} systems on α -glucosidase refolding in the presence of increasing concentrations of purified chaperones. 0.2 μ M α -glucosidase was denatured for 10 minutes at 75°C and the renaturation for 1.5 hours at 55°C was followed in the presence of DnaK_{Tth}-ClpB_{Tth} systems (KJEB, pure proteins: 1.6 μ M DnaK_{Tth}, 0.4 μ M DnaJ_{Tth}, 0.2 μ M GrpE_{Tth} and 1 μ M ClpB_{Tth}), lysate and lysate combined with pure chaperones added in increasing concentrations ([KJEB] x 2: two-fold KJEB etc). The refolding buffer: 50 mM MOPS/NaOH pH 7.5, 150 mM KCl, 10 mM MgCl₂, 5 mM ATP, 1 mM DTE). Aliquots of 20 μ l were taken at the end of incubation period and analyzed for α -glucosidase activity. The activity of α -glucosidase was set to 100 % for the reactivated enzyme by purified chaperones (KJEB). The lysate was added at a 0.8 mg/ml total protein concentration (corresponding to 10 μ l lysate/100 μ l total volume sample). In order to release the potential substrates bound to the chaperones, 5 mM ATP, 50 mM KCl and 5 mM MgCl₂ were added to the denatured lysate prior centrifugation.

3.3.2.3 Optimization of lysate composition

In order to obtain a chaperone containing *E. coli* cell extract that is not longer affecting the native luciferase, the lysate was subjected to various treatments. Following the steps presented in Figure 3-33A (see legend) a lysate that has no longer effect on native luciferase during luciferase assay was obtained. After this treatment the chaperones could still be detected in the lysate (data not shown).

The potential refolding activity of lysate obtained in this way was tested for luciferase (Figure 3-33B and C). Although addition of increasing amounts of lysate to denatured luciferase leads to an increase in luminescence (Figure 3-33C), the refolding obtained is insignificant when compared to the refolding assisted by DnaK_{Tth}-ClpB_{Tth} system (Figure 3-33B). Also, this treatment of the lysate didn't overcome its inhibitory effect on DnaK_{Tth}-ClpB_{Tth} system refolding activity (Figure 3-1B).

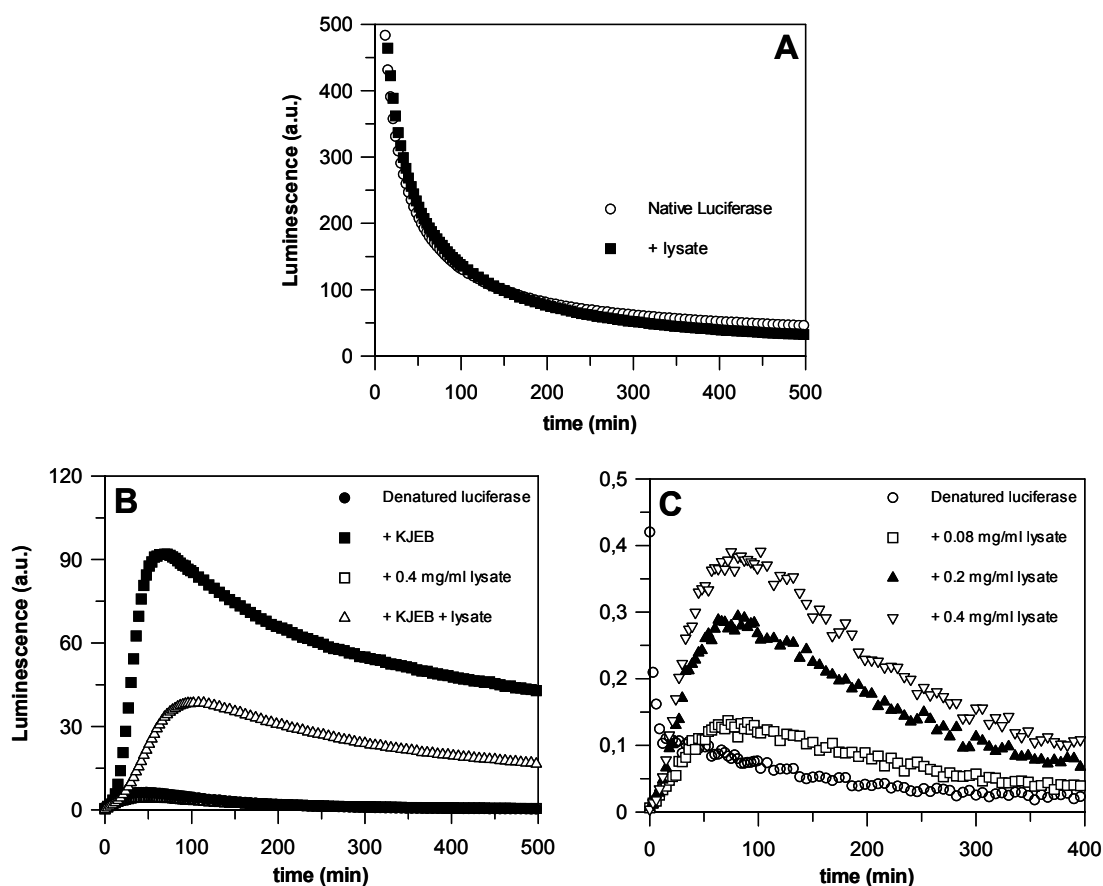


Figure 3-33: Optimization of the lysate composition and its effect of native and denatured luciferase. (A) The lysate was treated for 30 minutes at 70°C and 10 mM Mg·ATP was added before centrifugation. The supernatant was concentrated by ammonium precipitation (90 % saturation) and then dialyzed against 50 mM Tris/HCl pH 7.5, 100 mM KCl, 2 mM EDTA (12 kDa cut off) and subsequently, one-fold “Complete” protease inhibitors was added. The lysate obtained was tested for its influence on native luciferase (0.4 mg/ml total protein, 50 μl lysate to 250 μl total sample volume). (B) The lysate treated as described in (A) was added to denatured luciferase (30 minutes incubation at room temperature in buffer containing 7 M urea) in the absence (□) or in the presence (Δ) of purified chaperones. The refolding in the presence of pure chaperones (■) was used as control. Concentration of chaperones: 3.2 μM DnaK_{Th}, 0.4 μM DnaJ_{Th}, 0.8 μM GrpE_{Th} and 0.5 μM ClpB_{Th}. (C) Luciferase refolding in the presence of various amount of lysate (expressed as mg/ml total protein).

Addition of an excess of Mg·ATP to the refolding reaction seems to improve the luciferase refolding yield when both, lysate and purified chaperones are present (Figure 3-34). This could be an indication either that other ATP-ases are present in the lysate, thus diminishing the Mg·ATP concentration needed for chaperones, or that binding of luciferase by DnaK_{Th}-ClpB system is competed by other protein substrates in the lysate. In this last case, additional Mg·ATP would facilitate the releasing of these substrates and binding of luciferase. However, a too large excess of Mg·ATP (20 mM) is unfavorable for refolding due to impairment of luciferase binding by chaperones.

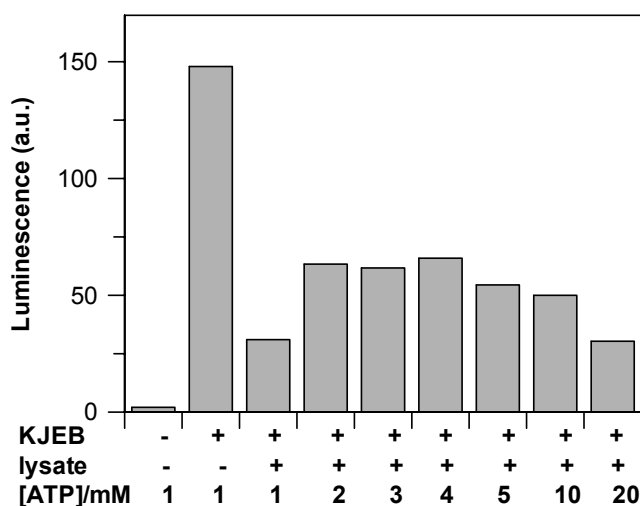


Figure 3-34: Influence of Mg·ATP excess on luciferase refolding assisted by DnaK_{Tth}-ClpB_{Tth} systems in the presence of *E. coli* lysate containing co-expressed thermophilic chaperones. The refolding of denatured luciferase assisted by DnaK_{Tth}-ClpB_{Tth} systems was monitored in the presence of lysate (0.8 mg/ml total protein) and increasing concentrations of Mg·ATP. The lysate was treated as described in **Figure 3-33A**. The refolding in the presence of pure chaperones was used as control. Concentration of chaperones: 3.2 μ M DnaK_{Tth}, 0.4 μ M DnaJ_{Tth}, 0.8 μ M GrpE_{Tth} and 0.5 μ M ClpB_{Tth}.

Though a small improvement in luciferase refolding was obtained by increasing the Mg·ATP concentration, an refolding yield compared to the chaperones only sample (Figure 3-34, KJEB, 1 mM ATP sample) could not be achieved in the presence of the lysate and pure chaperones. The partial inhibitory effect of lysate on DnaK_{Tth}-ClpB_{Tth} chaperone activity is still present.

Studies of Y. Groemping (Groemping Y., 2000) have shown that the chaperone assisted refolding of luciferase is dependent on the ratio in which the chaperones are used. The concentration of DnaK_{Tth} seems to be critical for luciferase refolding. At concentrations exceeding 3.2 μ M DnaK_{Tth} the refolding yield decreases dramatically. As the SDS-PAGE and western blotting analyses have shown, DnaK_{Tth} is highly expressed when compared to the expression levels of DnaJ_{Tth}, GrpE_{Tth} and ClpB_{Tth} (see 3.3.1). To check whether the inhibitory effect of the lysate on the activity of pure DnaK_{Tth}, DnaJ_{Tth}, GrpE_{Tth} and ClpB_{Tth} is not determined by an unfavorable chaperones stoichiometry, more exactly by a too high concentration of DnaK_{Tth}, a refolding experiment using lysate and increasing concentrations of DnaJ_{Tth}, GrpE_{Tth} and ClpB_{Tth} was performed (Figure 3-35).

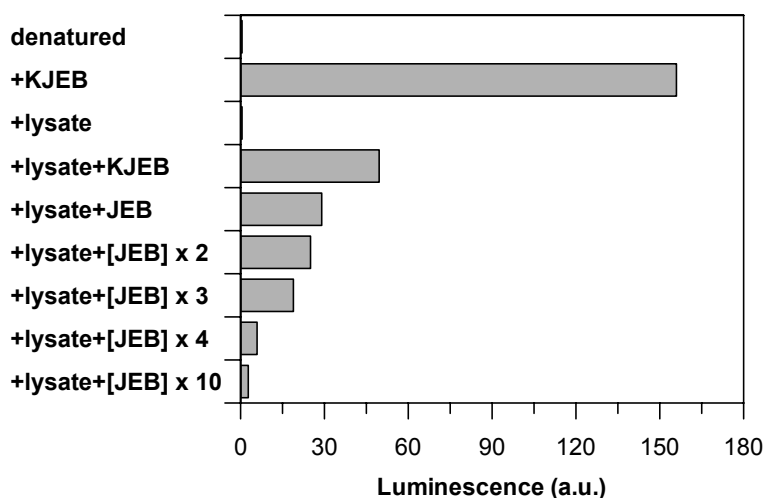


Figure 3-35: Luciferase refolding in the presence of DnaK_{Tth}-ClpB_{Tth} systems and of *E. coli* lysate containing co-expressed thermophilic chaperones: the influence of excess DnaJ_{Tth}, GrpE_{Tth} and ClpB_{Tth}. The refolding of denatured luciferase assisted by DnaK_{Tth}-ClpB_{Tth} systems was monitored in the presence of lysate (0.8 mg/ml total protein) and increasing concentrations of DnaJ_{Tth}, GrpE_{Tth} and ClpB_{Tth}. The lysate was treated as described in **Figure 3-33A**. The refolding in the presence of pure chaperones was used as control. Concentration of chaperones in the control: 3.2 μ M DnaK_{Tth}, 0.4 μ M DnaJ_{Tth}, 0.8 μ M GrpE_{Tth} and 0.5 μ M ClpB_{Tth}. The assay buffer contains 4 mM Mg·ATP.

The result obtained shows no improvement of the refolding yield when DnaK_{Tth} was omitted and only DnaJ_{Tth}, GrpE_{Tth} and ClpB_{Tth} have been added to the refolding mixture. Moreover, increased concentrations of the last three chaperones have a negative effect on the refolding, indicating that the chaperone ratio becomes more and more suboptimal for refolding. Nevertheless, this experiment has shown that it is not an excess of DnaK_{Tth} from the *E. coli* lysate which is determining the inhibition of chaperone assisted refolding.

Although without providing clear answers, the refolding studies presented here lead to the hypothesis of an inhibitor existent in *E. coli* cells that affects the DnaK_{Tth}-ClpB_{Tth} chaperone systems. Since the possibility of an inhibition directed to the activity of the substrate proteins was eliminated, the inhibition of refolding elicited by the lysate could be only caused by an interference with the chaperones activity. Whether the inhibitor present in *E. coli* is a homologue of DafA_{Tth} or not represents an issue that needs further investigation.

4 DISCUSSION

The findings presented in the results section will be discussed here with an emphasis on the new potential role of DafA_{Tth} in regulation of heat shock response at the translational level. This potential new function of DafA_{Tth} will be correlated with its essential role in mediating the DnaK_{Tth}-DnaJ_{Tth} assembly.

4.1 Properties of free DafA(L2V)_{Tth}

4.1.1 DafA(L2V)_{Tth} is a thermostable protein

As expected for a protein which originates from a thermophilic organism, DafA(L2V)_{Tth} possesses increased thermal stability. Differential scanning calorimetry experiments (see 3.1.5) show that the thermal unfolding of DafA(L2V)_{Tth} displays two transitions, both occurring at temperatures above the optimal growth temperature for *Thermus thermophilus* (75°C). The first transition has a maximum at ca. 89°C and represents the unfolding of DafA(L2V)_{Tth} monomers given that the unfolding is highly cooperative, a feature of many single-domain proteins. The second thermal transition of DafA(L2V)_{Tth} has a maximum at around 110°C and it might be attributed to the disassembly/denaturation of a small percent of DafA(L2V)_{Tth} oligomers. The correlation of the calorimetric data with analytical ultracentrifugation calculations (provided by Dr. Urbanke, Medizinische Hochschule, Hannover) leads to the assumption that the transition from 110°C derives from the unfolding of DafA(L2V)_{Tth} trimers. The presence of DafA(L2V)_{Tth} oligomers as trimers would be not at all surprising since DafA_{Tth} is found as a trimer within DnaK_{Tth}-DnaJ_{Tth}-DafA_{Tth} complex. The oligomerization of wild type DafA_{Tth}, outside of the complex, would be advantageous during heat shock conditions since oligomerization is a strategy often used by thermophilic proteins to enhance their stability (Jaenicke, 1996).

4.1.2 Denaturing agents have different effects on DafA(L2V)_{Tth} stability

Chaotropic agents-induced unfolding studies (see 3.1.3) based on the intrinsic fluorescence of DafA(L2V)_{Tth} revealed an increased stability of the protein in the presence of urea relative to mesophiles, but a sensitivity to the presence of GdmCl. The same behaviour was observed also for the other members of the DnaK_{Tth} chaperone system (Klostermeier, 1998; Groemping and Reinstein, 2001). Fluorescence spectroscopy and CD measurements have shown that 8 M urea has no influence on the secondary structure integrity of DnaJ_{Tth} and only residual effect on the stability of DnaK_{Tth}, GrpE_{Tth} and DafA(L2V)_{Tth}. In contrast, 6 M GdmCl induces the destabilization of the secondary structure of all these proteins. Tryptophane emission spectra of DafA(L2V)_{Tth} (see 3.1.3) have shown that the protein is fully unfolded at 5 M GdmCl. The transition midpoint for the GdmCl-induced denaturation of DafA(L2V)_{Tth} is around 4.1 M GdmCl.

The lack of a denaturing effect of urea on the thermophilic proteins was also shown in an experiment that follows the assembly/disassembly of the DnaK_{Th}-DnaJ_{Th}-DafA(L2V)_{Th} complex. The interaction between the three partners was not affected by the presence of urea up to a concentration of 4 M. On the other hand urea is able to disrupt the unspecific interactions between DafA(L2V)_{Th} molecules accumulated in *E. coli* cells as inclusion bodies.

4.1.3 Structural considerations

With its low molecular weight, DafA(L2V)_{Th} is a perfect candidate for structural studies using NMR-spectroscopy. Considering the tight relationship between protein structure and functional properties, determination of DafA(L2V)_{Th} structure would thus contribute to a better understanding of the particular function that wild type DafA accomplishes in *Thermus thermophilus*. However, the ¹H, ¹⁵N HSQC-NMR spectra (see 3.1.9) were not able to provide sufficient information in order to solve the protein structure. Nevertheless, the NMR results, combined with the fluorescence spectroscopy data, offered some information about the structural features of DafA(L2V)_{Th}. On this basis several structural considerations can be made.

The distribution of the amide group signals in the HSQC-NMR spectrum clearly indicates that DafA(L2V)_{Th} has a defined structure. From a total of ca. 50 residues visible in the spectrum 11 are found in the random coil region characteristic for peptides or unfolded proteins. The chemical shift of the remaining residues occupies specific areas that can be attributed to defined secondary structural elements. Most of these residues are concentrated in a region specific for α -helical structures. This observation is in agreement with the secondary structure prediction (see 3.1.7) that suggests a high α -helical content within the DafA(L2V)_{Th} structure. The region characteristic for extended structural elements (β -sheet) is also populated by several amino acids confirming again the structural prediction.

Spectroscopic measurements based on tryptophane fluorescence have shown that the two tryptophane residues comprised within DafA(L2V)_{Th} amino acid sequence are not very deeply embedded into the structure (see 3.1.3). The fluorescence emission derived from both residues has a maximum at around 343 nm which is characteristic for tryptophane located at the protein surface or in contact with polar groups. Nevertheless, the GdmCl-induced unfolding of DafA(L2V)_{Th} is accompanied by a decrease in the fluorescence emission and by a further red shift of ca. 5 nm of the emission maximum at the maximal concentration of denaturant. The completely denatured protein has an emission maximum very close to the one of free tryptophane in solution, showing that both tryptophane residues are fully exposed to the solvent. Consequently, at least one of the tryptophanes must be partially sheltered by other residues within the protein structure. These findings are sustained also by the NMR data. The HSQC-NMR spectrum of

DafA(L2V)_{Tth} (see Figure 3-14) reveals two different positions of the tryptophane residues. One of the indole NH signals is found in a region of the spectrum characterizing a surface-exposed tryptophane. The second signal is however shifted to a region specific for a tryptophane residue localized in the hydrophobic core or with its side chain somewhat embedded into the structure.

Although the NMR data offered direct evidence for different environment of the two tryptophanes, an assignment of the corresponding location for each residue was not straightforward. In this respect, site directed mutagenesis correlated with fluorescence spectroscopy could answer these questions. The alternative replacement of each tryptophane residue and the subsequent measurements of their fluorescence spectra in comparison to the spectrum of DafA(L2V)_{Tth} (see Figure 3-15) have allowed for the identification of the residue localized on the protein surface and of the one fully or partially embedded into the structure. In comparison to the DafA(L2V)_{Tth} spectrum, the maximum emission of DafA(L2V)W7C mutant is very slightly shifted toward a wavelength closer to the one of a fully exposed tryptophane, whereas the maximum of DafA(L2V)W41C is clearly shifted to the lower wavelength characteristic for a residue located in a more hydrophobic environment. Hence, W7 is the residue localized in the interior of the protein or partially embedded into the structure while W41 is the tryptophane residue exposed on the protein surface.

Fluorescent labeling of both tryptophane mutants and the assessment of their ability to interact with DnaK_{Tth} and DnaJ_{Tth} at equilibrium offered new information regarding the localization of these residues relative to the arrangement of the proteins within the complex. Consequently, several structural considerations might be suggested. This was facilitated by the observation that similar measurements done with other labeled cysteine mutants (e.g. F31C and A69C mutants) showed no changes in the fluorescent signal despite their ability to associate into the ternary complex. Compared to these mutants, both, labeled-DafA(L2V)W7C and DafA(L2V)W41C variants, show a change of fluorescence signal upon addition of DnaK_{Tth} and DnaJ_{Tth}. Since this is the result of an altered solvent accessibility of the fluorescent label it can be hypothesized that the tryptophane residues are somehow located at the interface between various (DafA(L2V)_{Tth} and DnaK_{Tth} or DnaJ_{Tth}) or identical molecules (DafA(L2V)_{Tth} monomers) inside the complex. Nevertheless, it can not be excluded that the observed fluorescence changes are not the result of a conformational change of DafA(L2V)_{Tth} molecules coupled to the complex assembly.

4.2 DafA(L2V)_{Tth} and its relationship with DnaK_{Tth} and DnaJ_{Tth}

4.2.1 DnaK_{Tth}-DnaJ_{Tth}-DafA(L2V)_{Tth} complex is unable to assist protein refolding

Competition experiments using fluorescent peptides have shown that in the presence of DnaJ_{Tth}, DafA(L2V)_{Tth} interferes with peptide binding to DnaK_{Tth} (Klostermeier et al., 1999). On the basis of this finding, a model for the regulation of the DnaK_{Tth} chaperone cycle was proposed (Klostermeier et al., 1999). This model suggests that there are two separate states of the DnaK_{Tth} system: a DnaK₃-DnaJ₃-DafA₃ complex representing the resting state and DnaK₃-substrate-DnaJ₃ complex as active chaperone species. According to the model the transition to the active state is determined by the critical concentration of denatured proteins as a consequence of stress conditions (e.g. heat shock) and results in the displacement of DafA_{Tth} by substrate. Rebinding of ATP under GrpE_{Tth}'s control allows the release of the substrate. This cycle of substrate binding and release may continue for several rounds or the complex returns to the resting state by rebinding of DafA_{Tth} ("switching off").

The incompatibility between the binding of peptide substrates and the presence of DafA(L2V)_{Tth} within the complex led to the assumption that DnaK_{Tth}-DnaJ_{Tth}-DafA_{Tth} can not represent the active form of the complex. Data presented here (see 3.1.6) support this hypothesis. For these studies the small peptides were replaced by firefly luciferase (Herbst et al., 1998; Kolb et al., 1994), a protein substrate used often in refolding assays. The refolding of GdmCl-denatured luciferase can be monitored on-line in a continuous assay where DnaK_{Tth} and its co-chaperones are added in a defined ratio (Groemping et al., 2001). The presence of an excess of DafA(L2V)_{Tth} in the refolding mixture has a strong inhibitory effect on luciferase renaturation (see 3.1.6.2). This inhibition of refolding does not occur through the binding of the substrate by DafA(L2V)_{Tth} since luciferase refolding assisted by the DnaK chaperone system from *E. coli* is not affected by the presence of DafA(L2V)_{Tth} (Groemping Y., 2000). DafA(L2V)_{Tth} prevents luciferase refolding by competing with its binding to DnaK_{Tth} and DnaJ_{Tth} through a mechanism not yet understood. There are indications that the inhibition of substrate binding to DnaK_{Tth}-DnaJ_{Tth} is related to the interaction between DafA(L2V)_{Tth} and DnaJ_{Tth} (Groemping Y., 2000). *In vitro* complementation experiments that use heterogeneous *T. thermophilus*-*E. coli* chaperone systems have shown that only in the presence of DnaJ_{Tth}, but not of DnaJ_{Eco}, DafA_{Tth} exhibits its inhibitory potential (Groemping Y., 2000).

These data corroborate a competitive mechanism of the binding of DafA_{Tth} and protein substrates to a DnaK_{Tth}-DnaJ_{Tth} complex and thus support the view that the DnaK_{Tth}-DnaJ_{Tth}-DafA_{Tth} complex can not be the active form of the refolding machinery.

4.2.2 DnaK-DnaJ-DafA(L2V) complex possesses high affinity and low rates of association and dissociation

Previous experiments (Klostermeier, 1998) and results presented in this work have revealed the increased stability of the DnaK_{Tth}-DnaJ_{Tth}-DafA(L2V)_{Tth} complex. These results indicate a high affinity between the three protein species involved. Analysis of DnaK_{Tth}-DnaJ_{Tth}-DafA(L2V)_{Tth} complex formation using a NBD-labeled DafA(L2V)S14C_{Tth} mutant (see 3.1.8) has shown that both association and dissociation represent slow processes. DafA(L2V)_{Tth} associates with DnaK_{Tth} and DnaJ_{Tth} with a rate constant k_{on} of $9.3 \cdot 10^3 \text{ M}^{-1} \text{ s}^{-1}$. The dissociation of the complex is characterized by a rate constant k_{off} of ca. $1.3 \cdot 10^{-3} \text{ s}^{-1}$. With the help of these parameters an apparent equilibrium dissociation constant K_D of ca. 140 nM for the complex formation could be calculated.

The rates characterizing complex formation were obtained at 25°C and in the absence of a protein substrate, thus their relevance for heat shock response of *T. thermophilus* is difficult to appreciate here. Studies of the DnaK_{Tth} chaperone cycle have shown that in general the properties of the cycle at 75°C do not differ significantly from the ones obtained at 25°C (Klostermeier et al., 1998). However, several quantitative results, e.g. equilibrium rate constants and acceleration rates of discrete cycle steps, were found to be slightly different at 75°C (Klostermeier, 1998). It is therefore conceivable that the on/off rates characterizing the assembly of the ternary complex might increase at higher temperatures. In this respect, the influence of increased temperature on the hydrophobic interactions suggested to be mainly involved in the complex formation (Klostermeier, 1998) might be considerable.

Nevertheless, the rates measured for DnaK_{Tth}-DnaJ_{Tth}-DafA(L2V)_{Tth} complex formation might reflect the dynamics of the complex during normal growth conditions of the thermophilic organism. The low values of association and dissociation rate constants have as consequence an enhanced kinetic stability of the complex assuring the co-existence of DnaK_{Tth}, DnaJ_{Tth} and DafA(L2V)_{Tth} complex in a stable form in the cell. The existence of a preformed DnaK_{Tth}-DnaJ_{Tth} ensemble mediated by the “glue” function of DafA_{Tth} might represent a mechanism required for a fast reply to the heat shock conditions. Once associated, DnaK_{Tth} and DnaJ_{Tth} would be available in the cell in a dormant but “ready to act” configuration. In this case, however, the prerequisite for a quick heat shock response would be the fast replacement of DafA_{Tth} by the increasing concentrations of denatured protein substrate. In this scenario, either DafA_{Tth} dissociation is much faster at 75°C or DafA_{Tth} release is accelerated in the presence of the substrate or of an additional regulator (e.g. a DafA_{Tth} exchange factor that accelerates exchange of DafA_{Tth} with protein substrate).

4.2.3 Point mutations in DafA(L2V)_{Tth} and the stability of the ternary complex

Several amino acids along the entire sequence of DafA(L2V)_{Tth} were replaced with a cysteine residue with the help of site directed mutagenesis (see 3.1.7). The cysteine residues were subsequently labeled with fluorescent probes and the labeled proteins were used in various assays. Functional studies which followed the association of DnaK_{Tth}, DnaJ_{Tth} and DafA(L2V)_{Tth} into the ternary complex have shown that none of these mutations suppress complex formation. Thus, the amino acid residues subjected to mutagenesis are not essential for the association of DafA(L2V)_{Tth} with DnaK_{Tth} and DnaJ_{Tth}. Also, these mutations do not abolish the interactions between DafA(L2V)_{Tth} monomers inside the complex. This result is most surprising in the case of the two tryptophane mutants (see Figure 3-16) since often these residues are important, if not essential, for a correct folding or a specific function of proteins.

Many of the residues mutated are hydrophobic amino acids. The high stability exhibited by the isolated DnaK_{Tth}-DnaJ_{Tth}-DafA(L2V)_{Tth} complex at high temperatures (75°C) or at high ionic strength (40 % ammonium sulphate) suggests that the interactions between the three partners are mainly of hydrophobic nature (Klostermeier, 1998). It is therefore very likely that some mutations might affect to some extent the binding affinity of DafA(L2V)_{Tth} to its partners or the interaction between DafA(L2V)_{Tth} monomers within the complex. Such changes in affinity are suggested by various binding kinetics observed with anisotropy experiments that measured complex assembly in the presence of various DafA(L2V)_{Tth} mutants (see 3.2.3). It can not be excluded however that these differences in the binding behavior are not also connected to the presence of the fluorescent label used for the measurements.

4.3 Functional studies reveal new potential functions for DafA_{Tth}

The predicted helix-loop-helix secondary structure and DNA/RNA-binding protein fold, the homology with the transcriptional regulator HspR from *S. coelicolor*, the co-elution of DafA(L2V)_{Tth} with RNA during purification (see 3.2.1.1) and the interaction with the pseudoknot RNA (see 3.2.1.2) indicate a regulatory function of DafA_{Tth} on the DNA/RNA level that might be connected to the heat shock response. This function could be directed to its own operon or to other important cellular sites possibly involved in the proposed regulatory role.

4.3.1 DafA_{Tth} is not implicated in transcriptional regulation of dnaK_{Tth} operon

The *dnaK* operon from *T. thermophilus* is preceded by a single promoter region which is homologous to *E. coli* consensus promoter sequences (Osipiuk and Joachimiak, 1997). Thus, this sequence could be recognized by the DNA-directed RNA polymerase σ^{32} subunit, the transcription factor which is responsible for heat shock regulation in the cytoplasm of Gram-negative bacteria (Bukau, 1993; Georgopoulos et al., 1994; Yura and Nakahigashi, 1999b; Yura and Nakahigashi, 1999a). In *E. coli*, during heat shock conditions σ^{32} levels increase transiently due to the increased translation of σ^{32} mRNA (*rpoH* mRNA) and transient stabilization of otherwise unstable σ^{32} without changes in *rpoH* gene transcription (Straus et al., 1990). The return to the steady-state levels of σ^{32} is done through the repression of *rpoH* mRNA translation (Morita et al., 1999) associated with degradation of σ^{32} mediated mainly by the ATP-dependent protease FtsH (Tomoyasu et al., 1995b; Tomoyasu et al., 1995a; Tomoyasu et al., 2001). The DnaK chaperone system participates in the down-regulation of σ^{32} in two ways: it is required for σ^{32} degradation (Straus et al., 1990) and it forms ATP-dependent ternary complexes with σ^{32} thus decreasing its activity with core RNA polymerase (Gamer et al., 1996). Although the thermophilic homologue for *E. coli* σ^{32} has not been identified yet, DnaK_{Tth} is nevertheless able to form complexes with a peptide derived from *E. coli* σ^{32} (Klostermeier et al., 1998). Hence, it is conceivable that the transcriptional regulation of the heat shock response in *T. thermophilus* is based on a mechanism that resembles the one from *E. coli* to some extent.

Assuming that free DafA_{Tth} may interfere with σ^{32} binding to regulatory regions found in the *dnaK*_{Tth} promoter, binding experiments that involved $\text{DafA}(\text{L2V})_{\text{Tth}}$ and DNA segments containing the -35 and -10 cassettes were carried out. The results obtained showed that $\text{DafA}(\text{L2V})_{\text{Tth}}$ does not recognize these regulating elements *in vitro*. Thus, a regulatory mechanism of *dnaK*_{Tth} gene expression involving DafA_{Tth} as a suppressor of σ^{32} action could not be confirmed.

Similar analyses were carried out with the transcriptional repressor HspR from *S. coelicolor*. The primary structure of HspR exhibits some homology (21 % amino acid identity) to the one of DafA_{Tth} . Furthermore, the organization of the *dnaK* operon in *T. thermophilus* is similar to the one from *S. coelicolor*. Within this organization, DafA_{Tth} occupies the same position as HspR in the sequence *dnaK-grpE-dnaJ-orfX*, *orfX* gene corresponding to DafA/HspR (see 3.2.1). In *S. coelicolor* HspR acts as a repressor of the *dnaK* operon gene expression by binding to several inverted repeat sequences (IRs) in the promoter region (Segal and Ron, 1996; Bucca et al., 2000; Bucca et al., 2003). HspR_{Sco} displays high similarity to the MerR family of eubacterial transcriptional regulators (Bucca et al., 1995). Also, DafA_{Tth} shares low homology with the DNA-binding domain of MerR proteins. Assuming that DafA_{Tth} could be a functional homologue of HspR_{Sco} or MerR

family members despite the relatively low amino acid identity, several binding experiments were performed to check whether DafA(L2V)_{Tth} interacts with the IRs identified in the thermophilic *dnaK* promoter. The experiments however, did not provide evidence that DafA(L2V)_{Tth} recognizes these DNA-sequences *in vitro*.

Thus, as far as the *in vitro* experiments have shown, the potential regulatory function of free DafA_{Tth} is pointed towards the *dnaK*_{Tth} operon in terms of transcriptional regulation of gene expression.

4.3.2 The 70 S ribosome, the new interaction partner of DafA(L2V)_{Tth}

Since a potential regulatory function at the transcriptional level could not be revealed and yet some RNA-binding was observed, the search for potential interaction partners of DafA_{Tth} has brought the attention to the translational machinery. The complex formation between DafA(L2V)_{Tth} and isolated *T. thermophilus* 70 S ribosomes was analyzed via various *in vitro* approaches, considering the specific features of the ribosomes (see 3.2.1.3). Sucrose cushion assays offer clear evidence of a binding event occurring between the two molecules, regardless of the DafA(L2V)_{Tth} variant used (DafA(L2V)_{Tth} or Alexa488-labeled DafA(L2V)S14C_{Tth} mutant). Furthermore, gel filtration experiments carried out with the labeled DafA_{Tth}-S14C variant supported the results obtained by the sucrose cushion assay. The increase in fluorescence signal of the 70 S ribosomes in the presence of DafA(L2V)S14C_{Tth}-Alexa488 clearly indicates that a ribosome-DafA(L2V)_{Tth} complex is formed. Competition experiments showed that the assembly of this complex is a specific process, excess of unlabeled DafA(L2V)_{Tth} being able to reduce the fluorescence signal to a value close to the one of the ribosome-free Alexa labeled DafA(L2V)S14C_{Tth}-Alexa488. Hence, it can be concluded that DafA_{Tth} is a novel ribosome-associated molecular chaperone when released from the DnaK_{Tth}-DnaJ_{Tth}-DafA_{Tth} complex.

4.3.3 Ribosome-DafA(L2V)_{Tth} complex and its relationship with DnaK-DnaJ-DafA(L2V)_{Tth} complex

The presence of ribosome associated chaperones was revealed in both prokaryotic and lower eukaryotic model systems (Hartl and Hayer-Hartl, 2002; Craig et al., 2003). The *E. coli* Trigger Factor (TF) and Ssb from *Saccharomyces cerevisiae* are the best studied ribosome-bound chaperones. Although both have chaperone activity while bound to the ribosomes, TF and Ssb do not share sequence similarity. TF belongs to the peptidyl-prolyl-cis-trans isomerase (PPIase) family (Hestekamp et al., 1996; Scholz et al., 1997; Stoller et al., 1995) whereas Ssb is a member of the Hsp70 family. TF is thought to function as a monomer on ribosomes (Patzelt et al., 2002) and it was demonstrated that it cooperates with DnaK in folding of newly synthesized proteins (Deuerling et al., 1999; Teter et al., 1999). The function of Ssb requires two additional proteins: Zuotin, a

DnaJ-like chaperone (Yan et al., 1998), and Ssz, another Hsp70 family member. All three assemble into a “ribosome-associated complex” (RAC) that also functions on the ribosome (Gautschi et al., 2001; Gautschi et al., 2002).

In relationship with these findings the question whether DafA_{Tth} recruits DnaK_{Tth} and DnaJ_{Tth} to the ribosome was addressed. Both gel filtration and the sucrose cushion assay results show that the DnaK_{Tth}-DnaJ_{Tth}-DafA(L2V)_{Tth} complex does not associate with the 70 S ribosomes (see 3.2.2). In contrary, assembly of these two complexes seems to be a competitive process, DafA(L2V)_{Tth} being shuttled between ribosomes and DnaK_{Tth}-DnaJ_{Tth}. From the protein folding point of view this finding is not too surprising considering that the DnaK_{Tth}-DnaJ_{Tth}-DafA(L2V)_{Tth} complex is unable to assist protein folding.

Taken together, these results lead to the proposal of a model for the DafA_{Tth} pathway that correlates the DnaK chaperone cycle with the translational machinery during heat shock response in *T. thermophilus*. The model is schematically represented in Figure 4-1. Since it was shown that DafA_{Tth} can not be part of the active chaperone system, it has to be released from the DnaK_{Tth}-DnaJ_{Tth}-DafA_{Tth} complex during heat shock and replaced by denatured protein substrates. Consequently, conform to the gel filtration and anisotropy findings presented in this work, monomeric rather than trimeric free DafA_{Tth} is targeted to the translational machinery without recruiting other members of the chaperone system.

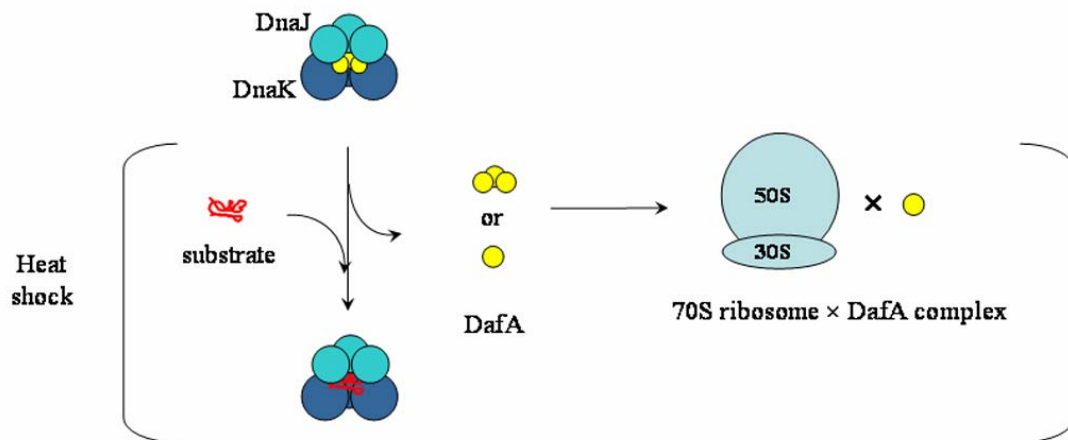


Figure 4-1: The model of DafA_{Tth} pathway during heat shock conditions. During heat shock DafA_{Tth} must be replaced from the complex by the denatured proteins. Since DafA_{Tth} is not a part of the active chaperone system it might have regulatory functions connected to the heat shock response after its releasing from the complex. The complex formed between DafA(L2V)_{Tth} and the 70 S ribosomes reconstructed *in vitro* indicates that monomeric DafA_{Tth} is targeted to the translational machinery. The assembly strongly suggests that DafA_{Tth} may act as a regulatory factor at the translational level. Though DafA(L2V)_{Tth} shows limited RNA-binding properties, the contribution of RNAs molecules (tRNA, mRNA) to the regulatory events is not yet clear.

DafA_{Tth} shuttling between the ribosome-DafA_{Tth} and DnaK_{Tth}-DnaJ_{Tth}-DafA_{Tth} complexes might have a regulatory meaning within the framework of a heat shock

response. The complete understanding of how the *T. thermophilus* DnaK chaperone system is regulated requires a more detailed understanding of DafA_{Tth}-ribosome interaction. In this respect, identification of a DafA_{Tth} docking site on the ribosome might be one of the first steps necessary. Competition experiments using (see 3.2.3.2) have shown that DafA_{Tth} and TF_{Tth} do not share the same binding site on the ribosome. Also, evidences that their binding sites are overlapping are lacking. Since the ribosomal binding site of TF is found close to the exit tunnel of newly synthesized polypeptides (Kramer et al., 2002; Blaha et al., 2003), a different location of DafA_{Tth} indicates once more that DafA_{Tth} is most likely not involved in co-translational protein folding. The RNA binding capacity of DafA_{Tth} suggests that binding to the ribosome could mainly be mediated by rRNA or rRNA and ribosomal proteins rather than ribosomal proteins only.

Although *in vivo* studies might drastically increase the knowledge about functional aspects of the ribosome-DafA_{Tth} interaction in respect to the heat shock response, this approach is not feasible at present, due to difficulties in genetic manipulation of *T. thermophilus* strains. On the other hand, the attempt to identify DafA_{Tth} in *T. thermophilus* lysates at various incubation temperatures including heat shock conditions was unsuccessful suggesting a very low abundance of DafA_{Tth} in the cell.

Interestingly, as the fluorescence anisotropy experiments have shown (see 3.2.3.3), DafA(L2V)_{Tth} is able to interact also with the 70 S ribosomal particle from *E. coli*. In the first place, this finding suggests that ribosomal binding site of DafA_{Tth} is located in a conserved region, probable present in many prokaryotic ribosomal particles. Second, this result might indicate that, despite the absence of a significant amino acid homology between DafA_{Tth} and other proteins in *E. coli*, a similar function at translational level could be accomplished by a yet unidentified factor. This hypothetical functional homolog of DafA_{Tth} might also interact transiently with DnaK and DnaJ since ternary complexes comparable in stability with the DnaK_{Tth}-DnaJ_{Tth}-DafA_{Tth} complex were not found in *E. coli*. Nevertheless, if such a homolog exists in *E. coli*, it is likely that also from the protein folding point of view; it functions in a way similar to DafA_{Tth}. In this respect, a detailed study on the inhibition of DnaK_{Tth}-ClpB_{Tth} assisted refolding elicited by *E. coli* lysates *in vitro* (see 3.3) might bring new information to support this hypothesis.

4.4 Outlook

The fully “decoding” of the DnaK_{Tth} chaperone cycle regulation requires also the understanding of DafA_{Tth}-ribosome interaction. Therefore, the DafA_{Tth}-ribosome complex has to be subjected to a detailed investigation. Although not an easy task, the DafA_{Tth} binding site on the ribosome has to be identified. In a first step it should be analyzed whether DafA_{Tth} needs the entire 70 S particle to bind or the binding site is located only on one of the ribosomal subunits. The controlled separation of the 30 S and 50 S subunits and subsequent analyses regarding DafA_{Tth} binding should answer this question. Identification

of the DafA_{Tth} binding site on ribosome would be a first step in revealing DafA_{Tth} function at the translational level.

Although several attempts to obtain kinetic information regarding the DafA_{Tth}-ribosome association have been here made, DafA(L2V)_{Tth} self-association makes this task very difficult to accomplish. One way to overcome this problem is the optimization of DafA(L2V)_{Tth} solubility and stability. The finding of such stabilizing conditions will enhance also the resolution of NMR spectra and will enhance the chance of DafA_{Tth} structure determination.

There are still many open questions concerning the DnaK_{Tth}-DnaJ_{Tth}-DafA_{Tth} complex and the interaction between the partners within the assembly. Electron microscopy provided images of the complex shaped as a trigonal particle. However, information about the arrangement of the proteins inside the complex is lacking. Klostermeier et al. proposed a model in which three molecules of DafA_{Tth} are “sandwiched” between three molecules of each DnaJ_{Tth} and DnaK_{Tth} (Klostermeier et al., 1999). Whether this is the real arrangement can be tested with the help of electron microscopy. Also, the contact regions between the proteins within the complex are not known for the moment. As shown in this work, several point mutations performed in DafA(L2V)_{Tth} did not abolish complex formation. This might suggest that rather extended amino acid areas and not single residues are involved in the interaction. Deletion of specific regions in DnaJ_{Tth} and DnaK_{Tth} might represent one way to understand what areas are necessary and sufficient for the complex formation.

The mechanism of DafA_{Tth}-induced inhibition of protein folding is not yet clarified. Refolding experiments using a real protein substrate for the DnaK_{Tth} system isolated from the same organisms would be in this case much more relevant especially for conditions simulating the heat shock response in *T. thermophilus*. Whereas the displacement of protein substrate from DnaK_{Tth} was occurring in the presence of DafA(L2V)_{Tth}, the replacement of DafA(L2V)_{Tth} from the complex by various model protein substrates used until present could not be observed at 30°C. Therefore, discovery of a real protein substrate for DnaK_{Tth} system is a prerequisite for the complete confirmation of the current model of DnaK_{Tth} cycle regulation.

Of a special interest is the inhibitory effect of *E. coli* lysates on the luciferase refolding assisted by DnaK_{Tth}-ClpB_{Tth} chaperone systems. Whether this inhibition is induced by an *E. coli* homolog of DafA_{Tth} is a matter that needs further analysis. If a DafA-like protein exists in *E. coli* its identification will greatly improve the knowledge about the *in vivo* function of DafA_{Tth} since, in contrast to the thermophilic strain, the genetic manipulation of *E. coli* is not longer a challenging task.

5 SUMMARY

DafA is a protein encoded by the *dnaK* operon of *Thermus thermophilus* and mediates the formation of a highly stable complex between the molecular chaperone DnaK_{Tth} and its co-chaperone DnaJ_{Tth}. This 87 amino acid residues protein is the only member of the DnaK_{Tth} chaperone system for which no corresponding protein has yet been identified in other organisms and whose particular function has remained elusive.

The main aim of this work was to characterize DafA_{Tth} using the stably expressed DafA(L2V)_{Tth} variant. The studies presented here involved the application of various biochemical and biophysical methods offering new insights into structural and functional features of DafA_{Tth}.

Although not complete, the structural analysis of free DafA(L2V)_{Tth} provided evidence for a well-folded protein comprising defined secondary structure elements including alpha-helical, beta-sheet and coiled coil regions. From these studies and from spectroscopical analyses of engineered DafA(L2V)_{Tth} point mutants it became also evident that the two tryptophane residues of DafA(L2V)_{Tth} have different localization with respect to solvent accessibility.

Studies on the dynamics of the DnaK_{Tth}-DnaJ_{Tth}-DafA(L2V)_{Tth} complex formation and dissociation using a fluorescently labeled DafA(L2V)_{Tth} cysteine mutant show that, at 25°C, both events occur at low rates. The rate constant characterizing complex assembly (k_{on}) is $9.3 \cdot 10^3 \text{ M}^{-1} \text{ s}^{-1}$, whereas the complex dissociation rate (k_{off}) is $1.3 \cdot 10^{-3} \text{ s}^{-1}$. As anticipated from previous studies, the affinity existing between the complex components is very high. The equilibrium dissociation constant K_D is in the submicromolar range (~140 nM). Also, these studies suggest once more that the complex formation is a highly synergic process occurring only in the presence of all three protein species. Fluorescent complexes comprising only two protein species could not be observed.

Except for its essential role in mediating in DnaK_{Tth}-DnaJ_{Tth} association, no other specific function could be assigned to DafA_{Tth}. Studies with peptides showed that DafA(L2V)_{Tth} competes with peptides binding to DnaK_{Tth} in the presence of DnaJ_{Tth}. The same inhibitory effect was observed here in a luciferase refolding assay. DafA(L2V)_{Tth} inhibits DnaK_{Tth}-assisted protein refolding thus confirming the model for DnaK_{Tth} chaperone cycle proposed by Klostermeier et al. Since DafA_{Tth} must be released from DnaK_{Tth}-DnaJ_{Tth}-DafA_{Tth} complex before substrate proteins can bind, free DafA_{Tth} might have regulatory function connected to the heat shock response. Here, the 70 S ribosomal particle was identified as the new binding target of DafA(L2V)_{Tth} thus supporting this hypothesis. DafA(L2V)_{Tth} is targeted *in vitro* to the translational machinery without recruiting DnaK_{Tth} and DnaJ_{Tth}. Competition experiments show that DafA(L2V)_{Tth} is shuttled between the two complexes. These findings strongly suggest the involvement of

DafA_{Tth} in regulatory processes occurring at a translational level, which could represent a new mechanism of heat shock response as an adaptation to elevated temperature.

The second part of this study involved the cooperation between DnaK_{Tth} and ClpB_{Tth} chaperone systems in reactivation of protein aggregates. The aim of this work was to establish *in vitro* conditions that will allow for protein-aggregate reactivation using the co-expressed DnaK_{Tth}-ClpB_{Tth} systems. The *dnaK*_{Tth} operon containing both DnaK and ClpB chaperone systems was cloned into an expression vector and the corresponding proteins were produced in *E. coli*. Importantly, the *dafA* gene was successfully removed from the operon, a prerequisite for a DnaK_{Tth} system functionally active in protein refolding. During this study it became evident that *E. coli* lysates containing the thermophilic proteins are not able to reactivate protein aggregates. Moreover, the lysates have a strong inhibitory effect on DnaK_{Tth}-ClpB_{Tth}-assisted refolding in an assay using purified chaperones. This observation raises the question of a DafA-like protein produced also by *E. coli* cells.

6 REFERENCES

Reference List

- Anfinsen,C.B. (1973). Principles that govern the folding of protein chains. *Science* *181*, 223-230.
- Anfinsen,C.B., HABER,E., SELA,M., and WHITE,F.H., Jr. (1961). The kinetics of formation of native ribonuclease during oxidation of the reduced polypeptide chain. *Proc. Natl. Acad. Sci. U. S. A* *47*, 1309-1314.
- Banecki,B., Liberek,K., Wall,D., Wawrzynow,A., Georgopoulos,C., Bertoli,E., Tanfani,F., and Zylicz,M. (1996). Structure-function analysis of the zinc finger region of the DnaJ molecular chaperone. *J. Biol. Chem.* *271*, 14840-14848.
- Barth,S., Huhn,M., Matthey,B., Klimka,A., Galinski,E.A., and Engert,A. (2000). Compatible-solute-supported periplasmic expression of functional recombinant proteins under stress conditions. *Appl. Environ. Microbiol.* *66*, 1572-1579.
- Beinker,P., Schlee,S., Groemping,Y., Seidel,R., and Reinstein,J. (2002). The N terminus of ClpB from *Thermus thermophilus* is not essential for the chaperone activity. *J. Biol. Chem.* *277*, 47160-47166.
- Ben Zvi,A.P. and Goloubinoff,P. (2001). Review: mechanisms of disaggregation and refolding of stable protein aggregates by molecular chaperones. *J. Struct. Biol.* *135*, 84-93.
- Blaha,G., Wilson,D.N., Stoller,G., Fischer,G., Willumeit,R., and Nierhaus,K.H. (2003). Localization of the trigger factor binding site on the ribosomal 50S subunit. *J. Mol. Biol.* *326*, 887-897.
- Braig,K., Otwinowski,Z., Hegde,R., Boisvert,D.C., Joachimiak,A., Horwich,A.L., and Sigler,P.B. (1994). The crystal structure of the bacterial chaperonin GroEL at 2.8 Å. *Nature* *371*, 578-586.
- Brown,N.L., Stoyanov,J.V., Kidd,S.P., and Hobman,J.L. (2003). The MerR family of transcriptional regulators. *FEMS Microbiol. Rev.* *27*, 145-163.
- Bucca,G., Brassington,A.M., Schonfeld,H.J., and Smith,C.P. (2000). The HspR regulon of *Streptomyces coelicolor*: a role for the DnaK chaperone as a transcriptional co-repressordagger. *Mol. Microbiol.* *38*, 1093-1103.
- Bucca,G., Brassington,A.M.E., Hotchkiss,G., Mersinias,V., and Smith,C.P. (2003). Negative feedback regulation of dnaK, clpB and lon expression by the DnaK chaperone machine in *Streptomyces coelicolor*, identified by transcriptome and in vivo DnaK-depletion analysis. *Molecular Microbiology* *50*, 153-166.
- Bucca,G., Ferina,G., Puglia,A.M., and Smith,C.P. (1995). The dnaK operon of *Streptomyces coelicolor* encodes a novel heat-shock protein which binds to the promoter region of the operon. *Mol. Microbiol.* *17*, 663-674.

- Bucca,G., Hindle,Z., and Smith,C.P. (1997). Regulation of the dnaK operon of *Streptomyces coelicolor* A3(2) is governed by HspR, an autoregulatory repressor protein. *J. Bacteriol.* *179*, 5999-6004.
- Buchberger,A., Schroder,H., Hestekamp,T., Schonfeld,H.J., and Bukau,B. (1996). Substrate shuttling between the DnaK and GroEL systems indicates a chaperone network promoting protein folding. *J. Mol. Biol.* *261*, 328-333.
- Buchberger,A., Theyssen,H., Schroder,H., McCarty,J.S., Virgallita,G., Milkereit,P., Reinstein,J., and Bukau,B. (1995). Nucleotide-induced conformational changes in the ATPase and substrate binding domains of the DnaK chaperone provide evidence for interdomain communication. *J. Biol. Chem.* *270*, 16903-16910.
- Buchner,J. (1999). Hsp90 & Co. - a holding for folding. *Trends Biochem. Sci.* *24*, 136-141.
- Bukau,B. (1993). Regulation of the *Escherichia coli* heat-shock response. *Mol. Microbiol.* *9*, 671-680.
- Bukau,B., Deuerling,E., Pfund,C., and Craig,E.A. (2000). Getting newly synthesized proteins into shape. *Cell* *101*, 119-122.
- Bukau,B. and Horwich,A.L. (1998). The Hsp70 and Hsp60 chaperone machines. *Cell* *92*, 351-366.
- Chen,L. and Sigler,P.B. (1999). The crystal structure of a GroEL/peptide complex: plasticity as a basis for substrate diversity. *Cell* *99*, 757-768.
- Chen,S., Roseman,A.M., Hunter,A.S., Wood,S.P., Burston,S.G., Ranson,N.A., Clarke,A.R., and Saibil,H.R. (1994). Location of a folding protein and shape changes in GroEL-GroES complexes imaged by cryo-electron microscopy. *Nature* *371*, 261-264.
- Choudhury,P., Liu,Y., and Sifers,R.N. (1997). Quality control of protein folding: Participation in human disease. *News in Physiological Sciences* *12*, 162-166.
- Chuang,S.E., Burland,V., Plunkett,G., III, Daniels,D.L., and Blattner,F.R. (1993). Sequence analysis of four new heat-shock genes constituting the hslTS/ibpAB and hslVU operons in *Escherichia coli*. *Gene* *134*, 1-6.
- Clemons,W.M., Jr., Brodersen,D.E., McCutcheon,J.P., May,J.L., Carter,A.P., Morgan-Warren,R.J., Wimberly,B.T., and Ramakrishnan,V. (2001). Crystal structure of the 30 S ribosomal subunit from *Thermus thermophilus*: purification, crystallization and structure determination. *J. Mol. Biol.* *310*, 827-843.
- Cowan,N.J. and Lewis,S.A. (2001). Type II chaperonins, prefoldin, and the tubulin-specific chaperones. *Adv. Protein Chem.* *59*, 73-104.
- Craig,E.A., Eisenman,H.C., and Hundley,H.A. (2003). Ribosome-tethered molecular chaperones: the first line of defense against protein misfolding? *Curr. Opin. Microbiol.* *6*, 157-162.
- Csonka,L.N. (1989). Physiological and Genetic Responses of Bacteria to Osmotic-Stress. *Microbiological Reviews* *53*, 121-147.

- Davis,G.D., Elisee,C., Newham,D.M., and Harrison,R.G. (1999). New fusion protein systems designed to give soluble expression in *Escherichia coli*. *Biotechnol. Bioeng.* *65*, 382-388.
- Dekker,P.J. and Pfanner,N. (1997). Role of mitochondrial GrpE and phosphate in the ATPase cycle of matrix Hsp70. *J. Mol. Biol.* *270*, 321-327.
- DeLuca,M. (1976). Firefly luciferase. *Adv. Enzymol. Relat Areas Mol. Biol.* *44*, 37-68.
- Deuerling,E., Schulze-Specking,A., Tomoyasu,T., Mogk,A., and Bukau,B. (1999). Trigger factor and DnaK cooperate in folding of newly synthesized proteins. *Nature* *400*, 693-696.
- Diamant,S., Ben Zvi,A.P., Bukau,B., and Goloubinoff,P. (2000). Size-dependent disaggregation of stable protein aggregates by the DnaK chaperone machinery. *J. Biol. Chem.* *275*, 21107-21113.
- Diamant,S., Eliahu,N., Rosenthal,D., and Goloubinoff,P. (2001). Chemical chaperones regulate molecular chaperones in vitro and in cells under combined salt and heat stresses. *J. Biol. Chem.* *276*, 39586-39591.
- Dobson,C.M. (1999). Protein misfolding, evolution and disease. *Trends Biochem. Sci.* *24*, 329-332.
- Dobson,C.M. and Karplus,M. (1999). The fundamentals of protein folding: bringing together theory and experiment. *Curr. Opin. Struct. Biol.* *9*, 92-101.
- Ehresman,B., Imbault,P., and Weil,J.H. (1973). Spectrophotometric Determination of Protein Concentration in Cell Extracts Containing Transfer-Rna and Ribosomal-Rnas. *Analytical Biochemistry* *54*, 454-463.
- Ellis,R.J. (1994a). Chaperoning nascent proteins. *Nature* *370*, 96-97.
- Ellis,R.J. (1994b). Molecular chaperones. Opening and closing the Anfinsen cage. *Curr. Biol.* *4*, 633-635.
- Ellis,R.J. (2001). Macromolecular crowding: an important but neglected aspect of the intracellular environment. *Curr. Opin. Struct. Biol.* *11*, 114-119.
- Ellis,R.J. and Hartl,F.U. (1999). Principles of protein folding in the cellular environment. *Curr. Opin. Struct. Biol.* *9*, 102-110.
- Ellis,R.J. and van der Vies,S.M. (1991). Molecular chaperones. *Annu. Rev. Biochem.* *60*, 321-347.
- Ewalt,K.L., Hendrick,J.P., Houry,W.A., and Hartl,F.U. (1997). In vivo observation of polypeptide flux through the bacterial chaperonin system. *Cell* *90*, 491-500.
- Fayet,O., Ziegelhoffer,T., and Georgopoulos,C. (1989). The groES and groEL heat shock gene products of *Escherichia coli* are essential for bacterial growth at all temperatures. *J. Bacteriol.* *171*, 1379-1385.
- Flaherty,K.M., DeLuca-Flaherty,C., and McKay,D.B. (1990). Three-dimensional structure of the ATPase fragment of a 70K heat-shock cognate protein. *Nature* *346*, 623-628.

- Freedman,R.B., Hawkins,H.C., and McLaughlin,S.H. (1995). Protein disulfide-isomerase. *Methods Enzymol.* *251*, 397-406.
- Frydman,J. and Hartl,F.U. (1996). Principles of chaperone-assisted protein folding: differences between in vitro and in vivo mechanisms. *Science* *272*, 1497-1502.
- Frydman,J., Nimmegern,E., Erdjument-Bromage,H., Wall,J.S., Tempst,P., and Hartl,F.U. (1992). Function in protein folding of TRiC, a cytosolic ring complex containing TCP-1 and structurally related subunits. *EMBO J.* *11*, 4767-4778.
- Frydman,J., Nimmegern,E., Ohtsuka,K., and Hartl,F.U. (1994). Folding of nascent polypeptide chains in a high molecular mass assembly with molecular chaperones. *Nature* *370*, 111-117.
- Gamer,J., Bujard,H., and Bukau,B. (1992). Physical interaction between heat shock proteins DnaK, DnaJ, and GrpE and the bacterial heat shock transcription factor sigma 32. *Cell* *69*, 833-842.
- Gamer,J., Multhaupt,G., Tomoyasu,T., McCarty,J.S., Rudiger,S., Schonfeld,H.J., Schirra,C., Bujard,H., and Bukau,B. (1996). A cycle of binding and release of the DnaK, DnaJ and GrpE chaperones regulates activity of the Escherichia coli heat shock transcription factor sigma32. *EMBO J.* *15*, 607-617.
- Garnier J, Gibrat J-F, and Robson B (1996). GOR Method for Predicting Protein Secondary Structure from Amino Acid Sequence. In *Methods in Enzymology: Computer Methods for Macromolecular Sequence Analysis, Vol 266, Section IV. Secondary Structure Considerations*, R.F.Doolittle, ed. (CA: Academic Press), pp. 540-553.
- Gautschi,M., Lilie,H., Funfschilling,U., Mun,A., Ross,S., Lithgow,T., Rucknagel,P., and Rospert,S. (2001). RAC, a stable ribosome-associated complex in yeast formed by the DnaK-DnaJ homologs Ssz1p and zuotin. *Proc. Natl. Acad. Sci. U. S. A* *98*, 3762-3767.
- Gautschi,M., Mun,A., Ross,S., and Rospert,S. (2002). A functional chaperone triad on the yeast ribosome. *Proc. Natl. Acad. Sci. U. S. A* *99*, 4209-4214.
- Genevaux,P., Schwager,F., Georgopoulos,C., and Kelley,W.L. (2002). Scanning mutagenesis identifies amino acid residues essential for the in vivo activity of the Escherichia coli DnaJ (Hsp40) J-domain. *Genetics* *162*, 1045-1053.
- Georgopoulos,C., Liberek,K., Zylicz,M., and Ang,D. (1994). Properties of the Heat-Shock Proteins of Escherichia coli and the Autoregulation of the Heat-Shock Response. In *The Biology of Heat Shock Proteins and Molecular Chaperones*, R.I.Morimoto, A.Tissieres, and C.Georgopoulos, eds. (Cold Spring Harbor, NY: Cold Spring Harbor Laboratory Press), pp. 209-249.
- Georgopoulos,C. and Welch,W.J. (1993). Role of the major heat shock proteins as molecular chaperones. *Annu. Rev. Cell Biol.* *9*, 601-634.
- Glover,J.R. and Lindquist,S. (1998). Hsp104, Hsp70, and Hsp40: a novel chaperone system that rescues previously aggregated proteins. *Cell* *94*, 73-82.

- Goldberg, M.E., Expert-Bezancon, N., Vuillard, L., and Rabilloud, T. (1995). Non-detergent sulphobetaines: a new class of molecules that facilitate in vitro protein renaturation. *Fold. Des* 1, 21-27.
- Goldberg, M.E., Rudolph, R., and Jaenicke, R. (1991). A kinetic study of the competition between renaturation and aggregation during the refolding of denatured-reduced egg white lysozyme. *Biochemistry* 30, 2790-2797.
- Goloubinoff, P., Christeller, J.T., Gatenby, A.A., and Lorimer, G.H. (1989). Reconstitution of active dimeric ribulose biphosphate carboxylase from an unfoiled state depends on two chaperonin proteins and Mg-ATP. *Nature* 342, 884-889.
- Goloubinoff, P., Mogk, A., Zvi, A.P., Tomoyasu, T., and Bukau, B. (1999). Sequential mechanism of solubilization and refolding of stable protein aggregates by a bichaperone network. *Proc. Natl. Acad. Sci. U. S. A* 96, 13732-13737.
- Gottesman, S., Clark, W.P., Crecy-Lagard, V., and Maurizi, M.R. (1993). ClpX, an alternative subunit for the ATP-dependent Clp protease of *Escherichia coli*. Sequence and in vivo activities. *J. Biol. Chem.* 268, 22618-22626.
- Gottesman, S., Clark, W.P., and Maurizi, M.R. (1990). The ATP-dependent Clp protease of *Escherichia coli*. Sequence of clpA and identification of a Clp-specific substrate. *J. Biol. Chem.* 265, 7886-7893.
- Gottesman, S., Maurizi, M.R., and Wickner, S. (1997). Regulatory subunits of energy-dependent proteases. *Cell* 91, 435-438.
- Gray, T.E. and Fersht, A.R. (1991). Cooperativity in ATP hydrolysis by GroEL is increased by GroES. *FEBS Lett.* 292, 254-258.
- Greene, L.E., Zinner, R., Naficy, S., and Eisenberg, E. (1995). Effect of nucleotide on the binding of peptides to 70-kDa heat shock protein. *J. Biol. Chem.* 270, 2967-2973.
- Greene, M.K., Maskos, K., and Landry, S.J. (1998). Role of the J-domain in the cooperation of Hsp40 with Hsp70. *Proc. Natl. Acad. Sci. U. S. A* 95, 6108-6113.
- Groemping Y. Kinetische und funktionelle Untersuchungen des DnaK-Systems aus *Thermus thermophilus* und heterogener Komplexe aus *T. thermophilus* und *E. coli*. 2000.
Ref Type: Thesis/Dissertation
- Groemping, Y., Klostermeier, D., Herrmann, C., Veit, T., Seidel, R., and Reinstein, J. (2001). Regulation of ATPase and chaperone cycle of DnaK from *Thermus thermophilus* by the nucleotide exchange factor GrpE. *J. Mol. Biol.* 305, 1173-1183.
- Groemping, Y. and Reinstein, J. (2001). Folding properties of the nucleotide exchange factor GrpE from *Thermus thermophilus*: GrpE is a thermosensor that mediates heat shock response. *J. Mol. Biol.* 314, 167-178.
- Harrison, C.J., Hayer-Hartl, M., Di Liberto, M., Hartl, F., and Kuriyan, J. (1997). Crystal structure of the nucleotide exchange factor GrpE bound to the ATPase domain of the molecular chaperone DnaK. *Science* 276, 431-435.
- Hartl, F.U. (1996). Molecular chaperones in cellular protein folding. *Nature* 381, 571-579.

- Hartl,F.U. and Hayer-Hartl,M. (2002). Molecular chaperones in the cytosol: from nascent chain to folded protein. *Science* 295, 1852-1858.
- Hayer-Hartl,M.K., Martin,J., and Hartl,F.U. (1995). Asymmetrical interaction of GroEL and GroES in the ATPase cycle of assisted protein folding. *Science* 269, 836-841.
- Hennessy,F., Cheetham,M.E., Dirr,H.W., and Blatch,G.L. (2000). Analysis of the levels of conservation of the J domain among the various types of DnaJ-like proteins. *Cell Stress. Chaperones*. 5, 347-358.
- Herbst,R., Gast,K., and Seckler,R. (1998). Folding of firefly (*Photinus pyralis*) luciferase: aggregation and reactivation of unfolding intermediates. *Biochemistry* 37, 6586-6597.
- Hesterkamp,T. and Bukau,B. (1996). The Escherichia coli trigger factor. *FEBS Lett.* 389, 32-34.
- Hesterkamp,T., Hauser,S., Lutcke,H., and Bukau,B. (1996). Escherichia coli trigger factor is a prolyl isomerase that associates with nascent polypeptide chains. *Proc. Natl. Acad. Sci. U. S. A* 93, 4437-4441.
- Hohfeld,J. and Jentsch,S. (1997). GrpE-like regulation of the hsc70 chaperone by the anti-apoptotic protein BAG-1. *EMBO J.* 16, 6209-6216.
- Horovitz,A., Fridmann,Y., Kafri,G., and Yifrach,O. (2001). Review: allostery in chaperonins. *J. Struct. Biol.* 135, 104-114.
- Houry,W.A., Frishman,D., Eckerskorn,C., Lottspeich,F., and Hartl,F.U. (1999). Identification of in vivo substrates of the chaperonin GroEL. *Nature* 402, 147-154.
- Hunt,J.F., Weaver,A.J., Landry,S.J., Gierasch,L., and Deisenhofer,J. (1996). The crystal structure of the GroES co-chaperonin at 2.8 Å resolution. *Nature* 379, 37-45.
- Jaeger,J., Restle,T., and Steitz,T.A. (1998). The structure of HIV-1 reverse transcriptase complexed with an RNA pseudoknot inhibitor. *EMBO J.* 17, 4535-4542.
- Jaenicke,R. (1987). Folding and association of proteins. *Prog. Biophys. Mol. Biol.* 49, 117-237.
- Jaenicke,R. (1991). Protein folding: local structures, domains, subunits, and assemblies. *Biochemistry* 30, 3147-3161.
- Jaenicke,R. (1996). Stability and folding of ultrastable proteins: eye lens crystallins and enzymes from thermophiles. *FASEB J.* 10, 84-92.
- Karzai,A.W. and McMacken,R. (1996). A bipartite signaling mechanism involved in DnaJ-mediated activation of the Escherichia coli DnaK protein. *J. Biol. Chem.* 271, 11236-11246.
- Kelley,L.A., MacCallum,R.M., and Sternberg,M.J. (2000). Enhanced genome annotation using structural profiles in the program 3D-PSSM. *J. Mol. Biol.* 299, 499-520.

- Kim, K.I., Cheong, G.W., Park, S.C., Ha, J.S., Woo, K.M., Choi, S.J., and Chung, C.H. (2000). Heptameric ring structure of the heat-shock protein ClpB, a protein-activated ATPase in *Escherichia coli*. *J. Mol. Biol.* *303*, 655-666.
- Klostermeier, D. Der Funktionszyklus des DnaK-Chaperonsystem aus *Thermus thermophilus*. Dissertation. 1998.
Ref Type: Thesis/Dissertation
- Klostermeier, D., Seidel, R., and Reinstein, J. (1998). Functional properties of the molecular chaperone DnaK from *Thermus thermophilus*. *J. Mol. Biol.* *279*, 841-853.
- Klostermeier, D., Seidel, R., and Reinstein, J. (1999). The functional cycle and regulation of the *Thermus thermophilus* DnaK chaperone system. *J. Mol. Biol.* *287*, 511-525.
- Kolb, V.A., Makeyev, E.V., and Spirin, A.S. (1994). Folding of firefly luciferase during translation in a cell-free system. *EMBO J.* *13*, 3631-3637.
- Kramer, G., Rauch, T., Rist, W., Vorderwulbecke, S., Patzelt, H., Schulze-Specking, A., Ban, N., Deuring, E., and Bukau, B. (2002). L23 protein functions as a chaperone docking site on the ribosome. *Nature* *419*, 171-174.
- Ladokhin, A.S. (2000). *Encyclopedia of Analytical Chemistry*, Meyers R.A, ed. (Chichester: John Wiley & Sons Ltd.).
- Laemmli, U.K. (1970). Cleavage of structural proteins during the assembly of the head of bacteriophage T4. *Nature* *227*, 680-685.
- Langer, T., Lu, C., Echols, H., Flanagan, J., Hayer, M.K., and Hartl, F.U. (1992). Successive action of DnaK, DnaJ and GroEL along the pathway of chaperone-mediated protein folding. *Nature* *356*, 683-689.
- Laufen, T., Mayer, M.P., Beisel, C., Klostermeier, D., Mogk, A., Reinstein, J., and Bukau, B. (1999). Mechanism of regulation of hsp70 chaperones by DnaJ cochaperones. *Proc. Natl. Acad. Sci. U. S. A* *96*, 5452-5457.
- Lehane, S.A. and Chowdry, B.Z. (1998). Thermodynamic background to differential scanning calorimetry. In *Biocalorimetry: Applications of Calorimetry in the Biological Sciences*, J.E. Dabury and B.Z. Chowdhry, eds. (Chichester, UK: John Wiley), pp. 157-182.
- Liberek, K., Marszalek, J., Ang, D., Georgopoulos, C., and Zylicz, M. (1991). *Escherichia coli* DnaJ and GrpE heat shock proteins jointly stimulate ATPase activity of DnaK. *Proc. Natl. Acad. Sci. U. S. A* *88*, 2874-2878.
- Linke, K., Wolfram, T., Bussemer, J., and Jakob, U. (2003). The roles of the two zinc binding sites in DnaJ. *J. Biol. Chem.* *278*, 44457-44466.
- Lu, Z. and Cyr, D.M. (1998). Protein folding activity of Hsp70 is modified differentially by the hsp40 co-chaperones Sis1 and Ydj1. *J. Biol. Chem.* *273*, 27824-27830.
- Manaiá, C.M., Hoste, B., Gutierrez, M.C., Gillis, M., Ventosa, A., Kersters, K., and Dacosta, M.S. (1995). Halotolerant *Thermus* Strains from Marine and Terrestrial Hot-

- Springs Belong to Thermus-Thermophilus (Ex Oshima-And-Imahori, 1974) Nom-Rev-Emend. *Systematic and Applied Microbiology* 17, 526-532.
- Maurizi,M.R. (2002). Love it or cleave it: tough choices in protein quality control. *Nat. Struct. Biol.* 9, 410-412.
- Mayer,M.P., Brehmer,D., Gassler,C.S., and Bukau,B. (2001). Hsp70 chaperone machines. *Adv. Protein Chem.* 59, 1-44.
- Mayer,M.P., Rudiger,S., and Bukau,B. (2000a). Molecular basis for interactions of the DnaK chaperone with substrates. *Biol. Chem.* 381, 877-885.
- Mayer,M.P., Schroder,H., Rudiger,S., Paal,K., Laufen,T., and Bukau,B. (2000b). Multistep mechanism of substrate binding determines chaperone activity of Hsp70. *Nat. Struct. Biol.* 7, 586-593.
- Mayhew,M., da Silva,A.C., Martin,J., Erdjument-Bromage,H., Tempst,P., and Hartl,F.U. (1996). Protein folding in the central cavity of the GroEL-GroES chaperonin complex. *Nature* 379, 420-426.
- McCarty,J.S., Buchberger,A., Reinstein,J., and Bukau,B. (1995). The role of ATP in the functional cycle of the DnaK chaperone system. *J. Mol. Biol.* 249, 126-137.
- Minton,A.P. (2000). Implications of macromolecular crowding for protein assembly. *Curr. Opin. Struct. Biol.* 10, 34-39.
- Mogk,A., Mayer,M.P., and Deuerling,E. (2002). Mechanisms of protein folding: molecular chaperones and their application in biotechnology. *Chembiochem.* 3, 807-814.
- Mogk,A., Tomoyasu,T., Goloubinoff,P., Rudiger,S., Roder,D., Langen,H., and Bukau,B. (1999). Identification of thermolabile Escherichia coli proteins: prevention and reversion of aggregation by DnaK and ClpB. *EMBO J.* 18, 6934-6949.
- Morita,M., Kanemori,M., Yanagi,H., and Yura,T. (1999). Heat-induced synthesis of sigma32 in Escherichia coli: structural and functional dissection of rpoH mRNA secondary structure. *J. Bacteriol.* 181, 401-410.
- Motohashi,K., Taguchi,H., Ishii,N., and Yoshida,M. (1994). Isolation of the stable hexameric DnaK.DnaJ complex from Thermus thermophilus. *J. Biol. Chem.* 269, 27074-27079.
- Motohashi,K., Watanabe,Y., Yohda,M., and Yoshida,M. (1999). Heat-inactivated proteins are rescued by the DnaK.J-GrpE set and ClpB chaperones. *Proc. Natl. Acad. Sci. U. S. A* 96, 7184-7189.
- Motohashi,K., Yohda,M., Endo,I., and Yoshida,M. (1996). A novel factor required for the assembly of the DnaK and DnaJ chaperones of Thermus thermophilus. *J. Biol. Chem.* 271, 17343-17348.
- Mullis,K.B. and Faloona,F.A. (1987). Specific synthesis of DNA in vitro via a polymerase-catalyzed chain reaction. *Methods Enzymol.* 155, 335-350.

- Osipiuk, J. and Joachimiak, A. (1997). Cloning, sequencing, and expression of dnaK-operon proteins from the thermophilic bacterium *Thermus thermophilus*. *Biochim. Biophys. Acta* *1353*, 253-265.
- Packschies, L., Theyssen, H., Buchberger, A., Bukau, B., Goody, R.S., and Reinstein, J. (1997). GrpE accelerates nucleotide exchange of the molecular chaperone DnaK with an associative displacement mechanism. *Biochemistry* *36*, 3417-3422.
- Pahl, A., Brune, K., and Bang, H. (1997). Fit for life? Evolution of chaperones and folding catalysts parallels the development of complex organisms. *Cell Stress. Chaperones.* *2*, 78-86.
- Parsell, D.A., Kowal, A.S., and Lindquist, S. (1994). *Saccharomyces cerevisiae* Hsp104 protein. Purification and characterization of ATP-induced structural changes. *J. Biol. Chem.* *269*, 4480-4487.
- Patzelt, H., Kramer, G., Rauch, T., Schonfeld, H.J., Bukau, B., and Deuerling, E. (2002). Three-state equilibrium of *Escherichia coli* trigger factor. *Biol. Chem.* *383*, 1611-1619.
- Pearl, L.H. and Prodromou, C. (2001). Structure, function, and mechanism of the Hsp90 molecular chaperone. *Adv. Protein Chem.* *59*, 157-186.
- Pelham, H.R. (1986). Speculations on the functions of the major heat shock and glucose-regulated proteins. *Cell* *46*, 959-961.
- Pellecchia, M., Montgomery, D.L., Stevens, S.Y., Vander Kooi, C.W., Feng, H.P., Gierasch, L.M., and Zuiderweg, E.R. (2000). Structural insights into substrate binding by the molecular chaperone DnaK. *Nat. Struct. Biol.* *7*, 298-303.
- Pellecchia, M., Szyperski, T., Wall, D., Georgopoulos, C., and Wuthrich, K. (1996). NMR structure of the J-domain and the Gly/Phe-rich region of the *Escherichia coli* DnaJ chaperone. *J. Mol. Biol.* *260*, 236-250.
- Pfanner, N., Craig, E.A., and Honlinger, A. (1997). Mitochondrial preprotein translocase. *Annu. Rev. Cell Dev. Biol.* *13*, 25-51.
- Pleckaityte, M., Mistiniene, E., Michailoviene, V., and Zvirblis, G. (2003). Identification and characterization of a Hsp70 (DnaK) chaperone system from *Meiothermus ruber*. *Mol. Genet. Genomics* *269*, 109-115.
- Privalov, P.L. and Potekhin, S.A. (1986). *Methods in Enzymology: Scanning microcalorimetry in studying temperature-induced changes in proteins.*, R.F. Doolittle, ed. (CA: Academic Press), pp. 4-51.
- Radford, S.E. (2000). Protein folding: progress made and promises ahead. *Trends Biochem. Sci.* *25*, 611-618.
- Rohrwild, M., Pfeifer, G., Santarius, U., Muller, S.A., Huang, H.C., Engel, A., Baumeister, W., and Goldberg, A.L. (1997). The ATP-dependent HslVU protease from *Escherichia coli* is a four-ring structure resembling the proteasome. *Nat. Struct. Biol.* *4*, 133-139.

- Roseman, A.M., Chen, S., White, H., Braig, K., and Saibil, H.R. (1996). The chaperonin ATPase cycle: mechanism of allosteric switching and movements of substrate-binding domains in GroEL. *Cell* 87, 241-251.
- Rudiger, S., Buchberger, A., and Bukau, B. (1997). Interaction of Hsp70 chaperones with substrates. *Nat. Struct. Biol.* 4, 342-349.
- Rudiger, S., Schneider-Mergener, J., and Bukau, B. (2001). Its substrate specificity characterizes the DnaJ co-chaperone as a scanning factor for the DnaK chaperone. *EMBO J.* 20, 1042-1050.
- Russell, R., Wali, K.A., Mehl, A.F., and McMacken, R. (1999). DnaJ dramatically stimulates ATP hydrolysis by DnaK: insight into targeting of Hsp70 proteins to polypeptide substrates. *Biochemistry* 38, 4165-4176.
- Ryan, M.T., Naylor, D.J., Hoj, P.B., Clark, M.S., and Hoogenraad, N.J. (1997). The role of molecular chaperones in mitochondrial protein import and folding. *Int. Rev. Cytol.* 174, 127-193.
- Ryan, M.T. and Pfanner, N. (2001). Hsp70 proteins in protein translocation. *Adv. Protein Chem.* 59, 223-242.
- Rye, H.S., Burston, S.G., Fenton, W.A., Beechem, J.M., Xu, Z., Sigler, P.B., and Horwich, A.L. (1997). Distinct actions of cis and trans ATP within the double ring of the chaperonin GroEL. *Nature* 388, 792-798.
- Saibil, H.R., Horwich, A.L., and Fenton, W.A. (2001). Allostery and protein substrate conformational change during GroEL/GroES-mediated protein folding. *Adv. Protein Chem.* 59, 45-72.
- Sakikawa, C., Taguchi, H., Makino, Y., and Yoshida, M. (1999). On the maximum size of proteins to stay and fold in the cavity of GroEL underneath GroES. *J. Biol. Chem.* 274, 21251-21256.
- Sambrook, J., Fritsch, E.F., and Maniatis, T. (1989). *Molecular Cloning: A Laboratory Manual*. (Cold Spring Harbor, NY: Cold Spring Harbor Laboratory).
- Samuel, D., Kumar, T.K., Ganesh, G., Jayaraman, G., Yang, P.W., Chang, M.M., Trivedi, V.D., Wang, S.L., Hwang, K.C., Chang, D.K., and Yu, C. (2000). Proline inhibits aggregation during protein refolding. *Protein Sci.* 9, 344-352.
- Sanchez, Y. and Lindquist, S.L. (1990). HSP104 required for induced thermotolerance. *Science* 248, 1112-1115.
- Santoro, M.M. and Bolen, D.W. (1988). Unfolding free energy changes determined by the linear extrapolation method. 1. Unfolding of phenylmethanesulfonyl alpha-chymotrypsin using different denaturants. *Biochemistry* 27, 8063-8068.
- Schagger, H. and von Jagow, G. (1987). Tricine-sodium dodecyl sulfate-polyacrylamide gel electrophoresis for the separation of proteins in the range from 1 to 100 kDa. *Anal. Biochem.* 166, 368-379.

- Schirmer,E.C., Glover,J.R., Singer,M.A., and Lindquist,S. (1996). HSP100/Clp proteins: a common mechanism explains diverse functions. *Trends Biochem. Sci.* *21*, 289-296.
- Schlee,S., Beinker,P., Akhrymuk,A., and Reinstein,J. (2004). A chaperone network for the resolubilization of protein aggregates: direct interaction of ClpB and DnaK. *J. Mol. Biol.* *336*, 275-285.
- Schlee,S., Groemping,Y., Herde,P., Seidel,R., and Reinstein,J. (2001). The chaperone function of ClpB from *Thermus thermophilus* depends on allosteric interactions of its two ATP-binding sites. *J. Mol. Biol.* *306*, 889-899.
- Schlee,S. and Reinstein,J. (2002). The DnaK/ClpB chaperone system from *Thermus thermophilus*. *Cell Mol. Life Sci.* *59*, 1598-1606.
- Schmid,F.X. (2001). Prolyl isomerases. *Adv. Protein Chem.* *59*, 243-282.
- Scholz,C., Stoller,G., Zarnt,T., Fischer,G., and Schmid,F.X. (1997). Cooperation of enzymatic and chaperone functions of trigger factor in the catalysis of protein folding. *EMBO J.* *16*, 54-58.
- Schroder,H., Langer,T., Hartl,F.U., and Bukau,B. (1993). DnaK, DnaJ and GrpE form a cellular chaperone machinery capable of repairing heat-induced protein damage. *EMBO J.* *12*, 4137-4144.
- Segal,G. and Ron,E.Z. (1996). Regulation and organization of the groE and dnaK operons in Eubacteria. *Fems Microbiology Letters* *138*, 1-10.
- Selkoe,D.J. (2002). Alzheimer's disease is a synaptic failure. *Science* *298*, 789-791.
- Sherman,M.Y. and Goldberg,A.L. (1996). Involvement of molecular chaperones in intracellular protein breakdown. *EXS* *77*, 57-78.
- Sigler,P.B., Xu,Z., Rye,H.S., Burston,S.G., Fenton,W.A., and Horwich,A.L. (1998). Structure and function in GroEL-mediated protein folding. *Annu. Rev. Biochem.* *67*, 581-608.
- Souren,J.E., Wiegant,F.A., and van Wijk,R. (1999). The role of hsp70 in protection and repair of luciferase activity in vivo; experimental data and mathematical modelling. *Cell Mol. Life Sci.* *55*, 799-811.
- Squires,C.L., Pedersen,S., Ross,B.M., and Squires,C. (1991). ClpB is the *Escherichia coli* heat shock protein F84.1. *J. Bacteriol.* *173*, 4254-4262.
- Stoller,G., Rucknagel,K.P., Nierhaus,K.H., Schmid,F.X., Fischer,G., and Rahfeld,J.U. (1995). A ribosome-associated peptidyl-prolyl cis/trans isomerase identified as the trigger factor. *EMBO J.* *14*, 4939-4948.
- Straus,D., Walter,W., and Gross,C.A. (1990). Dnak, Dnaj, and Grpe Heat-Shock Proteins Negatively Regulate Heat-Shock Gene-Expression by Controlling the Synthesis and Stability of Sigma-32. *Genes & Development* *4*, 2202-2209.

- Szabo,A., Langer,T., Schroder,H., Flanagan,J., Bukau,B., and Hartl,F.U. (1994). The ATP hydrolysis-dependent reaction cycle of the Escherichia coli Hsp70 system DnaK, DnaJ, and GrpE. *Proc. Natl. Acad. Sci. U. S. A* *91*, 10345-10349.
- Teter,S.A., Houry,W.A., Ang,D., Tradler,T., Rockabrand,D., Fischer,G., Blum,P., Georgopoulos,C., and Hartl,F.U. (1999). Polypeptide flux through bacterial Hsp70: DnaK cooperates with trigger factor in chaperoning nascent chains. *Cell* *97*, 755-765.
- Theysen,H., Schuster,H.P., Packschies,L., Bukau,B., and Reinstein,J. (1996). The second step of ATP binding to DnaK induces peptide release. *J. Mol. Biol.* *263*, 657-670.
- Thomas,P.J., Qu,B.H., and Pedersen,P.L. (1995). Defective protein folding as a basis of human disease. *Trends Biochem. Sci.* *20*, 456-459.
- Thompson,J.D., Higgins,D.G., and Gibson,T.J. (1994). CLUSTAL W: improving the sensitivity of progressive multiple sequence alignment through sequence weighting, position-specific gap penalties and weight matrix choice. *Nucleic Acids Res.* *22*, 4673-4680.
- Tobias,J.W., Shrader,T.E., Rocap,G., and Varshavsky,A. (1991). The N-end rule in bacteria. *Science* *254*, 1374-1377.
- Todd,M.J., Viitanen,P.V., and Lorimer,G.H. (1993). Hydrolysis of adenosine 5'-triphosphate by Escherichia coli GroEL: effects of GroES and potassium ion. *Biochemistry* *32*, 8560-8567.
- Todd,M.J., Viitanen,P.V., and Lorimer,G.H. (1994). Dynamics of the chaperonin ATPase cycle: implications for facilitated protein folding. *Science* *265*, 659-666.
- Tomoyasu,T., Arsene,F., Ogura,T., and Bukau,B. (2001). The C terminus of sigma(32) is not essential for degradation by FtsH. *J. Bacteriol.* *183*, 5911-5917.
- Tomoyasu,T., Gamer,J., Bukau,B., Kanemori,M., Mori,H., Rutman,A.J., Oppenheim,A.B., Yura,T., Yamanaka,K., Niki,H., and . (1995b). Escherichia coli FtsH is a membrane-bound, ATP-dependent protease which degrades the heat-shock transcription factor sigma 32. *EMBO J.* *14*, 2551-2560.
- Tomoyasu,T., Gamer,J., Bukau,B., Kanemori,M., Mori,H., Rutman,A.J., Oppenheim,A.B., Yura,T., Yamanaka,K., Niki,H., and . (1995a). Escherichia coli FtsH is a membrane-bound, ATP-dependent protease which degrades the heat-shock transcription factor sigma 32. *EMBO J.* *14*, 2551-2560.
- Vuillard,L., Braun-Breton,C., and Rabilloud,T. (1995). Non-detergent sulphobetaines: a new class of mild solubilization agents for protein purification. *Biochem. J.* *305 (Pt 1)*, 337-343.
- Wall,D., Zylicz,M., and Georgopoulos,C. (1994). The NH2-terminal 108 amino acids of the Escherichia coli DnaJ protein stimulate the ATPase activity of DnaK and are sufficient for lambda replication. *J. Biol. Chem.* *269*, 5446-5451.
- Walter,S. and Buchner,J. (2002). Molecular chaperones--cellular machines for protein folding. *Angew. Chem. Int. Ed Engl.* *41*, 1098-1113.

- Wawrzynow,A. and Zylicz,M. (1995). Divergent effects of ATP on the binding of the DnaK and DnaJ chaperones to each other, or to their various native and denatured protein substrates. *J. Biol. Chem.* *270*, 19300-19306.
- Weissman,J.S., Hohl,C.M., Kovalenko,O., Kashi,Y., Chen,S., Braig,K., Saibil,H.R., Fenton,W.A., and Horwich,A.L. (1995). Mechanism of GroEL action: productive release of polypeptide from a sequestered position under GroES. *Cell* *83*, 577-587.
- Wickner,S., Gottesman,S., Skowyr,D., Hoskins,J., McKenney,K., and Maurizi,M.R. (1994). A molecular chaperone, ClpA, functions like DnaK and DnaJ. *Proc. Natl. Acad. Sci. U. S. A* *91*, 12218-12222.
- Wickner,S., Hoskins,J., and McKenney,K. (1991). Function of DnaJ and DnaK as chaperones in origin-specific DNA binding by RepA. *Nature* *350*, 165-167.
- Wickner,S., Maurizi,M.R., and Gottesman,S. (1999). Posttranslational quality control: folding, refolding, and degrading proteins. *Science* *286*, 1888-1893.
- Williams,R.A.D. (1992). The Genus *Thermus*. In *Thermophilic Bacteria*, J.K.Kristjansson, ed. (Boca Raton: CRC), pp. 51-62.
- Wishart,D.S., Bigam,C.G., Holm,A., Hodges,R.S., and Sykes,B.D. (1995). ¹H, ¹³C and ¹⁵N random coil NMR chemical shifts of the common amino acids. I. Investigations of nearest-neighbor effects. *J. Biomol. NMR* *5*, 67-81.
- Wuethrich,K. (1986). *NMR of Proteins and Nucleic Acids*. (New York: Wiley & Sons).
- Xu,Z., Yang,S., and Zhu,D. (1997). GroE assists refolding of recombinant human pro-urokinase. *J. Biochem. (Tokyo)* *121*, 331-337.
- Yan,W., Schilke,B., Pfund,C., Walter,W., Kim,S., and Craig,E.A. (1998). Zuo1, a ribosome-associated DnaJ molecular chaperone. *EMBO J.* *17*, 4809-4817.
- Yifrach,O. and Horovitz,A. (1994). Two lines of allosteric communication in the oligomeric chaperonin GroEL are revealed by the single mutation Arg196-->Ala. *J. Mol. Biol.* *243*, 397-401.
- Yura,T. and Nakahigashi,K. (1999b). Regulation of the heat-shock response. *Curr. Opin. Microbiol.* *2*, 153-158.
- Yura,T. and Nakahigashi,K. (1999a). Regulation of the heat-shock response. *Curr. Opin. Microbiol.* *2*, 153-158.
- Zeiner,M., Gebauer,M., and Gehring,U. (1997). Mammalian protein RAP46: an interaction partner and modulator of 70 kDa heat shock proteins. *EMBO J.* *16*, 5483-5490.
- Zhu,X., Zhao,X., Burkholder,W.F., Gragerov,A., Ogata,C.M., Gottesman,M.E., and Hendrickson,W.A. (1996). Structural analysis of substrate binding by the molecular chaperone DnaK. *Science* *272*, 1606-1614.
- Zolkiewski,M. (1999). ClpB cooperates with DnaK, DnaJ, and GrpE in suppressing protein aggregation. A novel multi-chaperone system from *Escherichia coli*. *J. Biol. Chem.* *274*, 28083-28086.

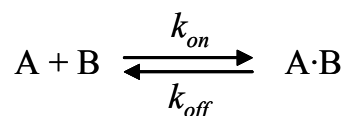
Zylicz, M., Ang, D., Liberek, K., and Georgopoulos, C. (1989). Initiation of lambda DNA replication with purified host- and bacteriophage-encoded proteins: the role of the dnaK, dnaJ and grpE heat shock proteins. *EMBO J.* 8, 1601-1608.

7 APPENDIX

7.1 Derivations

7.1.1 Determination of the k_{on} and k_{off} via k_{obs}

The interaction between two molecules A and B can be described by the following equation:



Equation 7-1

k_{on} association rate constant
 k_{off} dissociation rate constant

The concentration of A·B is modifying in time conform to equation:

$$d[A \cdot B]/dt = k_{on} [A] [B] - k_{off} [A \cdot B]$$

Equation 7-2

[A] concentration of A at time t

[B] concentration of B at time t

[A·B] concentration of complex A·B formed at time t

At equilibrium the concentration of A is given by the difference between $[A_0] - [A \cdot B]$. In the case of $[B_0] \gg A_0$, the concentration of B will be $[B] \approx [B_0]$ (pseudo-first order reaction). Thus, the previous equation will become:

$$d[A \cdot B]/dt = k_{on} [B_0] [A_0] - (k_{on} [B_0] + k_{off}) [A \cdot B]$$

Equation 7-3

[A₀] initial concentration of A

[B₀] initial concentration of B

Because the only fluorescent species are A and A·B, by measuring the $k_{obs} = k_{on} [B_0] + k_{off}$ at different concentration of B₀ and by plotting the k_{obs} against these various [B₀] it is possible to calculate the rate constants k_{on} and k_{off} .

The equilibrium dissociation constant K_D for the complex formation was calculated using the equation:

$$K_D = k_{off} / k_{on}$$

Equation 7-4

7.2 Abbreviations

ADP, ATP	Adenosin-5'-diphosphate, Adenosin-5'-triphosphate
APS	Ammoniumperoxodisulfate
BSA	Bovine Serum Albumin
CD	Circular Dichroism
DEAE	Diehylammoniummethyl-
DMSO	Dimethyl Sulfoxide
DNA	Deoxyribonucleic acid
DNase	Deoxyribonuclease
DTE	1,4-Dithioerythritol
EDTA	Ehtylendiaminetetraacetic acid
<i>E. coli</i> , <i>Eco</i>	<i>Escherichia coli</i>
FPLC	Fast Performance Liquid Chromatography
GdmCl	Guanidinium hydrochlorid
HEPES	4-(2-Hydroxyethyl)-1-piperazinoethansulfonic acid
HPLC	High performance liquid chromatography
Hsc	Heat shock cognate
Hsp	Heat shock protein
IAEDANS	5-(((2-iodoacetyl)amino)ethyl)amino)naphthalene-1-sulfonic acid
IANBD ester	N-((2-iodoacetoxy)ethyl)-N-methyl)amino-7-nitrobenz-2-oxa-1,3-diazole
IPTG	Isopropyl- β -D-thiogalactosid
kD	kilo Dalton
K_D	Equilibrium dissociation constant
k_{on}	Association rate constant
k_{off}	Dissociation rate constant
λ	Wavelength
mRNA	Messenger RNA
MOPS	3-Morpholinopropanesulfonic acid
OD ₆₀₀	Optical Density at 600 nm
PCR	Polymerase chain reaction
PMSF	Phenylmethylsufonyl fluoride

RNA	Ribonucleic acid
RNaseA	Ribonuclease A
rRNA	Ribosomal RNA
rpm	Revolutions per minute
<i>S. cerevisiae</i>	<i>Saccharomyces cerevisiae</i>
SDS-PAGE	Sodiumdodecylsulfat-Polyacrylamide Gel Electrophoresis
tRNA	Transfer RNA
<i>T. thermophilus</i> , _{Tth}	<i>Thermus thermophilus</i>
TCA	Trichloroacetic acid
TEMED	N,N,N',N'-Tetramethylethylenediamine
TF	Trigger Factor
Tris	Tris-(hydroxymethyl)-aminomethane
wt	Wild type

Abbreviations for the amino acids:

A	Ala	Alanine	I	Ile	Isoleucine	R	Arg	Arginine
C	Cys	Cysteine	K	Lys	Lysine	S	Ser	Serine
D	Asp	Aspartic acid	L	Leu	Leucine	T	Thr	Threonine
E	Glu	Glutamic acid	M	Met	Methionine	V	Val	Valine
F	Phe	Phenylalanin	N	Asn	Asparagine	W	Trp	Tryptophane
G	Gly	Glycine	P	Pro	Proline	Y	Tyr	Tyrosine
H	His	Histidine	Q	Gln	Glutamine			

Abbreviations for the nucleobases:

A	Ade	Adenine
C	Cyt	Cytosine
G	Gua	Guanine
T	Thy	Thymine

AKNOWLEDGEMENTS

I am very grateful to my Ph.D. supervisor Prof. Dr. Roger Goody for offering me the great opportunity to carry out my Ph.D. studies in MPI-Dortmund and for his support, scientific and moral, during the course of my Ph.D.

I would like to thank also Prof. Dr. Roland Winter for supervising my PhD work.

Many thanks to my coordinator Dr. Jochen Reinstein for giving me an exciting project that help me significantly improve my scientific knowledge and for his continuous scientific, moral and financial support during the entire Ph.D. period.

I would like to thank Dr. Ralf Seidel, the person incharge with cloning of the DnaK/ClpB systems, Dr. Peter Bayer for his help with the NMR spectra, Dr. Elke Deuerling (ZMBH, Heidelberg Universität) for the help with the ribosome experiments, Prof. Dr. Reinhard Hensel (Essen Universität) for help with fermentation of *T. thermophilus* cells, Dr. Dagmar Klostermeier (Bayreuth Universität) for interesting suggestions regarding my work.

Special thanks go to the entire “molecular chaperone” group with its actual (Hellen, Raji, Simone, Vinod, Sabine) and former (Petra, Philipp, Sandra, Thomas, Yvonne) members. They are responsible for a wonderful collegial and friendly climate within the group and for fruitful discussions in scientific and personal matters. Many thanks to Petra and Elisabeth for an excellent assistance in the lab.

I would like to thank also all my colleagues from Abt. III MPI-Dortmund and Abt. Biomol. Mech. MPI-Heidelberg for the friendly atmosphere in the department.

Special thanks to the whole Romanian community gathered over the years in MPI-Dortmund. The familiar atmosphere created by the presence of Alex, Alice, Alexandra, Stefan, Tudor, Vali and especially Anca, Betty and Cristina, made me often forget the long way home.

Special thanks also to Tatjana and Roman for their unlimited support in difficult times.

I send many thanks to Romania, to my whole family and my friend Rodica for their love and support.

Last, but not least, thank you Michael for everything!

CURRICULUM VITAE

Personal Information

Name	Georgeta Liliana Dumitru
Born on	December 13 th 1973 in Cosereni, Romania
Marital status	single
Email address	georgeta.dumitru@mpimf-heidelberg.mpg.de

School education

1980 – 1984	Elementary school in Bucharest, Romania
1984 – 1988	Gymnasium school in Bucharest
1988 – 1992	Theoretical High School “A. Vlaicu” in Bucharest
1992	High School Graduation

Studies in biochemistry

1993 – 1997	Studies of Biochemistry at the University of Bucharest, Faculty of Biology, Romania
1997 – 1998	Licentiate Thesis with the title "Biological, chemical and immunological characterisation of alpha-fetoprotein". Supervisor: Prof. Dr. Grigore Mihaescu, University of Bucharest, Faculty of Biology.
1998	Degree: Diploma in biochemistry
1998 – 1999	Research Assistant, Institute of Biochemistry of Romanian Academy, “Molecular Glycobiology” group
2000 – 2004	Ph.D. thesis at the Max-Planck Institut für Molekulare Physiology in Dortmund under supervision of Dr. Jochen Reinstein (Dept. of Prof. Dr. Roger Goody)

Publications

Dumitru, G.L., Groemping, Y., Klostermeier, D., Restle, T., Deuerling, E., and Reinstein, J : DafA Cycles Between the DnaK Chaperone System and Translational Machinery. **JMB** (2004) **339**, 1179-1189